NOISE MODELING FOR STANDARD CENELEC A-BAND POWER LINE COMMUNICATION CHANNEL

A RESEARCH REPORT
SUBMITTED TO THE FACULTY OF ENGINEERING AND THE BUILT ENVIRONMENT
OF UNIVERSITY OF THE WITWATERSRAND, JOHANNESBURG
IN PARTIAL FULFILMENT OF THE REQUIREMENTS
FOR THE DEGREE OF
MASTERS OF SCIENCE IN ENGINEERING (ELECTRICAL)

Ayokunle Damilola Familua
FEBRUARY 2012

Declaration

I declare that this project report is my own, unaided work, except where otherwise acknowledged. It is being submitted for the degree of Master of Science in Engineering at the University of the Witwatersrand, Johannesburg, South Africa. It has not been submitted before for any degree or examination at any other university.

Candidate Signature : .....

Name : .....

Date : (Day)..... (Month)..... (Year).....

Abstract

Power line communications (PLC) usage of low-voltage electrical power supply network as a medium of communication provides an alternative for the telecommunication access and in-house communication. Historically, power lines were majorly used for controlling appliances, however, with recent technology advancements power lines are now able to compete favorably and successfully with other relatively stable home automation and networking technologies like fixed line and wireless.

Regardless of the advantages PLC has to offer, like every other communication technology, it has its own technical challenges it must overcome to be fully deployed and maximize its full potential. Such challenges includes noise, which can originate from appliances connected across the network or can be coupled unto the network. Harmful interference to other wireless spectrum users such as broadcast stations, and signal attenuation are other challenges faced by usage of the power line as a communication medium. PLC suffers the risk of not living up to its full development as a reliable means of communication if proper understanding of the channel potential and characteristic is not known. Therefore, understanding of the channel potential and characteristics can be obtained through measurement and modeling of the PLC channel. This model and measurements of the channel characteristics can then be utilized in designing a good PLC system which is able to withstand and mitigate the effect of the different kind of noise and disturbance present on the PLC network.

This research therefore aims at formulizing and modeling the error pattern/behavior of noise and disturbances of an in-house CENELEC A-band based on experimental measurements. This is achieved by carrying out a real time experimental measurement of noise over a complete day to show the noise behavior. Error sequences are then generated from the measurement for the different classes of noise present on the CENELEC A-band and the use of Fritchman model, a Markovian chain model, is then employed to model the CENELEC A-band channel. This involves the use of Baum-Welch algorithm (an iterative algorithm) to estimate the model parameters of the three-state Markovian Fritchman model assumed. This precise channel model can then be used to design a good PLC system and facilitate the design of efficient coding and/or modulation schemes to enhance reliable communication on the PLC network. Therefore, answering the question of "*how to formulize and model the error pattern/behavior of noise and disturbances of an in-house CENELEC A-band based on experimental measurements"*.

Dedication

This Research Report is dedicated to the Almighty God, the author of wisdom for giving me the grace to complete this degree.

Acknowledgement

I wish to express my profound gratitude to the following people for their contributions towards the successful completion of my MSc degree.

My Lord and personal savior, who has being my strength through thick and thin and has inspired me to the completion of this degree, I will forever be grateful Lord;

My dear parents, Engr. and Mrs. Ajewole Joseph Familua, who instilled in me a desire for formal education and has been supportive financially and morally. I am forever indebted to you for the foundation you laid for me in life;

My Supervisor, Dr. Ling Cheng for your guidance, supervision, commitment, encouragement and rare thoroughness during the period of this research. I am most grateful for your thorough editing of this research report and for providing direction. Thanks for the opportunity you gave me to develop and also prove my ability;

My beloved brothers Dr. Franklin Oluwamayowa Familua, Mr. Victor Olanrewaju Familua, Oluwafemi Familua, Taye and Kehinde Familua; my sister-in-laws, Mrs. Lara Familua and Mrs. Abiola Familua for your encouragement and financial support;
Center for Telecommunications Access and Services (CeTAS) headed by Prof. Van Olst for your financial assistance;

My colleagues in the School of Electrical and Information Engineering; Muhammad Saeed, Sibonginkosi Ntuli, Mehran Asmi Muhammad, Rohaan Shaah, Benjamin Sim and Peter and those that I fail to mention. I recognize your immense contributions. I want to especially thank Reevana Balmahoon for helping in proof-reading my report;

The University of Witwatersrand Financial Aids and Scholarships office for your financial assistance;

To my spiritual fathers: Pastor J.O. Akinbodewa, Pastor Ebenezer Bobade, Pastor Ogunyemi, Pastor Odukunle and all members of the Christ Apostolic Church, Oke-Itura, Akure for your prayers and moral support; and

I will be ungrateful if I fail to acknowledge the assistance of Professor Petrus A. Janse Van Rensburg and my colleague Abdirashid Osman Qatarey. Thanks for your contributions.

List of Publications

Conference Publications

Familua, A.D., Qatarey, A.O., Van Rensburg, P.A.J., and Ling Cheng, "Error pattern/behavior of noise in in-house CENELEC A-Band PLC channel," *Power Line Communications and Its Applications (ISPLC), 2012 16th IEEE International Symposium on*, pp.114-119, 27-30 March 2012.

Ayokunle Damilola Familua and Ling Cheng, "Modeling of In-House CENELEC A-Band PLC Channel using Fritchman Model and Baum-Welch Algorithm" *Power Line Communications and Its Applications (ISPLC), 2013 17th IEEE International Symposium on*, pp.173-178, 24-27 March 2013.

Table of Contents

List of Abbreviations

AC	Alternating Current
AMI	Advance Metering Infrastructure
AMR	Automatic Meter Reading
ANSI	American National Standards Institute
ARIB	Association of Radio Industries and Businesses
AWGN	Additive White Gaussian Noise
BAN	Building Area Network
BB	Broad Band
BER	Bit Error Rate
BN	Background Noise
BNC	Bayonet Nut Connector or *Bayonet Neill Concelman Connector*
BPL	Broadband over Power Lines
CENELEC	Comité Européen de Normalization Electrotechnique
CISPR	International Special Committee on Radio Interference
CSMA	Carrier Sense Multiple Access
DPL	Digital Power Line Protocol
DSM	Demand Side Management
DSP	Digital Signal Processing
DS-CDMA	Direct Sequence Code Division Multiple Access
EIA	Electronic Industries Alliance
EMC	Electromagnetic Compatibility

ETSI	European Telecommunications Standards Institute
FCC	Federal Communications Commission
FEC	Forward Error Correction
FFT	Fast Fourier Transform
HAN	Home Area Networks
HD-PLC	High Definition Power line Communications
HDR	High Data Rate
HF	High Frequency
HMM	Hidden Markov Model
HV	High Voltage
IAT	Inter-Arrival Time
ICTSB	Information and Communications Technologies Standards Board
IEC	The International Electro-technical Commission
IN	Impulse Noise
ISI	Inter-Symbol Interference
ISO	International Organization for Standardization
ITU	International Telecommunication Union
LDR	Low Data Rate
LF	Low Frequency
LPTV	Linear and Periodically Time-Varying
LonWorks	Local Operation Networks
LV	Low Voltage
MF	Medium Frequency

MTL	Multi-conductor Transmission Line
MUI	Multi User Interference
MV	Medium Voltage
NBN	Narrowband Noise
OFDM	Orthogonal Frequency Division Multiplexing
OPERA	Open PLC European Research Alliance
PC	Personal Computer
P_E	Probability of Error or Error Probability
PHY	Physical Layer
PLC	Power Line communications
PLN	Power Line Network
PLX	Power Line Exchange Protocol
PRIME	Power line Related Intelligent Metering Evolution
PSD	Power Spectrum Density
PSU	Power Supply Utility
RCS	Ripple Control System or Ripple Carrier Signaling
RMS	Root Mean Squared
SNR	Signal to Noise Ratio
SST	Spread Spectrum Technique
TL	Transmission Line
TWACS	Two-Way Automatic Communication System
UNB	Ultra Narrowband
UPA	Universal Power line Association

UPS	Uninterruptible Power Supply
VHF	Very High Frequency
VLF	Very Low Frequency
VLSI	Very Large Scale Integration (Integrated Circuits)
QPSK	Quadrature Phase Shift Keying

List of Figures

List of Tables

Chapter 1: Introduction

1.0 Introduction

Power line communications (PLCs) technology has been classified into two major categories namely broadband (wideband) and narrowband PLC. This two major classification is based on their frequency bandwidth. Broadband (wideband) PLC is utilized for broadband applications, with the bandwidth ranging from 1-30 MHz, while narrowband PLC utilizes low frequency bandwidth ranging from 3-148 kHz for narrowband applications as defined by the European CENELEC standard for Europe and below 450 kHz in Japan [1], [2]. Despite the fact that broadband over power line (BPL) has attracted extensive interest and research over the last decade due to its use for high speed internet access and 'last mile' access services to all homes and offices, narrowband PLC is still highly relevant for some high speed narrowband applications.

The in-house narrowband PLC utilizes the existing power line networks that were originally meant for electrical energy distribution to provide a communication media and a means of interconnecting and controlling home appliances through the power outlets already and universally present in every rooms of the homes. Its relevance can also be found in various other narrowband applications namely: its historic use for control of power grid through meter reading, street lighting control, control of ground-lights of airport runways [3], home automation, and its application in communications of control data with 40 kb/s in street car/subway systems on 750V direct current networks [4].

Power line communication generally experiences a hostile environment on the existing power line network utilized as a medium of communication. Hence, this leads to performance degradations as a result of the intrinsic channel attributes and several other disturbances and challenges such as noise, which makes reliable data transmission over the power line channel difficult.

CENELEC A-band, with 3-95 kHz frequency bandwidth is plagued with a lot of noise and disturbances emanating from various electrical appliances connected across the network (due to their intrinsic properties) or from noise sources outside the power line network coupled unto the network. The use of these appliances is not coordinated as users connect or switch them on and off at will and the noise introduced causes burst error and loss of data at the receiving end during transmission. The characteristics of these noise and disturbances change with time of day, place, source and frequency. To achieve a robust PLC system design and for full realization of the potential of PLC system, it is crucial that these channel impairments, other additive noise and disturbances encountered during data transmission in PLC be thoroughly characterized. Hence, the need for measurement and modeling of the channel remains highly essential.

In this research report, we show noise measurement and modeling of the three major categories of noise present on the CENELEC A-band, and aim at answering the question of "*how to formulize and model the noise and disturbances present on the in-house CENELEC A-band based on experimental measurement*". The resulting models are experimental channel models based on real channel measurement.

This aim is achieved by carrying out experimental measurement of the three major classes of noise present on the PLC channel namely: background noise, narrowband noise and impulse noise. The measurement is carried out at two different locations; the residential and a laboratory environment. The output sequences (error sequences or observations) for these three major types of noise are generated separately from the measurement data, analyzed and modeled using a three-state partitioned hidden Markov model (HMM), namely Fritchman model [5]. The motivation behind the use of a Fritchman model is because it depicts the bursty nature of the power line communication channel which results due to the severe impairments present on the channel. This makes it useful in modeling of the PLC noise. The Fritchman model, which is a burst-noise channel model, assumes the probability of having a series of good states and also bad states based on the characteristics of the channel considered. Unlike other channel models such as the Gilbert-Elliot model [6], this only proposed a good and a bad state which is not a true representation of the noisy and burst-noise characteristics of the PLC channel.

An HMM iterative training algorithm, Baum-Welch algorithm [7], is then employed for likelihood evaluation and parameter estimation of the given Fritchman model parameters. Hence,

the resulting channel models can then be used for narrowband PLC system design for optimal performance. It also helps in selection and design of appropriate error correction codes and/or modulation techniques to mitigate the effect of noise to increase accuracy and improve the performance of the overall power line communication system. Furthermore, it is useful in testing, analyzing and evaluating these coding and modulation techniques.

1.1 Problem Definition

The in-house power line channel (medium) is shared with a lot of electrical devices that generate noise, as the network was originally designed for electricity distribution to these electrical devices and appliances, and not for data communication. This makes it susceptible to noise and disturbances. The noise and disturbances is mainly caused by switching transients caused by on and off switching of power supplies found in various household appliances as they occur all over a power supply network at irregular intervals. Moreover, the noise is also caused by radiation coupled to the power line network from a broadcast station sharing the same frequency band. As a result, the noise gives rise to signal distortion, consequent corruptions of data and burst error during transmission on the PLC network. Multipath fading, high signal attenuation and noise with random time-varying impulsive behavior are the most undesirable characteristics the power line network possesses.

Over the years research has shown through practical measurement in the PLC environment that impulsive noise has the most powerful and harsh effect on signal communication when compared to other kinds of noise. Significant performance degradation can result from the occurrence of this high-power impulsive noise due to burst errors that occurs as a result of this noise at the receiving end.

Therefore, due to this harsh environment faced by data communication on a PLC channel, a better understanding of the channel potential and noise (disturbances) behavior on the network is essential and its characterization crucial for the design of a reliable PLC system.

Furthermore, it is also of great importance to investigate the effects of this noise on data communications and realize a precise channel model that can be used to design modulation techniques and/or coding techniques to mitigate the damaging effects of this noise and optimize the performance of the power line communication in this harsh ubiquitous wired network. The

research addresses the problem of *"how to formulize and model the error pattern/behavior of noise and disturbances of an in-house CENELEC A-band based on experimental measurements"*.

1.2 Motivation

Firstly, this work is motivated by the need to further the advancement of research in power line communication field, as it is a fast growing alternative for last mile access network to end subscribers of telecommunication services and in-house home automation and interconnection. There is also need for more research input to harness the full potential PLC offers over other medium of communication and realize the full practical implementation of PLC channel as a reliable communication medium.

Secondly, this research is further motivated by the need to formulize and present a precise channel model that depicts the bursty characteristics of the PLC channel, i.e. *model the error pattern/behavior of noise and disturbances of an in-house CENELEC A-band based on real experimental measurements and not simulations*. The noise and disturbance characterization and modeling can effectively be used to facilitate the design of efficient coding and/or modulation schemes to mitigate the effects of these noise and disturbances for a reliable communication.

1.3 Scope and Research Objectives

Recently, PLC technology has received a lot of increasing interest as a means to provide offices and homes with interconnectivity, internet access in addition to local area networking using the already existing in-building wiring. PLC technology provides low-speed narrowband communications and potential to provide also high-speed broadband communications through the universal and most ubiquitous wired network without further need for new wiring installation. However, this ubiquitous wired network (power line network) was originally designed for energy transmission and distribution at 50 and 60 Hz depending on the country. Thus, the power line network presents a hostile or harsh environment for both low-speed and high speed communications.

This research is thus aimed at *formulizing and modeling the error pattern/behavior of noise and disturbances of an in-house CENELEC A-band based on experimental measurements.* This objective is achieved within the scope of the procedures mentioned as follows:

First, experimental measurement of noise is carried out on the CENELEC A-band PLC at two metropolitan locations of South Africa (a residential detached building with major household electrical appliances which are sources of noise on the PLC network, and the digital signal processing laboratory of the department of Electrical and Information Engineering Department of the University of Witwatersrand, Johannesburg, South Africa). Analysis of measured noise is done to present changes in noise characteristics over a complete day and show the noise pattern/behavior on the CENELEC A-band PLC channel.

Second, the noise measurement data is then analyzed according to the three major kinds of noise described in this report. The error observation sequence is generated for the three kinds of noise and modeled separately because of their different effects on data communication. Fritchman hidden Markov model, which is a Markovian chain model is employed to model the three kinds of noise assumed in this research. Baum-Welch algorithm is used to estimate the model parameters based on the training data i.e. the three error observation sequences generated from experimental measurement in this project. A precise channel model based on measurement is then realized.

1.4 Organization of this Research Report

To achieve the stated objectives, the layout of this report is as follows:

Chapter 1 contextualizes the study presented in this report. The problem definition is presented followed by the motivation for working on the project. The research objectives and scope of this research are also specified. This chapter is concluded by the organization of this research report.

Chapter 2 presents an overview of relevant works related to this project. An historical overview on PLC is done followed by relevant works on PLC channel and noise modeling. Furthermore, a literature review of the hidden Markov Fritchman model utilized in this project work is done, and this chapter is concluded by a review of the iterative Baum-Welch algorithm used for the model parameter estimation.

Chapter 3 presents basic technical details of power line communications topics relevant to this research work. An overview of PLC technology is first carried out in Section 3.1, followed by a study of the narrowband PLC standardization and regulatory landscape in Section 3.2. Section 3.3 examined PLC channel characteristics while Section 3.4 discusses the classification of noise on the PLC channel. In Section 3.5 an in-depth study of the coupling circuit is done while Section 3.6 gives a technical details of the hidden Markov models. This chapter concludes with the background details of the iterative Baum-Welch algorithm for parameter estimation in Section 3.7.

Chapter 4 presents the experimental measurement methodology used in this research as well as the discussion of the measurement results. This chapter starts by describing the measurement site in Section 4.1, followed by the measurement methodology and categorization of noise on the narrowband PLC channel in Section 4.2. Furthermore, the experimental measurement setup for noise data captured is described in Section 4.4. This chapter concludes with the presentation and discussion of the measurement results showing variation and behavior of noise on the CENELEC A-band over a complete day for the two different locations over two year span in Section 4.4.

Chapter 5 discusses the Baum-Welch Algorithm Parameter Estimation of the Fritchman Model. Section 5.1 presents the Fritchman model parameters assumed for the model, while Section 5.2 shows the error observation sequence generated for the three noise types. This chapter concludes with the presentation of the modeling results for 2011 and 2012 noise model in Section 5.3.

Chapter 6 concludes this research work with a research summary in Section 6.1, while conclusion and recommendation is presented in Section 6.2. Conclusively, Section 6.3 ends this chapter.

Chapter 2: Literature Review

2.0 Introduction

Power line networks (PLN), were earlier invented and designed for the transmission of electric power from power generating substations to a very large number of end-users (consumers) in the 50-60 Hz frequency range. PLN is in fact one of the most ubiquitous and robust structures ever built. The use of PLC technology historically has very limited applications but recently, it is fast becoming an alternative medium for long-haul data communication (both narrowband and broadband applications) and a solution for bridging the last mile problem for delivering telecommunications services in a cost effective way. This chapter presents a literature review of works related to this research. Section 2.1 takes us down memory lane by discussing the emergence of PLC and its historical overview. Section 2.2, 2.3, 2.4, presents literature review of works related to PLC channel and noise modeling, Fritchman model and Baum-Welch algorithm respectively.

2.1 PLC Historical Overview

Communications over power lines is not a new technology but an old idea which can be historically traced back to the 1900s, when power line communication recorded its first patent in this area [8]. Subsequently, electric power utilities worldwide have been utilizing this technology for load control and remote metering using single carrier narrowband solutions [9].

The emergence of PLC came with the power utilities making use of long distance High Voltage (HV) power lines with voltage level above 100 kV for voice and data communications. Historically, HV power lines apart from being used for power transmission have alternatively been used as medium of voice communications since as early as the 1920s [8].

Moreover, the historical motivation behind the use of power lines as a data transmission medium was primarily done to protect power distributions systems in the emergence of faults. In the event of a fault, quick exchange of information between power plants, power substations and power distribution centers is highly necessary to minimize the detrimental effects of these faults. The robustness and the availability of power line networks make it useful in solving this

problem. The use of HV power lines for PLC purposes by power utilities engineers in those early years was an alternative means of communication due to the poor coverage of telephones. The utility engineers who operate transformer stations and power plants use PLC for operational management with other power utilities colleagues who are stationed at other far geographical locations. Low data rates (few hundreds of bits per seconds) were later achievable for support of telemetry and tele-control applications with the emergence of digital communication techniques [9], [10].

Narrowband PLC emerged as a result of wide-spread of electrical power supply network. In the early 1920s, the first carrier frequency system became operational utilizing high-tension lines (15-500 kHz frequency range) for telemetry application, which is still in existence presently [11]. Consumer products such as baby alarms were introduced since the 1940s [12].

Historically, the usage of PLC for load control management was another essential driver for the use of PLC by power utilities. This enabled power utilities to remotely switch ON/OFF high energy consuming electrical appliances and equipment such as water heaters, air conditioner etc. Its application can been found in the control of peak event at the demand side using the Ripple Control System or Ripple Carrier Signaling (RCS), with the power utilities sending control signals to end users to switch off heavy duty appliances to achieve Demand Side Management (DSM) by saving energy [9]. The deployment of RCS was quite successful in the European context, finding its application in street light control, equipment control on power grid, and day/night tariff switching. Another important motivation for the use of PLC has been its usage for meter reading. From study meter reading utilizes an average information rate of about 1 bits/sec [13], with field trials of meter reading reported in [14].

Giving careful consideration to the fact that PLC has been around for quite a long time, but recently it is receiving a lot of renewed attention and interest despite the fact that it offers low data rate (a few kb/sec) for telemetry and protection applications which is not comparable to the Mb/sec data rate required in the present digital multimedia application age. This increasing interest was as a result of combinational effects of the some technological changes and events which includes the explosive internet growth that occurred in the 1990s, extremely large leaps in the Very Large Integrated Circuit (VLSI), Digital Signal Processing (DSP) technologies, and

also the deregulation of the telecommunication market which first took place in the US, and followed by Europe and Asia [15]. All these technological changes and events awakened the increasing interest in PLC technology thus making this technology a feasible technology for numerous applications. Such applications include: Home Automation, Home Networking and Internet Access (Broadband over Power Lines, BPL), Narrowband PLC-Radio Broadcasting, Automotive, and other specific applications by end-users such as: quality of power measurement using PLC [16], and a solution by Cavdar to remotely detect illegal electricity usage in [17].

The emergence of Broadband PLC systems (2-30 MHz frequency range) was birthed thus widening the application space and achieving data rates up to 200 Mb/sec. Over the years there has been increasing industry interest in high data rate application using narrowband-PLC. The technology is based on multicarrier schemes which operate in the 3-500 kHz frequency band. Evolution of PLC in the three main classes of PLC technologies is further discussed below.

Ultra-Narrowband PLC

Over the last couple of decades, several Ultra-Narrowband (UNB) solutions such as Automatic Meter Reading and Advance Metering Infrastructure (AMI) utilizing power line communications were deployed into the market by power utilities. Based on literatures, PLC first deployment involving the use of UNB-PLC technologies was first launched in applications such as the Turtle system [18] and TWACS (two-way automatic communications system) [85], [86]. The out-band communication (substation-to-meter) makes use of disturbances of voltage waveform while, the in-bound communication (meter-to-substation) makes use of disturbances of current waveform. Turtle has been widely used for AMR applications with its emerging products allowing only a one-way in-bound connectivity while a two way version was later released in 2002. TWACS on the other hand finds its application in Distribution Automation, AMI and Demand response and widely used especially in the US.

A narrowband TWACS-like method that could offer a high data rate than TWACS for inbound communication has been proposed recently [19].

Due to the increasing demand for higher data rates which motivated the emergence of Narrowband PLC which will be discussed as follows.

Narrowband PLC

The European CENELEC body recognizing the increasing demand for higher data rate PLC published a standard EN 50065 in 1992 [1]. The EN 50065 CENELEC Standard permitted data communication over the Low Voltage (LV) power distribution network and it allows operation in the (3-148.5 kHz) frequency range. This frequency allocation was further classified into four bands as discussed in Table 3.1. This standard also assigned specific bands for the exclusive use of power utilities unlike the FCC band (10-490 kHz) and the ARIB band (10-450 kHz) that allow any device to have access without any co-existence protocol as we have in the C-band of the CENELEC classification.

Broadband PLC

The deregulation of the telecommunication in the 1990s and the increasing demand for high data rate internet connectivity lead to the emergence of broadband PLC which was initially for internet access applications but successively developed for its eventual use in Home Area Network (HAN), and Building Area Network (BAN) applications. Early interest in Broadband-PLC for internet access emerged in Europe when Norweb and Nortel Communications proclaimed their development of a PLC technology to provide access to residential end-users (customers) in 1997 [20].

Limited test runs of broadband internet access over the power lines were carried out in Manchester, UK utilizing the Norweb prototypes, and it was found to be able to achieve communication of data at data rates around 1 Mb/sec. But the continued implementation this technology was brought into abrupt termination in 1999 due to high cost of implementation which was more than the anticipated cost and the electromagnetic compatibilities issues. Other BB internet deployment campaign was launched in Europe by Siemens and Ascom, but they were also confronted with similar fates encountered by Norweb.

The Open PLC European Research Alliance (OPERA) funded many multiyear research efforts on BB-PLC for internet access [21]. As a result of the failed projects on BB-PLC for internet access experienced by Norweb, Siemens and Ascom, research interest began to shift towards BB-PLC usage for in-home applications in the early 2000. Over the last decade, several industry-alliances had been constituted towards setting BB-PLC in-home technology specification. Such

alliances include: HomePlug Power line Alliance regarded as HomePlug, UPA (Universal Power line Association), Home Grid Forum and the High Definition Power line Communications (HD-PLC). Details about these alliances can be found in [101]. These alliances resulted into the following in-home BB-PLC technologies products which have been readily and progressively available in the market over past years:

HomePlug 1.0 which allows a PHY data rates of 14 Mb/sec.

HomePlug Turbo which can achieve a PHY data rates of 85 Mb/sec.

HD-PLC, UPA and *HomePlug AV* which offers a PHY data rates of 200 Mb/sec.

Although all the above mentioned technologies suffer from interoperability issues as they are not interoperable with each other, however, they offer an excellent home networking BB-PLC technologies essential in complementing Wi-Fi technologies even though they have not gained a significant market share and are not yet widely adopted.

2.2 PLC Channel and Noise Modeling

The harsh and noisy nature of PLC channel as a transmission medium makes it difficult to model [22]. Apart from being time-varying, frequency-selective, it is also suffers from colored background and impulsive noise impairments. In addition these technical challenges aforementioned, the grid and the indoor wiring topology and structure differ from country to country and also within a specific country.

From a communication perspective, each section of a particular grid possesses its own channel characteristics. Attenuation and dispersion present on the transmission side of the grid are very small and can be well dealt with. In contrast, as we approach the distribution side of the grid, towards the home, there is increase in dispersion and attenuation which is more prominent at higher frequencies [22], [23].

The power line network itself represents a noise source, apart from other several noises present on the network which are often dependent on frequency, time and weather.

The electrical appliances connected across the Low Voltage (LV) and Home Area Networks (HAN) are major sources of cyclo-stationary noise and Linear and Periodically time-varying

behavior of the channel impulse response. The presence of non-linear components such as diodes and transistors present in electrical devices (loads) connected across the power line results in the Linear and Periodically Time-Varying (LPTV) behavior of the channel impulse. This is because contrary to the small rapidly changing communication signals, these non-linear components appear as resistances that are biased by the AC mains voltage. A periodically time-varying change of the resistance of these devices is induced as a result of the periodically changing AC signal which sways these loads over dissimilar regions of their non-linear current versus voltage curve. Thus, the total impedance is seen as bye-pass impedance through the Line and neutral wires and, it is naturally periodic as a result of the dependence of its time variability on the periodic AC mains waveform [24].

Furthermore, based on Nyquist criterion, noise seems to be cyclo-stationary as electrical devices present on the network are also noise generators [24]. Narrowband noise is also often present as the power line itself is a source of electromagnetic interference as well as a victim.

PLC system design thus remains challenging, particularly dealing with the several noise sources present on the PLC channel being the major challenge.

Thus PLC channel modeling is essential in the design of a reliable communications system, as the design ought to be in agreement with the peculiar channel characteristics. Specifically, lack of unified and generalized model for the PLC channel has likely led to the slow rate of PLC transceiver optimization [22].

A lot of research has gone into the pursuit of having a more adept understanding of the power line channel attributes. Among several literature and works carried out on understanding the PLC channel attributes are the most salient ones highlighted as follows [25]: PLC channel Isotropic nature [26], The Multipath Model [27], RMS delay spread and the log-normal distribution of channel attenuation on the PLC channel [28], analysis of the grounded and ungrounded link under the same school of thought based on the relationship between both [29]. The PLC channel Linear and Periodic Time-Varying attribute [30], Noise classification and Modeling [2].

A review of current PLC channel modeling is presented in four categories and various models that fall under these categories are also reviewed as follows:

Top-Down Approach for Transfer Function Modeling: This approach is also regarded to as a *phenomenological* approach, and a *posteriori* methodology (an empirical approach) is often used in the computation of the transfer function. This empirical modeling approach implies the use of measurements in determining the model parameters, though it has been found to be computationally efficient and could be easily implemented but has high tendency of measurement errors [31]. The most cited PLC channel modeling empirical approach in literature are the studies carried out by Zimmermann and Dostert [27], and Philipps [32]. The advantage of Multipath model approach is that PLC channel simulation requires less computation which makes the algorithm implementation comparatively easy. This implementation is easy once measurement has been carried out and the modeling parameters have been derived from the measurement. But its major drawback is, in the event of changes in network, new measurement is highly essential which makes it difficult to use this model for the general purpose simulation tool.

Since the power grid is made up of branches of interconnected wiring joints, which results in multiple paths for signal propagation. It leads to a phenomenon called echo. Due to the imbalance in the characteristic impedance and load impedances of these numerous branches, a mismatch occurs resulting into portion of the propagated signal being reflected at each joint, load and open circuit. Hence, at the receiving side, the propagated signal added to the arriving echoes creates a complex resultant signal, whose amplitude is attenuated as a result of multipath propagation.

The empirical model approach proposed in [33] described the transfer function of the PLC channel by an echo model. Furthermore, in [34-35] the transfer function of the PLC channel is described using TL-theory and a two-port network theory. Also a different viewpoint a TL model based on two port networks with Z-parameters was proposed in [36]. These Z-parameters are easily measurable and computable and are expressed in terms of the port impedances.

Bottom-Up Approach for Transfer Function Modeling: This approach is normally regarded to as an analytical approach. A *priori* methodology (a deterministic approach) is used in the computation of the transfer function. The modeling parameters of deterministic models are deduced from a theoretical basis. Apart from being more computationally intensive when compared to the empirical approach, it also permits the prediction of change in the transfer

function which might occur due to the occurrence of changes in the network [31]. The major disadvantage of this deterministic modeling is that knowledge concerning the whole network is highly essential, i.e. having accurate and full knowledge of all the modeling parameters such as the topology, the terminating impedance on every branch and the types of cables and their corresponding characteristics [29]. It is evident that knowing all the model parameters can be time consuming and difficult. Initially, empirical approach was used for PLC channel modeling. The multipath model was the first major popular model that gave a phenomenological explanation of how signals are been transmitted over the power lines. The multipath model is being introduced by Zimmermann in [27], [32], [35], [37]. In this model, a set of limited parameters (delay, attenuation, number of paths, etc.) was used to demonstrate a simple model that describes the typical power line channel's complex transfer function. The drawback of this model is based on the fact that it is not linked to the power line channel physical parameters, but is founded on physical signal propagation effects. The signal propagation effect that arises from the presence of numerous branches and impedance mismatch phenomenon that causes multiple reflections. This model also studies frequency-selective fading that occurs as a result of multipath propagation. Deriving analytically the multipath model parameters utilizing a classical two-conductor transmission line theory (TL-theory) helps to overcome the problem of multipath model, provided an assumption is made that the link topology is known a priori [39]. Although, as the number of discontinuities increases, it increases the computational complexity of this method, hence, it becomes higher in in-building cases [29]. Furthermore, several authors have made contributions which focus on a deterministic model in the frequency domain based on the TL-theory [26], [29], [31], [40-43]. Also, a model that includes grounding in low voltage indoor cases and the multi-conductor transmission line modeling approach (MTL) is proposed [26], [29], [43].

Finally, a deterministic model which makes use of a single parameter to describe the power line channel complex transfer function was presented in [44]. Power line networks are classified into different groups based on the phase response and the average magnitude of the channels.

Noise Modeling: The noise power spectral density (PSD) is majorly dependent on location and time. In addition, various measurement campaign carried out shows it comprises of narrowband

noise, colored background noise, periodic impulse noise and asynchronous impulsive noise [2], [45].

A lot of research campaigns carried out to model PLC noise has been based on empirical measurement. This is as a result of difficulty in the characterization of PLC noise by pure analytical derivation. PLC noise modeling can be realized in both time and frequency domain based on the nature of the measurements. Background noise is often modeled in the frequency domain while impulse noise is modeled both in time and frequency domains [46].

Background Noise Models: Background noise is broadly modeled in the frequency domain and modeling of this kind of noise is achieved by fitting a decreasing function with its power spectral density or voltage profile. Examples of this model were proposed in [47-48], [125]. Based on these examples, a model for background noise was proposed by OPERA consortium [49]. Inclusion of specific power density functions (PDF) in the model makes it possible for the statistical behavior of the background noise to be characterized. For instance log-normal distribution, Nakagami distribution, Gaussian distribution and Rayleigh distribution were proposed in the following references [46-47], [50-51].

Impulse Noise Models: In spite of the short duration or interval of the occurrence of impulse noise, it is conceived as the main error source when data are communicated over the PLC channel. This is as a result of its high PSD [52]. The impulse noise has been analyzed both in the frequency and time domains, although analysis in the time domain is the most available in literature. Using the time domain model, impulse noise is characterized by random variables namely: the impulse width t_w, the impulse amplitude A, and the inter-arrival time (IAT), t_{arr}. The statistical properties of these random variables might be deduced from measurements. An impulse noise model denoted as n_{imp} is proposed in [23], [45], [125-126]. This model is based on a popular impulse function, denoted by $imp\ (t)$, and this impulse function possesses unit amplitude and unit width and mathematically represented below:

$$n_{imp} = \sum_i A_i imp\left(\frac{t - t_{arr,i}}{t_{w,i}}\right) \tag{2.1}$$

To model the PDF of the aforementioned random variables, several authors have proposed the inclusion of additional underlying random process with the aim of defining the variance. For

instance, according to [45], [49], in order to define the PDF of the IAT and the impulse width the authors proposed stochastic models founded on a partitioned Markov chain. In contrast, a Middleton's class-A noise model was proposed for both impulse noise and background noise, so as to generate a worst case scenario. Ultimately, impulse noise and background noise were regarded and analyzed as a cyclo-stationary process in some literatures. The noise is assumed as a Gaussian process with a periodic time function instantaneous variance [2], [53].

Narrowband Noise Model: The primary sources of this type of noise are broadcast stations occupying the short, middle and long wave frequency range. It can be modeled as a sum of multiple sinusoidal noises represented mathematically below, since the noise are modulated signals from the broadcast stations [45].

$$\mathrm{n}_{narrowband}(t) = \sum_{i=1}^{N} A_i\,(t)\,.\sin(2\pi f_i t\ +\ \varphi_i) \qquad (2.2)$$

Number of carriers reckoned with in the model is denoted as *N,* and each of these carriers having different amplitude A_i (*t*), and also different phase denoted by φ_i. With regards to a basic model, some of the parameters can be assumed as a constant, which is not ideal for a more realistic model where it is necessary to consider some specific modulation techniques [49].

PLC Modeling using Simulation Tools: Research effort has been dedicated to the development of PLC channel simulation tools. The basic intent behind this approach is the implementation of an algorithm formulated based on any of the PLC channel model that has been developed. These simulation tools help in testing and evaluating how accurate and reliable these models are, and often have Human-Machine Interface that is easy to understand and use [54]. Mostly, simulation tools implementation is the outcome of the channel model development process. Some authors have developed some PLC channel modeling tools using the deterministic approach. The development of some PLC channel modeling tools have been carried out utilizing the deterministic approach, likewise other development are based on empirical approach. However, the main approach used by simulation tool developers is the deterministic approach based on the fact that it permits the prediction of future changes which might occur due to network changes. Several simulation tools developed by various authors are found in the following references [35], [55-58].

Other models that are noteworthy are that of Canete et al. in [59], and Barmada et al. in [60].

2.3 Fritchman Model

Hidden Markov Models are commonly used in many applications such as: control theory, automatic speech recognition, queuing theory, weather prediction, digital signal processing, modeling of burst error channels, and several other interesting applications.

Fritchman model was proposed by Fritchman [5], where he described a simple Markov chain model for modeling of digital data channels. In the proposition, an assumption of a binary channel was made which implies that a correct bit symbolizes a noise free occurrence while on the other hand the error bit depicts the presence of noises.

Based on broad literature review on how signals are propagated on the PLC channel, a reasonable assumption that supports the use of a simple Markov chain for modeling of the PLC channel has been made. Nevertheless, PLC channels are fairly different from other simple digital channels. In the PLC channel, occurrences of impulsive noise that could lead to burst error are quite common and high. Hence, to properly describe or depict PLC channel's unusual characteristics, the partitioned Markov chain is the most appropriate and a good choice for characterization of the PLC channel.

The partitioned Markov chain model as proposed by Fritchman groups/partitions the data transmission mechanism into two states. The first state which represents an error-free transmission is regarded as the error-free state, while the other partition representing an error prone transmission is referred to as the error state. The error state is the most important state when the partitioned Markov chain is applied in modeling of digital channel because it is from this state that noise and long bursty error bits are generated. A further in-depth detail on Fritchman partitioned Markov model can be found in Section 3.6.2 and 3.6.3.

From literature, Fritchman model [5], has found its application in broad and diverse range of digital communication problems. Oosthuizen et al. [61] applied Fritchman model in the modeling of Hamming code error detection, misdetection and decoding error event. Drukarev and Yiu [62] and Knowles and Drukarev [63] modeled magnetic recording channel with the use of Fritchman Markov chain. Tsai in [64] applied the Fritchman model to the modeling of High Frequency

channels. Lotter et al. [65] utilized Fritchman modeling to model Multi User Interference (MUI) in Direct Sequence Code Division Multiple Access (DS-CDMA).

Furthermore, Swarts and Ferreira [66] and Antoni [67] also applied the Fritchman model to characterize a digital fading VHF channel. Garcias-Frias and Crespo [68] utilized this form of hidden Markov model for burst error characterization in indoor radio channels.

Finally, some recent applications of the popular Fritchman model to solve digital communication problems could be found in [69-71].

2.4 Baum-Welch Algorithm

The need for techniques which is robust and fast for fitting hidden Markov models to experimental data (training) is highly required. This is because methods such as conjugate gradient, Newton-Raphson (which are standard statistical techniques of maximum likelihood parameter estimation) are not robust, hence difficult for HMMs parameter fitting. In contrast, the Baum-Welch algorithm presents a robust method of HMMs parameter fitting.

Baum et al. [7], proposed a principle which forms the basis for the effectiveness of an iterative technique that takes place in utilizing maximum likelihood methodology in statistical estimation for probabilistic functions of Markov chains. They demonstrated a generalized technique useful for maximization of a function $P(\Gamma)$ with P belonging to a large category of probabilistically defined function. Refer to Section 3.7 for more detailed study of the Baum-Welch algorithm.

This proposed iterative technique is commonly used in hidden Markov model training for the estimation of the HMM parameters. Its ability to guarantee convergence to local maximum, maximum likelihood estimation despite an incomplete training data makes it popular. It also possesses superior numerical stability.

Below are some of the various applications of the Baum-Welch iterative technique.

Zhang et al. [72] utilized the Baum-Welch technique for hybrid speech recognition training method for HMM. Breuer and Radons [73] extended the common Baum-Welch algorithm to estimate the parameters of autonomous initialized stochastic sequential machines (ISSM's) to

feed forward networks of ISSM's. Kim and Wicker [74] used the Baum-Welch algorithm to solve the problem of APP decoding of single and parallel concatenated codes, by carrying out a simple extension, hence, providing channel-matching turbo decoding algorithms. Matuz et al. [75] utilized the Baum-Welch algorithm to model Land Mobile Satellite channel (LMSC), imposing some constraints on the algorithm in order to simplify the algorithm and improve its convergence.

Other recent applications of the Baum-Welch Algorithm can be found in the following references [76-83].

Chapter 3: Related Techniques

3.0 Introduction

This section presents basic background technical details of power line communication topics relevant to the work carried out in this research work. Section 3.1 gives an overview and motivation behind the PLC technology, while Section 3.2 focuses on PLC standardization and regulatory landscape. Moreover, Sections 3.3 discusses the PLC channel characteristic, while, Section 3.4 presents noise classification on the PLC channel. Section 3.5 gives details of coupling circuit and different modes of coupling available for PLC channel. Furthermore, Section 3.6 introduces hidden Markov models (HMMs), problems associated with this model and present Fritchman model which is an example of HMMs used in this research work. This chapter concludes with background details of the Baum-Welch algorithm an iterative procedure for Fritchman model parameter estimation in Section 3.7.

3.1 PLC Technology Overview

Over the last decade, there has been a rapid increase in telecommunication (telecoms) systems usage. The necessity for the emergence of new telecoms services and additional transmission capacities has prompted the need to develop new telecoms network and transmission technologies to further cater for the increasing demand of communication services and transmission capacities. Telecommunications from an economic point of view promises large amounts of revenue which is the motivating factor for large investment in this field.

Hence, high speed networks are been built by a large number of telecommunication enterprises so as to ensure the realization of various emerging telecommunication services which can be adopted worldwide. However, this investment does not reach the end customers as they are mainly provided for the transport network that interconnects different network provider's communication nodes. End customer's connection to the transport network is achieved over distribution and access networks that forms part of the overall communication system topology. The end customers or subscribers connection is physically or directly realized over the access networks. However, realization, installation and maintenance of this access networks require

very high cost, which over the years has been found to be about 50% of all network investments, being spent on the access network [84]. However, it takes longer time to realize the return on investment (ROI) because of the relatively high costs of the access network, calculated per connected subscriber. Hence, network providers seek possible low cost ways of realization of the access network [84].

Despite the deregulation of the telecommunications market in so many countries, the access networks still belong to the incumbent network providers who were former monopolistic telephone companies. This has prompted new network providers emerging in the telecommunication market to seek for other solutions of offering their own access network. Power line communications (PLC) technology offers an alternative solution that helps in the realization of the access network using the existing power supply network for communications.

The electrical power distribution network is one of the most ubiquitous networks worldwide. This network is made up of a wide universal wiring system with the primary purpose of power distribution to end user electrical household appliances. The use of this existing power line offers a communication media for data communication without the need for new cable or wiring installation. In other words, *power line communication* (PLC) technology describes a concept that utilizes the existing power line network infrastructure and cabling for the purpose of data communication. As a result of this, a cost effective and reliable communication can be built. Data is transmitted and travels over the same power line network used to supply electricity, which thus allows the existing power line infrastructure present in homes to serve the purpose of transporting data without the need for adding new wires. Therefore, power line communication technology allows the development and realization of an in-house network or providing "last mile" for telecommunication services to the end subscribers, which is achieved in a very cost effective way. This could be achieved at nearly no investment of universal infrastructure with many wall outlets.

Due to increasing research interest in this field, PLC technology is experiencing rapid growth and is been utilized in multiple commercialized applications and different market segments; this includes lighting control, smart grid, in-home automation, solar panel monitoring, electric cars and energy metering to mention but few. The global agitation for energy conservation is one of the driving forces propelling the need for intelligent systems (e.g. intelligent communication with

energy generation and devices that consume energy). PLC provides an unequaled no-new-infrastructure approach that can enable rapid deployment of in-home automation and smart or intelligent energy management technology available around the world. Power line communication is not faced with the problem of line-of-sight and short transmission range limitations like its wireless counterpart and it is cost-effective and easy-to-install for so many applications. The three main classes of Power line technologies are discussed as follows.

Ultra-Narrowband PLC Technology (UNB-PLC): The UNB-PLC technologies is operational in the ultra-low frequency range between (0.3-3 kHz), achieving a very low data rate at approximately 100 bps and has a very large operational range/coverage of (≥150 km). In this class of PLC technology the data rate per link is low but various forms of effective addressing and parallelization possessing dependable scalability is utilized by deployed systems. The UNB solutions have been deployed by power utilities and have been in the market for over two decades making it a mature technology despite been proprietary. A historic use can be found in its utilization in the following application: RCS (Ripple Control System), which is a one way communication link for load control support application, extremely low speed (0.001 bit/sec) Automatic Meter Reading (AMR) Turtle System, and TWACS (a Two-Way Automatic Communication System) [85-87].

Narrowband PLC Technology (NB-PLC) The NB-PLC technologies operate at Very Low Frequency (VLF), Low Frequency (LF) and the Medium Frequency band (MF), which all falls between the (3-500 kHz) frequency range. The narrow band frequency includes the CENELEC band (3-148.5 kHz) defined by the European Standard, the United States Federal Communications Commission (FCC) band which ranges from (10-490 kHz) and the Japanese Association of Radio Industries and Businesses (ARIB) band falling in the frequency range between (10-450 kHz). The NB-PLC is further categorized into two as follows:

Low Data Rate (LDR): These are Single carrier technologies with achievable data rates of few kb/sec. Devices that operates at Low data rates conforms to various standards and recommendations such as X10, LonWorks, CEBus, BacNet and other protocols recommended are typical examples of LDR NB-PLC technologies.

High Data Rate (HDR): These are multicarrier technologies with achievable data rates ranging between tens of kb/sec to 500 kb/sec. Devices that operates at High data rates conforms to various ongoing standards such as ITU-T G.hnem, PRIME, G3-PLC and IEEE 1901.2 are typical examples of HDR NB-PLC technologies [85-87].

***Broadband (BB) PLC Technology (BB-PLC)*:** The BB-PLC technologies are PLC technologies that operate at both High Frequency (HF) and Very High Frequency (VHF) and there frequency band ranges between (1.8-250 MHz) with achievable data rates also referred to as PHY rate ranging from Mb/sec to several hundreds of Mb/sec. Devices that operates and conforms to HomePlug 1.0, IEEE 1901, Gigle MediaXtreme are typical examples of BB-PLC technologies [85-87].

3.2 PLC Standardization and Regulatory Landscape

This section discusses and addresses the subject of standardizations and regulations in the PLC landscape. It gives a brief overview of the PLC standards in Section 3.2.1, and goes ahead to discuss some of the current Narrowband PLC standards available in Section 3.2.2 and concludes with CENELEC Standard and Band Classification in Section 3.2.3.

3.2.1 Overview of PLC Standardizations and Regulations

In order to ensure that PLC operates in a healthy environment and the system itself does not hinder the smooth operation of other communication technology, there is need for standardization. Several standard bodies and groups exist with many established standards that are meant to provide guidance and regulate the operational specifications of power line communication system. These bodies are still actively working towards more PLC standards to create a healthy environment for PLC technology and also ensure interoperability with other communication systems. The European Committee for Electro-technical Standardization (CENELEC) [88], is the standard body that governs regulatory rules in Europe and operates in the frequency range of (3-148.5 kHz), while the Federal Communications Commission (FCC) governs in the Northern America and operates in the frequency range of (10-490 kHz) [89], and the Japanese Association of Radio Industries and Businesses (ARIB) operates at (10-450 kHz) frequency range.

The need for these regulatory bodies in power line communications field is prompted and motivated by the fact that the PLC devices that transmit over the power line networks are electrical equipment which is then used for communication purposes. Therefore, Power line Communication is categorized under both telecommunication and the electric field. Hence, to prevent interference from and to other communication systems, the power line channel, PLC products and services must adhere to and work under certain operational regulations such as, electromagnetic compatibilities, electric safety and nets and communication services [90]. The various standard regulations under these three operational regulations are discussed briefly accordingly.

Electromagnetic capability: The standard regulation described in the CENELEC EN50065 standard addresses the subject of electromagnetic capability for narrowband application (low frequency, low data rates application like a typical in-home or in-building automation). Part 1 of this standard regulation also specifies the allowable limit for conducted disturbances at the main port in the frequency range (3-148.5 kHz).

Electric safety: According to the European standards *73/23/EEC, 93/68/EEC* and *EN 60950* governing the European community, it is specified that all equipment and appliances which are connected across the power line networks should be in total adherence to the low voltage directives. This is to ensure the safety of power line devices and information technology equipment using the power line network as a communication medium.

Nets and communication services: The *2002/19/EC* (Access Directive), *2002/20/EC* (Authorization Directive), *2002/21/EC* (Framework Directive) and *2002/21/EC* (Universal Service Directive) are European directives that deal with regulations implied by their name under the Net and communication services. The access directive addresses issues on access to, and the interconnection of electronic communication networks and other associated facilities. Moreover, the authorization directive deals with issues relating to services and electronic communications network authorization, while, the framework directive specify a common regulatory framework for the use of electronic communications networks and services. Finally, the universal service directive takes care of issues relating to universal services and users' right to electronic communication networks and services.

The major international standard bodies saddled with the responsibilities of regulating and approving standards in different existing areas by producing international standards for electronic and telecommunications equipment [91], are highlighted and briefly discussed as follows.

The International Electro-technical Commission **(IEC)** came into existence in 1906 and was responsible for the preparation and publishing of international standards for all electrical, electronics and related technologies [92]. All national standards are guided by the IEC standard.

The International Special Committee on Radio Interference **(CISPR)** is responsible for promotion of international agreement that pertains to the subject of radio interference therefore encouraging international trade. The CISPR standard body produces standards that protect radio reception from various interferences sources which includes but are not limited to electricity supply system, electrical appliances, and broadcast receivers. They also address issues on the methods and equipment used in the measurement of interference emanating from both electric and electronic equipment operating above the 9 kHz frequency band [93].

The International Organization for Standardization **(ISO)** came into existence in 1947 and is constituted of 140 national standard bodies from 140 different countries in the world. They are responsible for promoting worldwide development of standardization and other related activities [94].

The International Telecommunication Union **(ITU)** is saddled with the responsibility of creating telecommunication standards, as it also adopts international regulations and agreements. The ITU became a specialized agency of the United Nations in 1947 but was originally founded in 1865. Furthermore, ITU allows global telecommunications networks and services to be coordinated by both the private sector and government [95].

Other relevant standard bodies include: *American National Standards Institute* (ANSI) [96], *Electronic Industries Alliance* (EIA) [97], *Institute of Electrical and Electronics Engineers* (IEEE) [98], *European Telecommunications Standards Institute* (ETSI) [99], *Information and Communications Technologies Standards Board* (ICTSB) [100]. The first three aforementioned are American bodies while the latter two are European bodies. A detailed and comprehensive up-

to-date review of PLC standards can be found in [101]. The next section focuses on latest standards that are developed for narrowband applications.

3.2.2 Narrowband PLC Standards

This section describes briefly some of the standardization developments that are taking place in the narrowband PLC landscape.

***LonWorks*:** The ANSI/EIA 709.1 standard, also referred to as LonWorks was one of the first low data rate narrowband PLC standards to be sanctioned. This standard was issued in 1999 by ANSI before it metamorphosed into an international standard in 2008 (ISO/IEC 14908-1) [102]. It is a seven-layered OSI protocol that provides services that enables the application program embedded in a device to transmit and receive messages from other devices present in the network without prior knowledge of the network topology and/or the functions of this other devices. The LonWorks technology is now an open standard which is used worldwide because of its interoperability. It can be configured for use in electric utility applications making use of the CENELEC A-band. On the other hand, industrial, commercial and in-home application uses the C-band. Other multi-applications include but are not limited to: Smart Buildings (HVAC controls, elevators/escalator controls, irrigation, lighting and security); Smart Cities (Street lighting, buses and subway systems, theater and stage lighting); Smart Grid (Advanced metering, demand response, and distribution automation) [103].

***Power line Related Intelligent Metering Evolution* (PRIME):** This standard came into being as a result of the growing interest in exploiting high data rate narrowband PLC solutions that operates in the FCC, CENELEC, and ARIB frequency bands. This standard is fast becoming popular and gaining the support of European industries. PRIME has established and specified an Orthogonal Frequency Division Multiplexing (OFDM) based high data rate narrowband-PLC solution that operates and makes use of the CENELEC A-band frequency. PRIME initiative has capacity of PHY data rates up to 125 kb/s and it is an open standard [104]. Another high data rate narrowband PLC initiative similar to the PRIME initiative is the G3-PLC discussed below.

G3-PLC: Just like PRIME, G3-PLC is an open standard. It is an OFDM based high data rate narrowband-PLC that promotes interoperability as it can coexist with IEC 61334 and IEEE P1901.2. It operates in the 10-490 kHz frequency range thereby complying with CENELEC,

FCC and ARIB. It has also got built in robustness as it possess two layers of forward error correction and a robust mode that overcomes noisy channel conditions. Other key feature of the G3-PLC is cyber security as its 6LoWPAN adaptation layer supports IPv6 packets. The G3-PLC standard is useful in Distribution Automation and Smart Electricity Meters [105].

A well-articulated detail of PRIME and G3-PLC and comparison between both standards can be found in [106-107].

Other recent standards for narrowband application are the ITU-T G.hnem and IEEE 1901.2 which came into being in 2010. Details of both standards can be found in [108-110].

3.2.3 CENELEC Standard and Band Classification

CENELEC, *Comité Européen de Normalization Electrotechnique* is a European Committee for Standardization that was brought into being in 1973. It was saddled with the responsibility of preparing voluntary electro-technical standards which helped in the development of the single European Market/Economic Area for electrical and electronics goods and services [111]. It defines transmission on low voltage installation in the CENELEC EN50065-1 document [112], and makes it mandatory that power line products and services rendered by all member countries of the CENELEC organization must adhere and comply with this standard for home automation and other narrowband applications.

The CENELEC 50065-1 standard regulates all signaling within the frequency range 3 kHz to 148.5 kHz on the power line and specifically made provisions for five different categories of channels in this frequency range. The transmitted power allowed is dependent on channel specification and coupling method, but should not exceed 500 mW. Below is a table of the CENELEC band showing the band categorization, its frequency range (bandwidth), the corresponding maximum allowable transmission level limits, the access protocol utilized and the purpose of usage of the band.

Band Name	Frequency Range (kHz)	Maximum Allowable Transmitter Output Voltage [dB (μV)]	Access Protocol Utilized	Stipulated Band Usage
	3-9	134 dB (μV) ≡ 5V	No protocol required	Usage of this band is limited to energy providers and utility
A	9-95	134 dB (μV) ≡ 5V at 9 kHz 120 dB (μV) ≡ 1V at 95 kHz	No protocol required	Usage of this band is limited to energy provider and their concession-holders
B	95-125	116 dB (μV) ≡ 0.63V at 95-148.5 kHz but in exceptional cases 134 dB (μV)	No protocol required	Usage of this band is limited to energy providers' customers
C	125-140		Carrier Sense Multiple Access (CSMA) protocol using a carrier center frequency of 132 kHz	For Private use of energy providers' customers. The use of CSMA makes possible the simultaneous operation of several systems within this frequency band
D	140-148.5		No protocol required	For Private use of energy providers' customers (for Alarm and Security Systems)

Table 3.1: Overview of the CENELEC EN 50065 Standard Bands and Categorization.

3.3 PLC Channel Characteristics

Power line channel when compared with other conventional media such as coaxial cables, twisted pair cables and fiber-optic cables considerably differs in structure, physical properties and topology. It exhibits a rather hostile characteristic, as it was originally designed for power distribution at very low frequency of 50/60 Hz with no prior thought of its eventual use for high frequency data transmission.

Power line communication using this network as a medium of communication inherits the intrinsic properties and characteristics of the power line network. Hence, PLC inherits a hostile medium for its eventual use as a medium of data transmission at high frequency. PLC does not only inherit the nasty and hostile behavior of the power line network but in addition combines that of a communication channel. Variation in impedance, high attenuation as a result of

impedance mismatch, noise and disturbances present on the network or coupled unto the network are some of the main challenges PLC has to overcome to achieve its full potential and development as a reliable medium of data transmission when compared to other data transmission technology. In view of this, PLC transmission environment can be seen to be worse when compared to its mobile communication counterpart.

The channel characteristics could both be frequency and time-dependent, and there possibility of its dependence on where both the transmitter and receiver are located in the power line infrastructure. Thus, the channel is described generally as a random time varying with a frequency-dependent SNR (Signal to Noise Ratio) over the communication bandwidth.

The design of good power line communications systems demands a detailed knowledge of the channel characteristics such as impedance, noise scenario, interference and the channel capacity, which helps to design and/or choose suitable methods of data transmission. These channel characteristics are discussed briefly in the following section and literatures are referenced for a detailed and comprehensive knowledge of these channel characteristics.

3.3.1 Impedance

Impedance is one of the channel characteristics important in the design of PLC systems as impedance variation has a great effect on the PLC systems performance. Power line as a medium of communication has reflections and signal attenuation that is induced by its impedance properties.

Varying impedance on the PLC channel is one of the challenges PLC technology has to combat as it affects the performance and reliability of data transmission on the channel. The power line channel comprises of interconnection of wires or cables having different sizes and varying impedance value forming a branch in the power line topology. This variation in impedance of the wires and cables could lead to a phenomenon referred to as impedance mismatch resulting from unbalanced impedance [113]. Consequently this phenomenon leads to reflection, attenuation and multipath fading of signal transmitted on the PLC channel. Moreover, impedance mismatch is not only caused by the varying wires and cable impedance alone but also the impedances of several electrical loads connected onto the PLC channel have a great effect on signal attenuation [114]. The varying impedance encountered on the PLC channel is dependent upon frequency and

time the electrical loads are active on the network. Hence, the impedance that the transmitted signal encounters on the PLC channel has a great effect on the signal power the transmitter can couple onto the PLC channel.

Furthermore, single phase line act predominantly as inductive loads, with the magnitude of impedance value increasing with frequency, in the frequency range below 100 kHz (impedance increase from 1-2 ohms at 10 kHz to 10-20 ohms at 100 kHz has often been experienced) [114]. Apart from acting as inductive loads, the single phase line also possess distinctive capacitance of 30-60 pF/m, and a corresponding inductance of 0.3-0.6 μH/m and also, a resistance value of 0.04 ohm/m with a resultant impedance of between 75-150 ohms [114], [115].

The major electrical appliances commonly found in homes are majorly resistive and reactive loads. The major resistive loads prevailing in the lower frequency region often found in homes include but are not limited to this list: cloth dryers, incandescent lights, and electric heaters. On the other hand, reactive loads commonly found in homes include appliances or devices such as TV, PC, and motors prevailing in the higher frequency region of the spectrum [114]. Consequently, varying load impedance and cable/wire impedance often results to varying signal power, which consequently degrades the performance of the PLC. Signal power transmitted can be improved if and only if the impedance encountered by the signal on the PLC channel matches that of the transmitter, otherwise impedance mismatch takes place resulting in signal attenuation. Hence, it is important that the coupling circuit designed for signal injection has impedance adaptation attribute to prevent insertion loss and impedance mismatch. For instance, the bidirectional impedance-adapting transformer coupling circuit for low voltage power line communications designed in [113] was meant to achieve maximum signal transfer and prevent impedance mismatch.

Conclusively, modeling of the power line impedance helps in understanding the obscure nature and behavior of power line that changes at the connection of different loads across it. Network topology and loads connected across the network have a great effect on the network impedance. To combat these drastic impedance conditions on any power line channel PLC solutions must possess a low transmit impedance and on the other end a high receive impedance so as to ensure maximum voltage signal transfer or maximum power transfer between the two ends.

Summarily, the net or total impedance encountered on the power line channel is often influenced by the network topology and is a combination of the various impedances namely *impedance of the distribution transformer, load impedance or impedance of devices connected to the power line network and characteristic impedance of the various inter-connects of cables used in the power line network* [40].

3.3.2 Attenuation

The injection of high frequency signals unto the power line network can be achieved through a suitable high pass filter known as coupling circuit. The signal received at the receiver will be maximized if and only if the power line, transmitter and the receiver impedance are matched. Otherwise an impedance mismatch leads to a phenomenon called *attenuation*. Unlike other dedicated communication channels such as Ethernet which uses coaxial cables with known impedance, thus not faced with impedance matching problem, PLC channel is plagued with impedance mismatch problem. This phenomenon occurs due to the fact that power line networks are made up of variety of conductor types, with differing cross-sectional area which are joined almost at random. Hence, an extensive variety of characteristic impedances is encountered over the network as earlier discussed in Section 3.3.1.

Often, low impedances of the LV power line channel results in high signal attenuation. The impedance mismatch that occurs between the transmitter, PLC channel and the receiver are often triggered by the time-variant loading activities that occur on the channel. Consequently, this contributes vastly to high attenuation of signals often experienced, hence rendering the attenuation also time-variant. High attenuation experienced on LV PLC channel most times necessitates positioning of repeaters at distance of less than 1 km. On the contrary, HV PLC channels do not experience high signal attenuation as their LV counterpart does, as data communications at long distances in the range of hundreds of kilometers without repeaters have been achieved [117]. An analysis of signal attenuation on medium-voltage power line networks is given in [118]. Below is an overview of some factors that influence signal attenuation on PLC channels [116], [119].

Signal Attenuation Dependency on Time: Time of the day is one of the factors that influence the severity of signal attenuation on PLC channel. In reality, signal attenuation and network

impedance have a very close relationship. Hence, based on the fact that network impedance is time-dependent, such a dependency on time must be taken into consideration for signal attenuation investigation. The fact that several electrical appliances are active on the PLC channel during the peak period (daytime) results in firm day and night sensitivity. Hence, high attenuation will often occur during the day due to numerous active appliances during this time [116].

Signal Attenuation's Dependency on Frequency: Based on measurement reported on the Canadian LV power line network [43], it was observed that signal attenuation is independent of frequency for frequencies below 100 kHz while on the other hand, signal attenuation increase of 0.25 dB/kHz were observed for frequencies above 100 kHz. Signal attenuation is capable of rising extremely high at certain frequencies of cable length greater than 400 m as a result of transmission line effects [116].

Signal Attenuation's Dependency on Distance: Based on principle, signal attenuation is presumed to be linearly dependent on distance, and so far no loads exist between the data communication transmitter and the receiver. On the contrary in practical situations, several loads are often connected between the transmitting and receiving device with worst-case occurrence of signal attenuation of around 100 dB/km frequently recorded [116].

Signal Attenuation over Differing Network Phases: The impedance between two power line phases strongly defines the signal attenuation experienced between the two phases. According to [119], the signal attenuation experienced between two points that are connected unto the same phase is oftentimes smaller than that experienced between two points at the same distance but connected unto differing phases [116].

3.3.3 Noise

The CENELEC A-band remains the most noise susceptible band amidst the four standard CENELEC PLC frequency bands. Electrical appliances which draw their supply from the 50 Hz electric supply constitute the major sources of noise present on the power line network. These electrical appliances generate noise components which are injected unto the power line and such noise component extends into the high frequency spectrum. Other sources of noise that affects the power line network are noise coupled unto the network from various broadcast station and

spurious disturbances from other unknown such which impair certain frequency bands of the power line network. Generally, the characteristic of this channel noise varies strongly with frequency, load, time of the day, and source and geographical location [121].

In summary, the technical problems/challenges which the power line channel suffers from, that requires adequate attention in order to achieve a reliable PLC system are mentioned as follows: *unavailability of earthed neutral, low impedance characteristics of the grid which requires a very high transmit power, limitation in distance that could be covered due to high attenuation characteristic of the power line medium, impedance variation which occurs as a result of non-linear loads, significant changes of impedance over long durations caused by the ON and OFF switching of various loads connected across the network and varying high interference characteristics due to various noisy loads and noise injected into the network from other source* [122].

The three major types of noise believed to be present on the PLC channel are Background noise, Narrowband noise and Impulse noise. Refer to Section 3.4 for detailed description of the three major noise categories.

3.4 Noise Classification on PLC Channel

In contrast to many other available communication channels, power line noise cannot be described as an additive white Gaussian noise (AWGN) model, therefore a thorough understanding of power line noise is inevitable for an appropriate modeling of the noise which in turns helps in design of a power line system that achieves optimal performance. Noise is a major problem that has effect of data transmission on the power line. This is because the properties of this noise are not similar to the AWGN which can be easily analyzed.

Researchers have over the years categorized noise present over the power line network into five major categories. These literatures not only discuss types of noise present on the power line but also study the noise characteristics, distribution of duration, inter-arrival time and the amplitude of impulsive noise experienced on the power lines [123-127]. According to these literatures, noise on power line can be classified into five categories namely; Narrowband noise, Colored background noise, Periodic impulse noise synchronous with main, Periodic impulse noise asynchronous with mains and Asynchronous impulse noise as represented in the figure shown

below. Some of the major noise sources that affect communication over PLC channels are: light dimmer, universal motors, television receivers and computer monitors, microwave oven, air-conditioners and several other electrical appliances connected to the PLC channel.

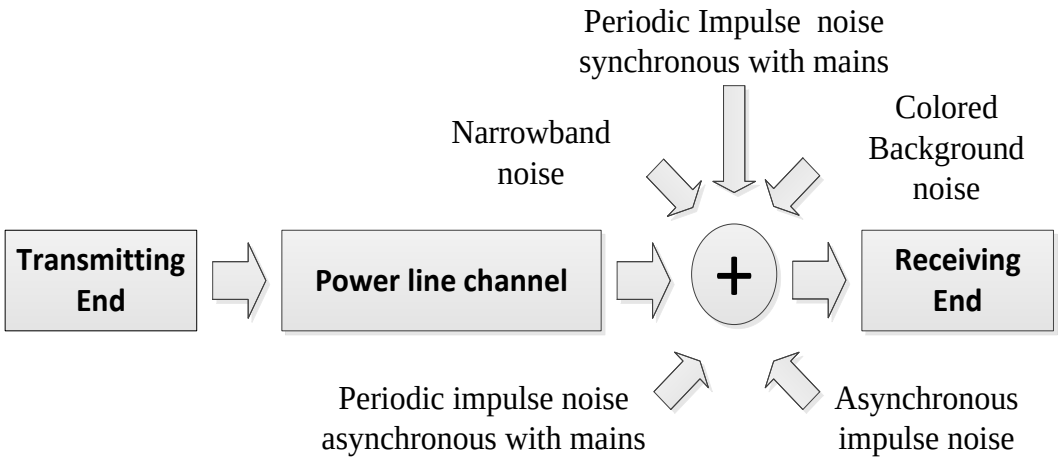

Figure 3.1: The Five Major Categories of Noise Present On the PLC Channel.

Further research has gone ahead to categorize noise on PLC channel into three major classes, the Background noise, Narrowband noise and Impulse noise. The noise model is further reduced to a simpler model as shown in the figure below.

The properties, sources and behavior of these three major classes of noise are further discussed accordingly in the following sections.

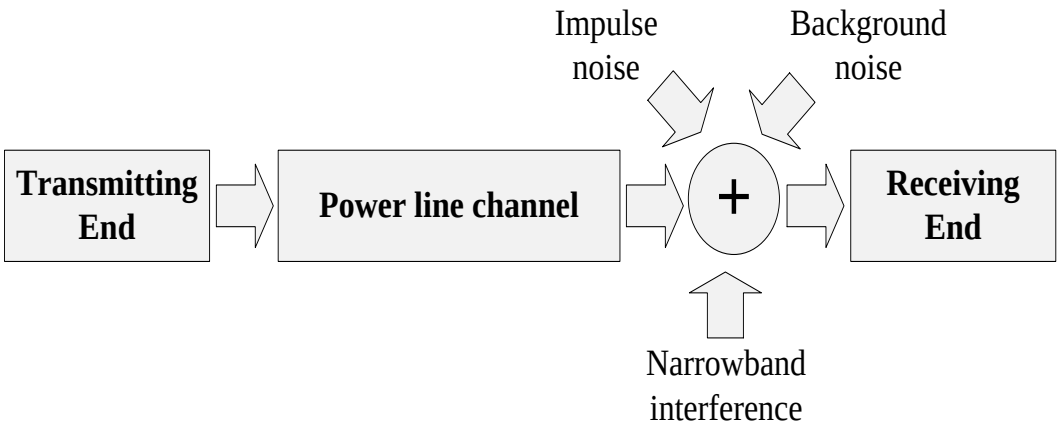

Figure 3.2: Simple PLC Noise Model Showing the Three Major Noise Classifications.

3.4.1 Background Noise

This type of noise is frequently characterized by constant envelope for a long duration (at least more than a few cycles of mains AC voltage) [128]. Background noise frequently includes flicker noise, thermal noise resulting from front-end amplifiers of receivers, and noise from universal motors often found in household electrical loads such as electric drilling machines, mixers, hair dryers, fans etc. Background noise (BN) is assumed to be cyclo-stationary in nature, possessing relatively low PSD emanating from a combination of numerous low power sources. By definition, background noise is quantifiable in the absence of other dominant noise sources and varies with frequency. Background noise often exists permanently on the PLC channel and non-whiteness is its most vital attribute, which implies that the PSD is frequency-dependent. In the CENELEC A-band frequency range (3-95 kHz), the PSD of the BN decays with increasing frequency having a slope of 20-25 dB/decade for an in-home environment [121]. This type of noise is mainly present in low frequencies allocated to PLC than in the high frequencies [129].

3.4.2 Narrowband Noise

This noise type normally occupies narrow portion of the frequency band of the spectrum under consideration. A typical example measured in this research is shown in Figure 4.3. Narrowband noise originates from sinusoidal signals that are coupled unto the PLC channel via radiation from amateur radios or broadcast stations sharing the same frequency spectrum with the narrowband PLC channels and system. It has also been reported that narrowband noise often originates from the horizontal retrace frequency of TVs. The horizontal retrace frequency for the European PAL TV system is 15.6 kHz and consequently, observation of some narrowband disturbances are often recorded at harmonics of this horizontal retrace frequency. Other narrowband noise sources are spurious disturbances that emanate from the various electrical loads having inbuilt transmitter and receiver. The severity of narrowband disturbances often varies depending on time of day [121], [128].

3.4.3 Impulse Noise

Despite the fact that this type of noise is transient in nature, it has been reported to be the major source of long bursty errors observed on the PLC channel. Unlike the narrowband noise which is confined to a narrow portion of the frequency band of interest, impulse noise occupies and

spreads randomly over a larger part of the frequency band of interest as a result of its high PSD. A typical impulse noise measured in this research is shown in Figure 4.4. Impulse noise is often characterized by its duration, magnitude, and inter-arrival time. Impulse noise is further classified into two categories as described below [126-128].

Periodic impulsive noise synchronous with the mains: This category of impulse noise is mainly regarded as a cyclo-stationary noise. The noise waveforms possess a train of impulses synchronous with the 50/60 Hz AC mains frequency or twice this frequency. Sources of this category of impulse noise include power supplies with silicon controlled rectifier and light dimmers with thyristors. In the case of the light dimmer, noise impulse synchronous to the AC mains voltage is been switched unto the PLC channel while the light dimmer is controlling the brightness of a light (it switches the AC current based on its phase). This noise type also originates from the commutating effect that occurs in a brush motor.

Periodic impulsive noise asynchronous with the mains: This noise type is also cyclo-stationary because it exhibits underlying period which is same as that of the mains. It has been conventionally considered to occur as a result of periodic impulse with repetition rates between 50-200 kHz and is typically caused by transient switching that occurs in power supplies. Consequently, because of this high repetition rate, a spectrum constituting discrete lines results with the frequency spacing based on the repetition rate [45].

A novel approach of modeling this kind of noise can be found in [130].

3.5 Coupling Circuit

The coupling circuit is not just a piece of circuit but a vital part of the PLC system. It is the interface circuit that is used to couple signals unto the PLC channel. Hence proper care must be taken when designing this circuit as it must adhere to operating standards set by PLCs international regulatory bodies. A coupling circuit is designed as a peculiar filter (band-pass filter) [114], [131] with the primary aim of coupling the signal unto the network, while it also blocks and filters the AC mains power waveform but allows PLCs high frequency communication signals to pass. A careful consideration of its constituent components must be made so as to overcome the challenging characteristic the PLC channel possesses. The coupling circuit must also be designed to provide galvanic isolation and on the other hand prevent excess

voltage from entering the sensitive measuring equipment used in noise data capture. Most importantly this circuit must be able to withstand and adapt to the varying impedance experienced on the PLC channel hence preventing insertion and coupling losses.

3.5.1 Coupling Circuit Modes

There are several ways of realizing the coupling communication signals unto the PLC channel. As spelt out in [114], [128] and [132], coupling circuit design can be realized through the use of two different closed current paths, namely, the common mode coupling and differential mode coupling which are further discussed in Section 3.5.1.1 and Section 3.5.1.2 below.

Differential Mode Coupling

This coupling mode requires the live terminal to constitute a terminal while the neutral terminal is utilized as the second terminal. This coupling mode is realizable and implementable with the existence of neutral terminal as we have in LV power line networks. On the contrary, differential coupling mode is not realizable and implementable on MV and HV power line networks due to the unavailability of a separate neutral line. Alternatively, though not recommended most often the ground (earth terminal) constitutes the second terminal in such cases [114], [128], [132].

Common Mode Coupling

The common mode coupling involves the interconnection of both the line (live) and neutral terminal to constitute one terminal while the ground (earth terminal) becomes the second terminal. This mode is unachievable theoretically, based on the fact that the ground and neutral wires are always connected at the transformer point. On the contrary, it is practically achievable because the inductance which exists between the coupling points and the short circuit point is big enough to outsmart this problem. This mode of coupling is preferred over its differential mode counterpart because of the 30 dB better coupling that it yields. In some countries, common mode coupling is highly prohibited on the LV power line network as a result of the danger it poses to end users. A solution to this danger is designing the input current not to exceed the sensitivity of the earth leakage protection device (30 mA for LV applications) present at the location where the coupling circuit is to be used. For the physical implementation of coupling circuit, there exist two possible ways of realizing this as described briefly below in Section 3.5.1.3 and 3.5.1.4.

Capacitive Coupling

In capacitive coupling mode a capacitor is basically used to impress or couple the communication signal unto the network. This is achieved by modulating the communication signal unto the network's voltage waveform. A capacitive coupling interface is connected in parallel to the power line network. It is an affordable and compact interface commonly used in LV applications such as AMR and other in-home applications [114], [128], [132].

Inductive Coupling

In this case the use of an inductor is utilized to impress and couple the communication signal unto the network. It is achieved by impressing the communication signal unto the network's current waveform. Inductive coupling circuit is connected in series with the loads in the power line network. This inductive coupling has been reported to be rather lossy. Nevertheless, since no physical connection is made with the power line network, this coupling mode is safer to implement than its capacitive coupling counterpart [114], [128], [132].

Capacitive coupling is mainly utilized on LV power line network due to power restriction (there is a maximum allowable power) on the LV network. Both inductive and capacitive coupling modes are allowable on MV power line networks.

3.5.2 Coupling Circuit Components Selection and Functions

In order to convey communication signals on a power waveform of the power line network, careful consideration must be taken in designing and interfacing both the power circuitry and the communication circuitry so that these two systems are optimally compatible as they both operate at differing extremes. Power systems typically operate at very low frequencies and very high power, current and/or voltage levels while on the other hand, communication systems operate at a very high frequencies and low power, currents and voltage levels [133], [134]. To design a proper interface (coupling circuit) that will achieve optimal compatibility between the power and communication systems, a fundamental understanding of the various components and circuitry for these systems capabilities at the two differing extremes must be carefully considered. Also, analysis of the performance of the coupling circuit can be done based on the following criteria: signal attenuation at the transmitter and receiver, over-voltage protection, galvanic isolation and both the installability and reliability of the coupling interface.

Coupling Capacitor

The coupling capacitors are to a large extent used in PLC to superimpose or couple the communication signal onto the power line [135]. They also constitute a part of more advanced high-order filters [136]. Coupling capacitor's basic and fundamental characteristics are well stated and standardized in ANSI C93.1-1972, [137]. These capacitors are required to be high-frequency capacitors (with self-resonant frequency being higher than the modulation frequency) since they carry the communication current [138]. Conversely, the coupling capacitor will have to be able to act as a filter, filtering the power voltage that is dropped across the component. It must also be able to prevent the effect of voltage surge and therefore need to be a high-voltage capacitor. According to [139], the coupling circuit filtering characteristics are to a degree dependent on electrical loads onto which the waveform terminates.

Coupling Transformer

The coupling transformer functions mainly to provide a galvanic isolation between the PLC equipment and the power line network (to prevent damage of the sensitive PLC equipment), as it also provides impedance adaptation (which is necessary due to the varying impedance that exists between the power line itself, loads connected across it and impedance of the PLC equipment). But, it also has to be designed to be able to pass the high-frequency communication signal freely and unhindered. Regrettably, the power waveform operates at much lower frequency and much higher voltage. Hence, the power waveform would have a saturating influence which is at least 10^5 when compared to the communication waveform [133]. Consequently, it is highly essential that the power waveform is first low-pass filtered before entering the coupling transformer [133], [138].

Zener Diode

A zener diode serves as a voltage regulator by regulating the voltage in the coupling circuit and also prevents the entry of excess voltage (over-voltage) from passing through the circuit and damaging sensitive measurement equipment.

Resistor

In the general design of coupling circuits, the use of resistors is often been avoided as it implies a loss of power, which can either be of the communication signal or power waveform.

Nevertheless, in the coupling circuit designed for carrying out measurement in this research, a resistor is used across the capacitor as a discharge resistor.

3.5.3 Transformer-Capacitor Coupling Circuit Design

Transformer-capacitor coupling circuits are used extensively in LV power line communications [138], [139], mainly because: *The transformer provides galvanic isolation from the power line network and the transformer acts as a limiter when saturated by high-voltage transients.*

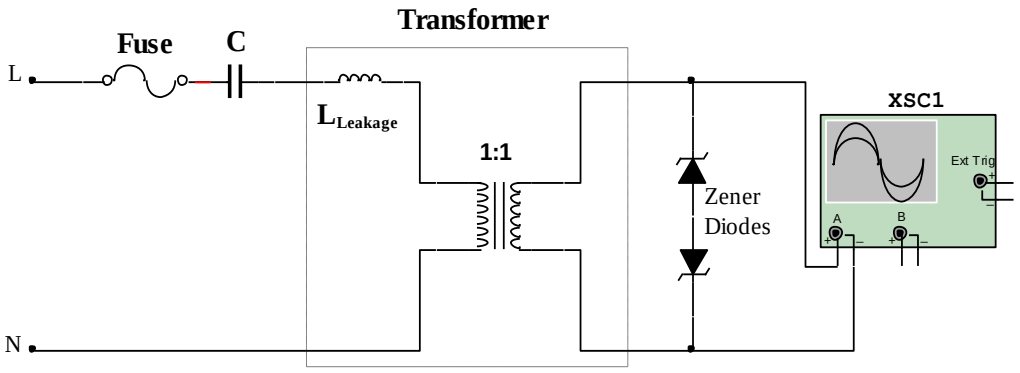

Figure 3.3: Coupling Circuit Schematic.

Figure 3.3 above shows the schematics of the coupling circuit. A 1:1 transformer winding ratio was used for transparent measurement of noise. A high-voltage, high frequency capacitor rated 0.1 µF, 250 VAC and 400 VDC was used to realize a high-order filter and couple the noise signal unto the measurement equipment for capture while blocking the low frequency power signal [135], [136]. The primary side (live and neutral terminals) is connected to the power line outlet, while the secondary side is connected to the BNC connector to connect the coupler to the oscilloscope for noise data capture.

As earlier stated the zener diode serves as a voltage regulator and overvoltage protection. It is typically connected in reversed bias and in parallel with the load as seen from the schematic. It regulates output voltage by keeping it constant (stabilized) regardless of varying load conditions and changes in the source voltage which is typical of the power line network. The back to back connection of the zener diode makes it act as a clipper which symmetrically clips the peaks of waveform at approximately the zener voltage of the zener diode. Therefore, for the circuit it clips at nearly 10 V which is the zener voltage of the zener diode used in the coupling circuit. Figure 3.4 below shows the connection of the low-cost coupling components used in designing the

transformer-capacitor coupling (coupling capacitor, discharge resistor, coupling transformer, zener diodes, and fuse). The coupling circuit is neatly packed in a three-pin plug as shown below.

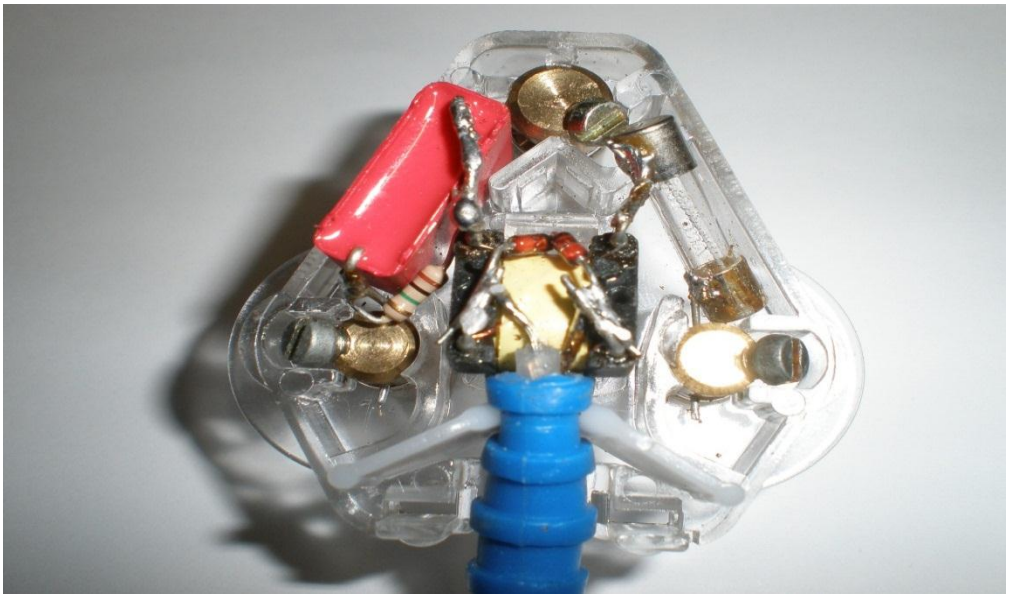

Figure 3.4: Coupling Circuit Neatly Packed In a Three-Pin Plug.

Figure 3.5: Coupling Circuit Showing the Final Termination with a BNC Connector.

Figure 3.5 shows the final termination of the coupling circuit with a 75Ω coaxial cable and a BNC connector for end connection to the oscilloscope. (The 3-pin plug side is end point connection to the power line network, while the BNC connector side is the end pint connection for coupling of the noise signal unto the oscilloscope for noise data capture).

After the completion of the coupling circuit design it is highly essential to measure the transfer function of the circuit to ascertain that it acts as a band pass filter for the frequency band it is to be used for. Figure 3.6 shows the transfer function measurement of the coupling circuit to ascertain its performing its function as a band pass filter. Take note of the linear frequency axis, and the band-pass filtering for CENELEC bands.

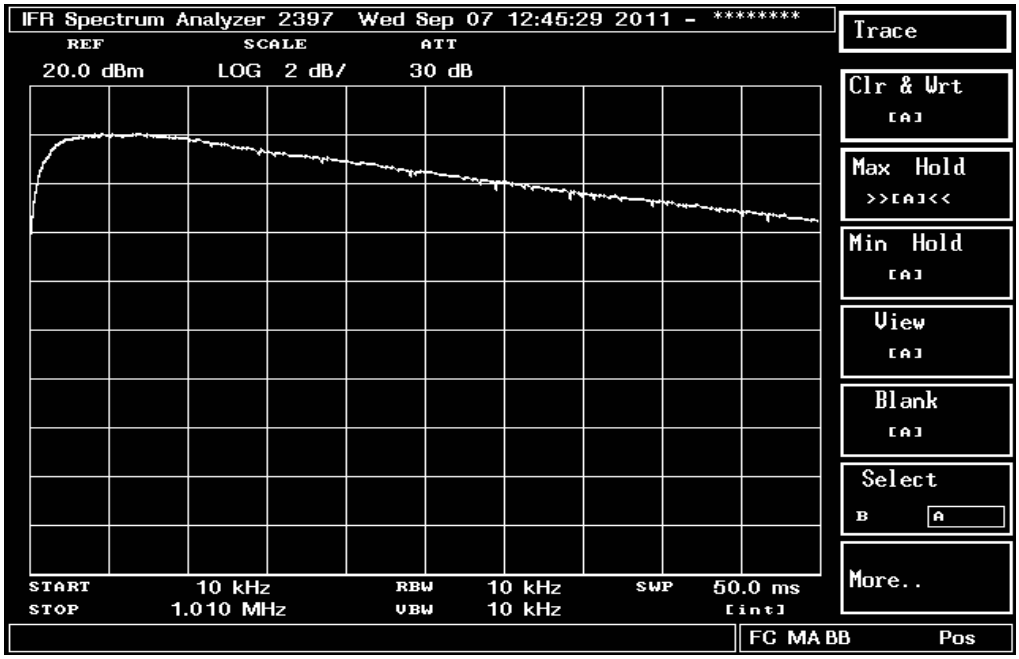

Figure 3.6: Transfer Function of the Coupling Circuit.

In order for the coupling circuit to reliably perform its function it must adhere to the following: Total adherence to the CENELEC standard on the allowable bandwidth, maximum allowable transmitted power and transmitted level limits (dB (μV)), the coupling circuit must act as a band pass filter allowing high PLC frequency to pass but block the mains 50 Hz supply. It must also provide galvanic isolation and surge protection and insertion and coupling losses must be avoided by making sure the coupling circuit has impedance adaptation characteristics to compensate for the varying impedance encountered on the power line.

3.6 Hidden Markov Model

According to Rabiner [140], hidden Markov model (HMM) is a twofold manner stochastic process having an underlying stochastic process that is hidden (not observable). Another set of stochastic process is needed to make it observable and this stochastic process gives the sequence of observed symbols.

Before a discussion of Fritchman model which is an example of an HMM, it is highly essential that the basic characteristic of HMM be spelt out. According to Rabiner [140] and [141], there are five major attributes that characterizes an HMM namely;

N, which represents the number of finite states in a given model. Where $S = \{S_1, S_2, S_3, \dots S_N\}$ describes the set of possible states, which is the at time *t* denoted by s_t *or* q_t.

M, which denotes the number of distinct or unique observation symbols per state. In other words, it is a representation of the distinct alphabet size of the output symbol. $E = \{e_1, e_2, e_3, \dots, e_M\}$ refers to all possible output symbols set, where O_t denotes the output symbol at a given time *t*. The observation symbol sequence is denoted by $O = \ O_1, O_2, O_3, \dots, O_T$. Where *T* is the length of the observation sequence.

A, denotes the state transition probability distribution, where $A = \{a_{ij}\}$ and a_{ij} is the probability of transitioning from state *i* at time *t* to state *j* at time *t+1* and it is denoted by the notation $a_{ij} = \Pr(s_{t+1} = j \mid s_t = i)$, with $1 \leq i, \ j \leq N$.

B, The output symbol probability distribution in *j* state. It can also be referred to as observation symbol probability and emission probability distribution. It is represented by the notation $B = \{b_j(e_k)\}$, which is the probability that the error symbol e_k occurs given that the model is in state *j* and at time *t* denoted by $b_j = \Pr(e_k|s_t = j)$, $1 \leq j \leq N$, $1 \leq k \leq M$.

Finally, π which represents the initial or prior state probability. It is the prior probability of being in state *i* at the start of the observations i.e. at time t=1 and it is denoted by $\pi = \{\pi_i\}$, where $\pi_i = \Pr(s_1 = i)$, $1 \leq i \leq N$.

The values of the Hidden Markov model parameters (*N*, *M*, *A*, *B*, and π) stated above can be used to generate the observation sequence given by $O = \ O_1, O_2, O_3, \dots, O_T$. But for the purpose of this

work, the observation sequence is obtained from experimental measurement data rather that simulation as will be discussed later.

3.6.1 Problems of Hidden Markov Models

There are three basic problems associated with Hidden Markov models namely [64]:

Probability Evaluation Problem: Given an observation sequence say $O = \{O_1, O_2, O_3, O_4, \dots\}$ and the model parameters denoted by Γ= {*A, B,* π}, how can we obtain the efficient computation of $\Pr(O|\Gamma)$, i.e. the likelihood of the observation sequence? The solution to this problem is given by the *Forward* and *Backward procedures of the Baum-Welch algorithm.*

Optimal State Sequence or Decoding Problem: Given an observation sequence $O = \{O_1, O_2, O_3, O_4, \dots\}$ and the model Γ, how can we choose a state sequence $Q = \{q_1, q_2, q_3, q_4, \dots\}$ that optimally explains our observation sequence? We are trying to figure out the most likely state sequence that emitted the observation sequence. The solution to this problem is given by the *Viterbi algorithm.*

Learning or Parameter Estimation Problem: How can the adjustment of the model parameters Γ= {*A, B,* π} be done to maximize the likelihood $\Pr(O|\Gamma)$? We are trying to look for the initial state probabilities, state transition probabilities and observation or error probabilities that best explain the given sequences. The solution to this problem is given by the *Baum-Welch algorithm parameter re-estimation procedure.* Hence, the introduction and description of the Baum-Welch algorithm in Section 3.7.

Hidden Markov models are a class of Markov chain models utilized in the description of bursty error channels. In hidden Markov models, it is assumed that the source that produces the bursty error is in one of the many states of the Markov chain. The error probability is also assumed to be state dependent; hence, we can only observe the error sequence while the underlying state sequence cannot be observed

3.6.2 Fritchman Model

Description of the statistical distribution of errors that occurs as a result of channel impairments is the main aim of discrete channel models. This mathematical description of the behavior of impairment and memory on the channel helps facilitate the design of good error coding strategy

that can be used on a particular channel. In this research our modeling effort is based mainly on the extensive use of the ideas centered on the hidden Markov model as introduced and discussed in [140]. In the past, modeling of discrete communication channel has been quite successful using the Markov process. A similar course is followed by applying the hidden Markov model to model PLC noise in this work.

This section presents a brief description of the Fritchman model proposed by Fritchman [5], [142-143], and it further presents a generalized Fritchman model employed for the implementation of the Baum-Welch algorithm, an iterative algorithm that will be discussed in the next section. In [5], Fritchman considered binary communication channel characterization utilizing functions of finite-state Markov chains. Fritchman derived the error-run distribution and error-free run distributions which are two distributions that are applicable to code evaluation. Furthermore, he described the partitioning of an *N*-state model into two groups of *k* error-free states and *N-k* error states, showing that the error-free run distribution general form is the weighted sum of at most *k* exponentials while on the other hand, the error-run distribution is the weighted sum of *N-k* exponentials.

Fritchman further showed the applicability of this model to characterize real communication channels by using this model for statistical representation of high frequency radio experimentally. Fritchman also showed that modeling of bursty binary channels can be done using the Markov chain models. Examples of bursty channels that can be modeled using the Markov model are channels that show an attribute of frequency fading. These channels can be modeled such that there error-free length distribution has finite exponential terms. Below is the figure of the state space partitioning.

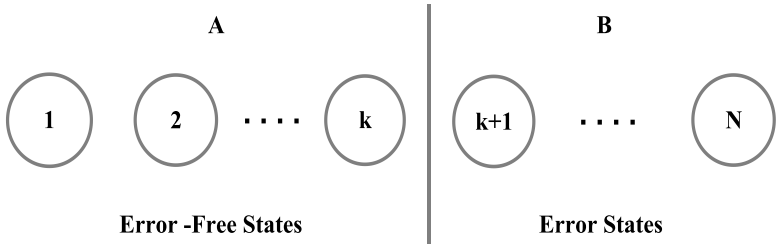

Figure 3.7: State Space Partitioning

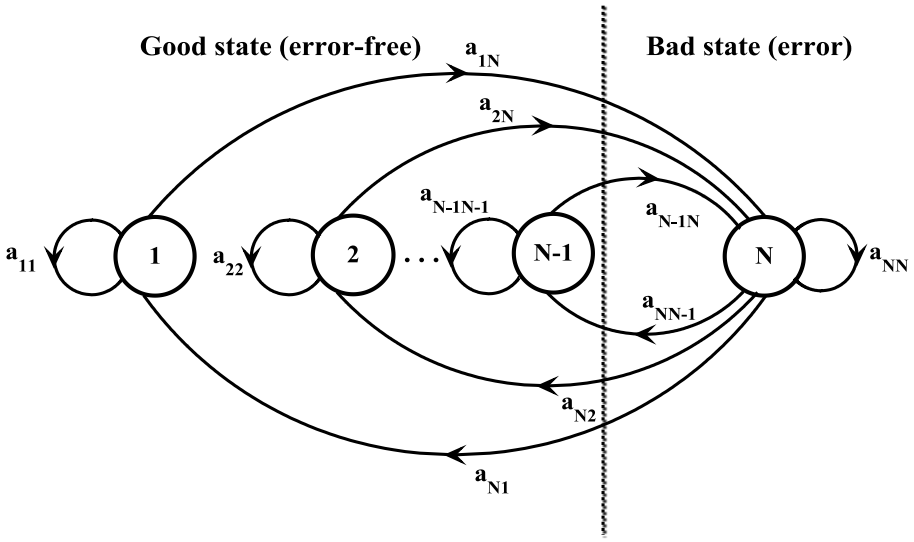

Figure 3.8: Generalized Fritchman Model

A three-state model with one error state is chosen for modeling of the noise on the PLC channel modeled in this research project because it is easier to parameterize.

3.6.3 A Three-state Fritchman Model

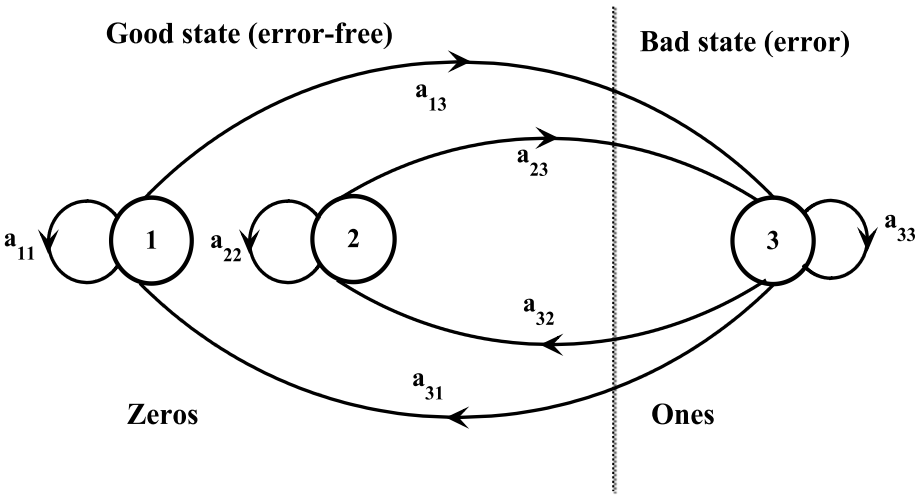

Figure 3.9: A Three-State Fritchman Model with Two Good States and One Bad State.

This model is highly useful for modeling of burst errors in communication channels which is why it has received a lot of attention lately. Figure 3.8 shows a generalized finite-state Fritchman Markovian chain model of a channel with memory and *N* finite states. A three-state Fritchman model is utilized in modeling of the power line channel in this research work. Figure

3.9 shows a three-state model with two good states and a bad state. From the three-state Fritchman model diagram shown above, it can be seen that each state has self-transition. Transitions exist between the error-free states and the error state in both directions, but transition is not allowed between the error-free states. This makes its suitable for modeling of real communication channels as it allows for existence of a multiple degree of memory in the model [5]. A three-state model is chosen based on Fritchman's paper [5], refer to Section 5.1 for the motivation behind the use of one error state.

Moreover, a single-error state is assumed for this model, therefore zero (0) denotes the conditional probability of error so far we are in an error-free state while one (1) denotes the conditional probability of error given that we are in an error-state. This makes it possible for the error-free distribution Pr ($0^m|1$) to uniquely specify the single error state. Simply put it means the model parameters can be obtained from the error-free run distributions and vice versa [8].
Generally, the state transition matrix *A* can be partitioned as presented below.

$$\boldsymbol{A} = \begin{bmatrix} A_{gg} & A_{gb} \\ A_{bg} & A_{bb} \end{bmatrix}$$

The sub-matrices A_{gg} and A_{gb} denote probabilities of transitioning between good states and the probabilities of transitioning from good to bad state respectively and are represented in math notation as follows.

$$\boldsymbol{A_{gg}} = \begin{bmatrix} a_{11} & a_{12} \\ a_{21} & a_{22} \end{bmatrix}$$

$$\boldsymbol{A_{gb}} = [a_{13}\ a_{23}\ ]$$

Likewise A_{bg} and A_{bb} denote probabilities of transitioning from bad to good state and self-transition in bad state respectively. A_{bg} and A_{bb} are mathematically represented as follows.

$$\boldsymbol{A_{bg}} = [a_{31}\ a_{32}]$$

$$\boldsymbol{A_{bb}} = [a_{33}]$$

The corresponding state transition matrix *A* and *B* matrix for the three-state model is represented below. It can be seen that for the state transition matrix *A*, there are no entries for both a_{12} and a_{21} which is due to non-occurrence of transition between the two good states (state one and two).

$$\boldsymbol{A} = \begin{bmatrix} a_{11} & 0 & a_{13} \\ 0 & a_{22} & a_{23} \\ a_{31} & a_{32} & a_{33} \end{bmatrix}$$

According to Fritchman for a three state model with two good states and a bad state, the two good states do not produce any error. Therefore, an observation of errors implies that these errors are generated from the only bad state [5]. Hence, the *B* matrix which is the error generation matrix is represented in binary form with the matrix notation as follows.

$$\boldsymbol{B} = \begin{bmatrix} 1 & 1 & 0 \\ 0 & 0 & 1 \end{bmatrix}$$

The *B* matrix represents the input-to-output symbol transition, which is the error probability. Note that the columns of the *B* matrix must sum to one [142]. For further details of how the *B* matrix is chosen, refer to Section 5.1. The first two columns represent the two good states (error-free states), while the last column represents the bad state (error-state).

Another parameter that needs to be defined is π, the initial state probability, which is the prior probability of being in any of the state

$$\boldsymbol{\pi} = [\pi_1 \ \pi_2 \ \pi_3].$$

The three-state Fritchman model utilized in modeling can also be regarded as a semi-hidden Markov model. This is based on the fact that occurrence of an error tells us that the observed symbol is emitted from the third state (bad state) which always emit errors. However, for an error free observation, we are not sure of the state that emitted the outcome since it is not physically observable given that we have two good states, hence the name semi-hidden Markov [5], [84].

3.7 Baum-Welch Algorithm

Baum-Welch algorithm [7], [142], [144], is an iterative algorithm for estimation of the partitioned Markov model parameters $\Gamma = (A, B, \pi)$ from a given error sequence obtained through measurement. This algorithm has been designed to converge to the maximum likelihood estimator of $\Gamma = (A, B, \pi)$ that maximizes Pr $(O|\Gamma)$ [17]. As an iterative algorithm, the number of iterations to be executed to achieve a required level of accuracy for the model should be determined by the display of the estimated values of A and π as the algorithm is executing its

operation and the required level of accuracy gotten as soon as there is no changes in the model parameters [7], [142].

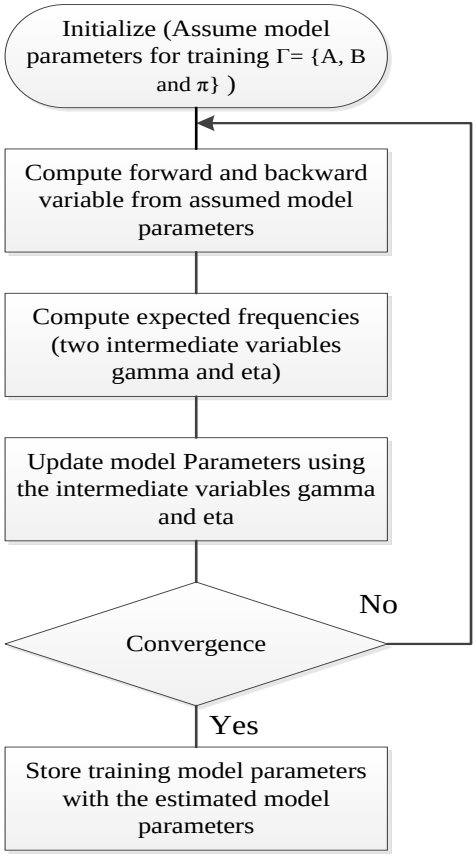

Figure 3.10: Baum-Welch Algorithm Flow Chart

Figure 3.10 above presents the Baum-Welch algorithm flow chart showing a description of the procedures carried out by the algorithm. This procedures are further discusses below and the corresponding equations computed and executed at each stage presented in Section 3.7.1. Below are brief description of variable computed and task executed by the Baum-Welch algorithm.

Step 1: Initial model parameters. Initialize the model parameters to some values (Assume a model $\Gamma = \{A, B, \pi\}$)

Step2: With the model parameters Γ assumed. Compute the *"forward variables"* and the *"backward variables"* Where the *forward variable* is denoted by $\alpha_t(i)$ is presented below as

$$\alpha_t(i) = \Pr[O_1, O_2, \dots, O_t, s_t = i \mid \Gamma] \quad (3.1)$$

Where $\alpha_t(i)$ represents the probability of emitting the partial observation sequence, $O_1, O_2, \dots, O_t$ **,** (up to time *t*), given that we are in state *i* at time *t***,** given the model Γ.

Also, the *backward variable* denoted by $\beta_t(i)$ is presented below as it denotes the probability of emitting the partial observation sequence $O_{t+1}, O_{t+2}, \dots, O_T$, given that we are in state *i* at time *t* and given the model Γ.

$$\beta_t(i) = \Pr[O_{t+1}, O_{t+2}, \dots, O_T \mid s_t = i, \Gamma] \quad (3.2)$$

Where $t = 1, 2, \dots, T \; and \; i = 1, 2, \dots, N$

Step 3: Using the forward and backward variables computed above we then calculate two intermediate variables which are the expected frequencies that will help in estimation of the model parameters.

The expected number of transitions from state *i* to state *j* which is denoted by $\xi_t(i,j)$ which represents the probability of being in state *i* at time *t*, and being in state *j* at time *t+1***,** given the model Γ and the observation sequence *O* and given as follows

$$\xi_t(i,j) = \Pr(s_t = i, s_{t+1} = j, O \mid \Gamma) \quad (3.3)$$

The expected number of transitions from i which is denoted by $\gamma_t(i)$ which represents the probability of being in state i at time *t*, given the model Γ and the observation sequence *O* and it is represented as follows

$$\gamma_t(i) = \Pr(s_t = i \mid O \mid \Gamma) \quad (3.4)$$

Other expected frequencies to be computed for the estimation of the model parameters are:

The expected number of times in state *i* at time (*t = 1*)

The expected number of starting in state *j* or transitioning from state *j* which is denoted by $\gamma_t(j)$.

The expected number of being in state *j* and observing $O_t = e_k$

Step 4: The expected frequencies computed in step 3 is used to estimate the model parameters; $\hat{a}_{ij}, b_j(e_k) \; and \; \pi_i$.

Step 5: if the model parameters converge. The resulting parameters is the estimated HMM parameter that produced the observation sequence i.e. $\hat{\Gamma} = \Gamma$ (equivalently). Otherwise, go back

to step 2 with the new values of the model parameters $\hat{\Gamma} = \{\hat{A}, \hat{B}, \hat{\pi}\}$ and repeat step 2-4 until the desired level of convergence is attained [142], [144].

3.7.1 Computation of Baum-Welch Algorithm Equations

This section presents a step by step computation of the Baum-Welch algorithm equations. The parameter estimation is realized through the five basic steps highlighted in the section above. This section shows in equation form the three major computation intensive steps (step 2-step 3). Since it is computational intensive, computations for the first four observations sequence is only shown in appendix A, for an understanding and clear view of computation executed by the Matlab code that implements Baum-Welch algorithm.

Forward Variables Computation

The computation of the forward variables is executed in three steps: initialization, induction and termination [142], [144].

Initialization Step:

$$\alpha_t(i) = Pr\ [O_1\ , O_2\ , \dots , O_t\ ] \tag{3.5}$$

$$\alpha_t(i) = \pi_i\ b_i\ (O_t\ ) \tag{3.6}$$

Induction Step:

$$\alpha_{t+1}(\mathrm{j}) = \left[\sum_{i=1}^{\mathrm{N}} \alpha_t(i)\, a_{ij}\right] \mathrm{b_j}\ (\mathrm{O_{t+1}}) \qquad 1 \leq \mathrm{t}\ \leq \mathrm{T}-1, 1\ \leq \mathrm{j} \leq \mathrm{N} \tag{3.7}$$

Termination Step: (t = T)

$$\alpha_T(i) = Pr\ [O_1\ , O_2\ , \dots , O_T\ , S_T = i \mid \Gamma] \tag{3.8}$$

$$\sum_{i=1}^{\mathrm{N}} \alpha_T(i) = \sum_{i=1}^{\mathrm{N}} Pr\ [O_1\ , O_2\ , \dots , O_T\ , \mathrm{S_T} = i \mid \Gamma] = \mathrm{Pr}\ [\overline{\mathrm{O}}\ |\Gamma] \tag{3.9}$$

$$Pr\ [\overline{\mathrm{O}}\ |\Gamma] = \sum_{i=1}^{\mathrm{N}} \alpha_T(i)\ \beta_{\mathrm{T}}\ (i) \tag{3.10}$$

Since, $\beta_{\mathrm{T}}(i) = 1$, Therefore for ($i$ = 1, 2,…, N and N=3 for the case considered)

$$\beta_4(1) = 1$$

$$\beta_4(2) = 1$$

$$\beta_4(3) = 1$$

Hence,

$$Pr\ [\bar{O}\,|\Gamma] = \sum_{i=1}^{N} \alpha_T(i)\ = \sum_{i=1}^{N} \pi_i\, b_i(O_T) \tag{3.11}$$

Backward Variables Computation

The computation of the backward variables unlike the forward variable is executed in two steps: initialization and induction [142] , [144].

Initialization: $\beta_T(i) = 1$, therefore,

$$\beta_4(1) = 1; \quad \beta_4(2) = 1; \ \beta_4(3) = 1 \tag{3.12}$$

Induction:

$$\beta_t\ (i) = \sum_{j=1}^{N} \beta_{t+1}(j) b_j(O_{t+1}) a_{ij}\ \ , \qquad 1 \le t \le T-1, 1 \le j \le N \tag{3.13}$$

Computation of the Expected Frequencies

The computation of the first expected frequency $\gamma_t(i)$ is computed mathematically as shown below [142], [144].

$$\gamma_t(i) = Pr\ [s_t = i\,|\bar{O}, \Gamma]\ = \frac{\alpha_t(i)\beta_t(i)}{P[\bar{O}\,|\Gamma]}\ ; \quad i = 1,2,\dots,N \tag{3.14}$$

While $\xi_t(i,j)$ is also mathematically computed as follows

$$\xi_t(i,j) = Pr\ [s_t = i\ , s_{t+1} = j\,|\bar{O}\ , \Gamma] \tag{3.15}$$

Where, $\xi_t(i,j)$ denotes the probability of being in state *i* at time *t*, and state *j* at time *t+1*, given the model Γ and the observation sequence $\bar{O}$. It is further simplified as follows.

$$\xi_t(i,j) = \frac{Pr[s_t = i\ , s_{t+1} = j\,|\bar{O}\ , \Gamma]}{P[\bar{O}\,|\Gamma]} \tag{3.16}$$

$$\xi_t(i,j) = \frac{\alpha_t(i)\ a_{ij}\ b_j(O_{t+1})\ \beta_{t+1}(j)}{P[\bar{O}\,|\Gamma]} \tag{3.17}$$

Model Parameter Estimation using the Expected Frequencies

Determining new state transition probability [142], [144].

$$\hat{a}_{ij} = \frac{\text{expected number of transitions from i to j}}{\text{expected number of transitions from i}} \tag{3.18}$$

$$\hat{a}_{\text{ij}} = \frac{\sum_{\text{t=1}}^{\text{T}-1} \xi_t(i,j)}{\sum_{\text{t=1}}^{\text{T}-1} \gamma_t\,(i)} \tag{3.19}$$

Computing $\hat{b}_j(e_k)$, defined by

$$\hat{b}_j(e_k) = \frac{\text{expected number of times } \text{e}_\text{k} \text{ is emmited from state j}}{\text{expected number of visits to state j}} \tag{3.20}$$

$$\hat{b}_j(e_k) = \frac{\sum_{\text{t=1}|O_t=e_k}^{\text{T}} \gamma_t(j)}{\sum_{\text{t=1}}^{\text{T}} \gamma_t(j)} \tag{3.21}$$

Computing the estimated initial state probability π_i (the expected number of times in state S_i at time t=1)

$$\hat{\pi}_i = \alpha_1(i)\beta_1(i) \tag{3.22}$$

Several methods have been proposed for the parameterization of the HMMs, but the Baum-Welch algorithm is the most popular technique. Other methods include: gradient search technique [148], interval distribution curve fitting technique [5], [64], [149].

Chapter 4: Measurement Methodology and Results

4.0 Introduction

In this section, we present the measurement methodology use in detecting the three types of noise measured in this work. First a description of the measurement site is done, followed by the measurement methodology. Furthermore, the experimental setup used for noise data captured was also discussed briefly. This chapter is concluded with the presentation of measurement result showing the statistical properties of the noises and a discussion on these results.

4.1 Description of Measurement Site

A brief discussion of the measurement sites is highly essential. This is because the network topology and loads present at different locations have an impact on the noise measurement taken due to the various scenarios that occur at these locations. An in-house noise data were captured at two different metropolitan locations of South-Africa. Even though these locations network topology (star topology) are similar, they differ in terms of numbers and types of electrical and electronics appliances and equipment connected across their power line network.

The laboratory site is situated in the Faculty of Engineering building which was undergoing renovation at the time the noise data were captured for 2011 measurement. The presence of motorized drilling machine, cutting machine and all other equipment used during the renovation were additional sources of noise connected onto the power line network. Equipment present at this site are computers, various laboratory equipment (oscilloscope, power supply, spectrum analyser etc.), and all these equipment constitute noise sources on the power line network when active.

The residential in-house noise data were captured at a densely populated residential area in the city of Johannesburg, South Africa. Household electrical and electronics appliances such as hair dryers, electrical ovens, electric heaters, microwave ovens, carpet vacuum cleaners, shaving machines, etc. may constitute sources of noise on the power line network.

The next section presents the methodology for classifying the three major noise types present and captured at the site.

4.2 Measurement Methodology and Categorization of Noise Types

It is highly essential to describe the rule guiding the classification of noise type present on the PLC channel, and this can only be achieved effectively by knowing the characteristics of the individual noise type. Below is the set methodology employed to categorize and measure noise data in this project (Measurement are carried out in the frequency domain).

Firstly, in order to measure narrowband noise, a threshold voltage in (mV) is set to discover permanent narrowband noise (NBN). Any noise spike that crosses above the threshold is regarded as narrowband noise (error-prone), while those below are regarded as error-free. This is done by predetermining a threshold in terms of the amplitude (mV) of the noise spike. The duration of this 'permanent' or 'semi-permanent' narrowband noise may be empirically chosen as some may last for hours based on how long the source stays active on the power line, and also dependent on the threshold chosen. During the course of measurement some occurrences of NBN measured lasted for duration of 1,800 seconds (30 minutes), i.e. the NBN duration was far greater than the typical 1ms, whilst experiencing noise levels higher than the chosen mV threshold in a single sub-channel. The frequency of occurrence of the permanent NBI is then recorded with the corresponding source-frequency sub-band and duration within the chosen time frame. Another characteristic of this type of noise that makes it easy to identify when compared to other noise types is that it is confined to narrow portion of the frequency band on which measurement is carried out.

To distinguish between these two classes of noise, the impulsive noise and the background noise, a threshold number is chosen (set) with respect to the minimum number of frequency sub-channels interfered by the noise data captured. Any captured noise data showing more of the frequency sub-channels above the threshold interfered by noise is categorized as impulsive noise, while noise data showing less frequency sub-channel interfered by noise below the threshold number set is regarded categorically as background noise. This is done based on the properties of these two noise types (refer to Section 3.4). Impulse noise interferes with almost all the

frequency band of use, while background noise interferes with fewer frequency sub-channels. Threshold duration is also set to distinguish between background noise and impulse noise, as background noise lasts longer than impulsive noise. Impulsive noise is transient in nature due to switching effects of regulators and other noise source that causes impulsive noise. Hence, disturbances that last a small time fraction in the range of perhaps say less than 100µs may be categorized as impulse noise, while background noise has higher duration than this as it is always present on the network in contrast to impulse noise which is transient. For the captured data, the frequency of occurrences of this noise type is recorded over a 24-hour time frame.

4.3 Experimental Measurement Setup

The measurement setup comprises of the following: a 2 channel 50 MHz Rigol DS1052E Digital Oscilloscope, a UPS with the oscilloscope connected to the UPS to disallow further introduction of noise into the measurement. A coupling circuit is essential for noise data capture. It is designed as a band pass filter to provide galvanic isolation of oscilloscope from the power line 220V/50Hz supply and also allowing the CENELEC high frequency signal to pass. Figure 4.1 below shows the setup for noise data capture.

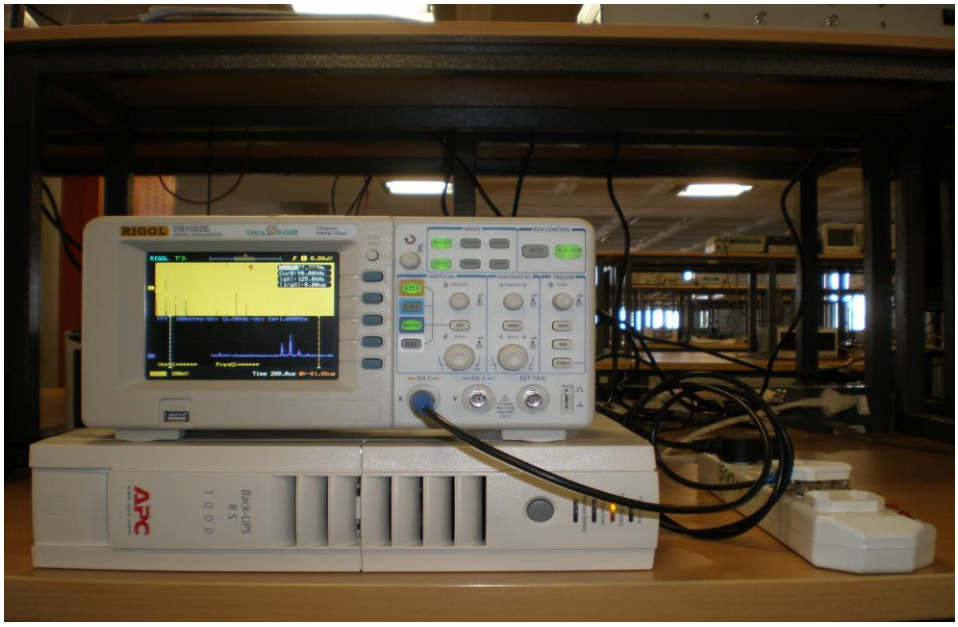

Figure 4.1: Experimental Setup for Noise Data Capture

Before noise data are been captured, the Uninterruptible Power Supply (UPS) is fully charged and disconnected from the mains supply. The oscilloscope is then connected to (UPS) to prevent noise from its power supply being further coupled onto the power line. It is highly essential that the UPS noise is been characterized as shown in Figure 4.2, with the coupler plugged out from the oscilloscope to measure the UPS noise-floor. The coupler is then plugged to the power line outlet and the BNC end connection point is plugged to the oscilloscope for measurement.

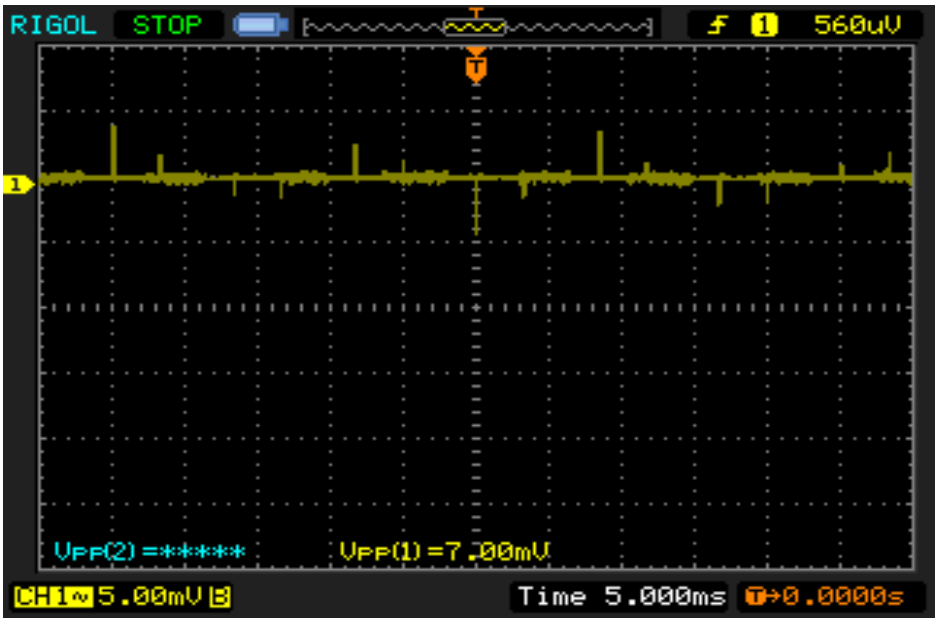

Figure 4.2: UPS Noise-Floor Measurement With Coupler Plugged Out.

All noise data are captured in the frequency domain using the Fast Fourier Transform (FFT) function of the digital oscilloscope. This is useful as analysis of the harmonics in power line and measurement of the harmonic content and distortion on power lines can be realized.

It can be observed from Figure 4.3 that the noise is confined to a narrow portion of the frequency band which shows the attribute of a narrowband noise while Figure 4.4 shows impulse noise spread across the whole frequency band.

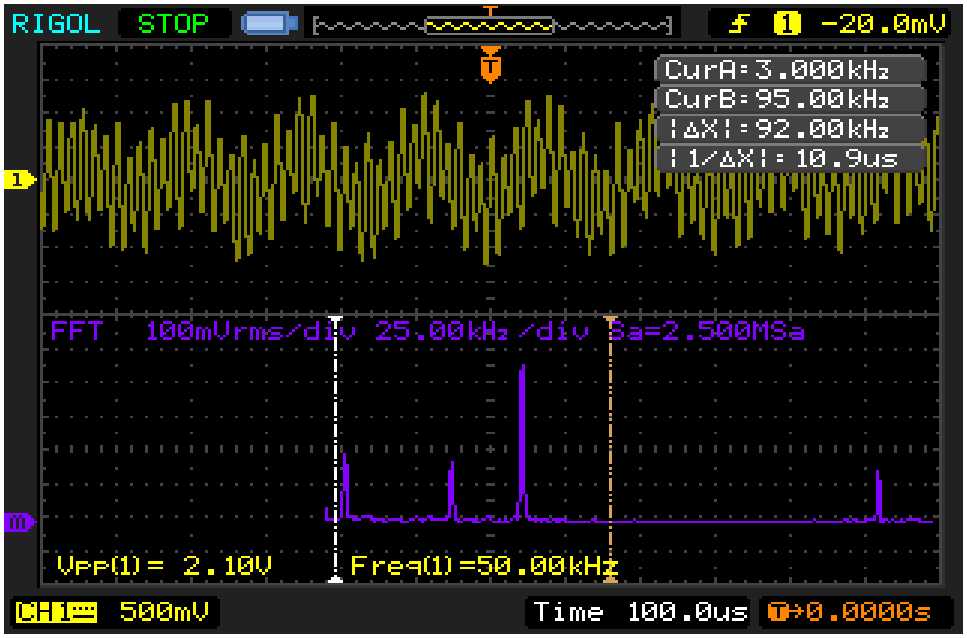

Figure 4.3: Sample Of A Narrowband Noise Captured.

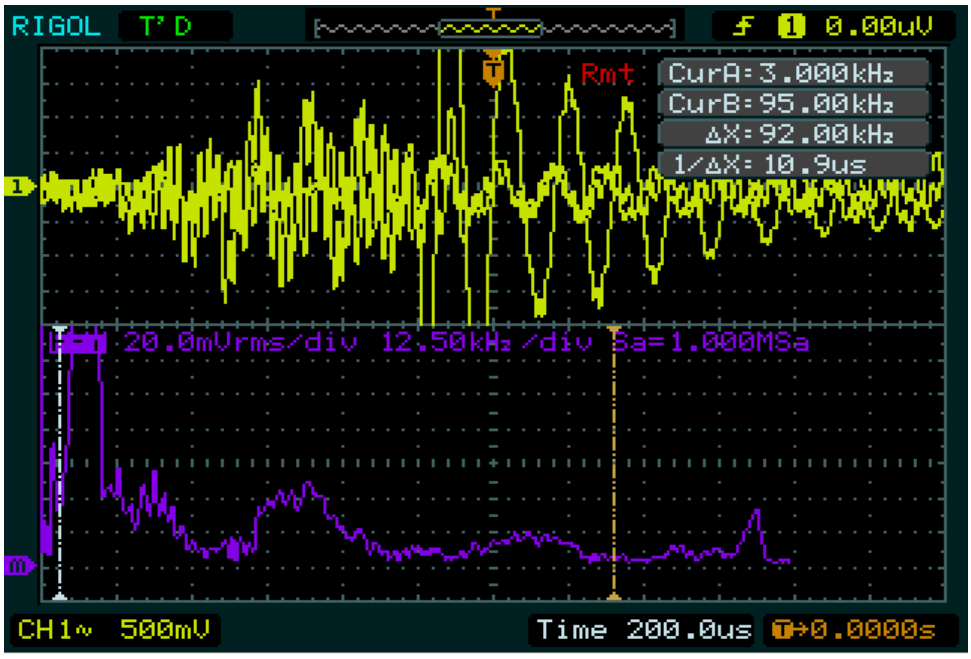

Figure 4.4: Sample Of Impulse Noise Captured.

4.4 Measurement Results and Discussion

This section presents statistical data of noise measurement taken during the 2011 and the 2012 measurement campaign. Based on the inter-arrival time of measurements taken, likewise the sum of noise impulses recorded per chosen time frame, several interesting observations were made for both the residential and laboratory in-house locations. Table 4.1 below shows the statistical data of laboratory in-house narrowband noise captured during 2011.

Time (Hours)	Number of Occurrences	Frequency (kHz)	Average Duration(Hour)
8-9am	3	10\41\63	0.61
9-10am	3	10\41\63	0.42
10-11am	2	7\66	0.46
11-12pm	1	7	0.83
12-1pm	2	58\66	0.83
1-2pm	4	7\34\66\69	0.54
2-3pm	3	7\58\68	0.61
3-4pm	3	7\58\68	0.44
4-5pm	2	7\66	0.5
5-6pm	2	7\66	0.21
6-7pm	2	7\68	0.23
7-8pm	2	7\68	0.3
8-9pm	2	41\66	0.46
9-10pm	2	41\66	0.54
10-11pm	3	41\68	0.46
11-12am	2	7\68	0.38
12-1am	1	66	0.58
1-2am	2	66\68	0.13
2-3am	1	66	0.33
3-4am	1	66	0.33
4-5am	1	66	0.33
5-6am	1	66	0.63
6-7am	1	66	0.16
7-8am	1	66	0.10

Table 4.1: Laboratory In-House Narrowband Noise for 2011.

Analysis of the noise occurrence is then considered between the same noise type for the residential in-house and the laboratory in-house measurement taken in 2011. Furthermore, a comparison is made between the same kind of noise at the same location but different year (2011 vs. 2012). Based on analysis, it was observed generally that at the residential location, on the

average, there are more occurrences of noise impulse recorded when compared to the laboratory in-house. This can be linked to the presence of more electrical loads (microwave oven, TV, hair dryer, air conditioner, electric heaters, shaving machines etc.) connected across the residential in-house site power line network and fewer loads present on the laboratory site network. Note that in Table 4.1 above narrowband disturbances were observed on many occasions at 7, 41, 66 and 68 kHz within the 24 hours duration of measurement in 2011 (laboratory in-house). Some sporadic occurrences of narrowband disturbances were also recorded at 10, 63 and 69 kHz with all this disturbances coming from unknown sources.

Table 4.2 below shows the statistical data of laboratory in-house narrowband noise captured during 2012.

Time (Hours)	Number of Occurrences	Frequency (kHz)	Average Duration(Hour)
8-9am	3	7\41\69	0.83
9-10am	1	41	0.84
10-11am	2	7 41	0.29
11-12pm	1	69	0.66
12-1pm	1	58	0.70
1-2pm	1	34	0.60
2-3pm	1	69	0.41
3-4pm	1	7	0.34
4-5pm	1	41	0.56
5-6pm	2	41\80	0.30
6-7pm	2	68\80	0.43
7-8pm	1	34	0.10
8-9pm	2	66\69	0.11
9-10pm	1	69	0.14
10-11pm	1	80	0.16
11-12am	1	7	0.33
12-1am	1	66	0.68
1-2am	1	69	0.10
2-3am	1	68	0.43
3-4am	1	68	0.40
4-5am	1	80	0.40
5-6am	1	68	0.53
6-7am	1	68	0.10
7-8am	3	66	0.83

Table 4.2: Laboratory In-House Narrowband Noise for 2012.

Note that in Table 4.2 above narrowband disturbances were observed often at 7, 41, 66, 68, 69, and 80 kHz and disturbances were seldom recorded at the following frequencies 34, 41, 58, 80 kHz within the 24 hours duration of measurement in 2012 (laboratory in-house).

Table 4.3 below shows the statistical data of residential in-house narrowband noise captured during 2011.

Time (Hours)	Number of Occurrences	Frequency (kHz)	Average Duration (Hour)
8-9am	6	8\31\32\33\34\90	0.11
9-10am	2	8\35	0.2
10-11am	3	8\9\36	0.2
11-12pm	3	8\9\45	0.29
12-1pm	1	8	0.5
1-2pm	2	7\8	0.42
2-3pm	3	7\8\9	0.4
3-4pm	3	8\50\51	0.25
4-5pm	2	8\43	0.15
5-6pm	3	8\42\60	0.2
6-7pm	4	8\9\48\49	0.24
7-8pm	2	8\50	0.29
8-9pm	3	8\9\48	0.25
9-10pm	3	9\32\91	0.2
10-11pm	2	8\80	0.2
11-12am	3	8\37\92	0.23
12-1am	3	9\35\91	0.2
1-2am	3	8\37\90	0.2
2-3am	3	8\37\91	0.21
3-4am	2	8\35	0.24
4-5am	3	8\37\90	0.2
5-6am	3	8\31\89	0.3
6-7am	3	8\36\90	0.2
7-8am	3	9\37\91	0.2

Table 4.3: Residential In-House Narrowband Noise for 2011.

Note that in Table 4.3 above narrowband disturbances were observed on many occasions at 8 kHz, lesser occurrence were recorded at 9, 90, 91 kHz and disturbances were seldom and sporadically recorded at 31, 32, 33, 34, 35, 36, 37, 42, 43, 45, 48, 50, 51, 60 kHz within the 24 hours duration of measurement in 2011 (residential in-house).

Table 4.4 below shows the statistical data of residential in-house narrowband noise captured during 2012.

Time (Hours)	Number of Occurrences	Frequency (kHz)	Average Duration (Hour)
8-9am	7	7\31\32\42\66\90\94	0.18
9-10am	5	8\9\42 \45\50	0.25
10-11am	5	36\43\50\51\90	0.22
11-12pm	5	32\48\60\80\91	0.32
12-1pm	4	31\32\42\50	0.45
1-2pm	4	8\9\32\80	0.56
2-3pm	5	48\50\51\80\91	0.40
3-4pm	3	8\9\32	0.34
4-5pm	3	66\90\94	0.22
5-6pm	2	7\31	0.40
6-7pm	2	7\31	0.33
7-8pm	3	48\80\91	0.33
8-9pm	2	32\80	0.30
9-10pm	2	42\66	0.30
10-11pm	2	90\91	0.40
11-12am	1	42	0.19
12-1am	1	80	0.10
1-2am	1	66	0.19
2-3am	1	66	0.23
3-4am	3	37\66\91	0.28
4-5am	3	8\32\66	0.19
5-6am	2	32\80	0.40
6-7am	4	8\35\48\80	0.40
7-8am	4	8\37\90\91	0.23

Table 4.4: Residential In-House Narrowband Noise for 2012.

Note that in Table 4.4 above narrowband disturbances were observed on many occasions at 8, 32, 66, 80, 90 and 91 kHz, lesser occurrences were recorded at 7, 9, 31, 42, 48, 50 kHz and disturbances were seldom and sporadically recorded at 37, 43, 45, 51, 60 and 94 kHz within the 24 hours duration of measurement in 2012(residential in-house).

Table 4.5 below shows the statistical data of laboratory in-house impulse noise captured during 2011 and 2012.

Note that from Table 4.1 and 4.3, carrying out comparisons between narrowband noise occurrences measured at both the residential and laboratory site in 2011, it was observed that more narrowband noises were recorded in the residential site when compared to the laboratory site. 68 narrowband noises were recorded for the residential site while 46 narrowband noises were observed at the laboratory site. Similarly for 2012, narrowband noise recorded was higher at the residential site where 74 narrowband noises were observed as opposed to the 32 recorded for the laboratory site. Several narrowband noises measured originated from modulated signals coupled unto the power line network at the two sites and from electrical devices having built-in transmitter and receiver such as TV.

For Table 4.5-4.8, note that the probability of background noise is defined as the ratio of the summation of the number of background noise occurrences and the product of number of A-band frequency sub-channels and the number of observations. On the other hand the probability of impulse noise is defined as the ratio of the number of impulse noise occurrences and the number of observation. The background noise probability is represented below mathematically:

$$Pr_B = \frac{\sum N_{BN}}{N_f \times N_{obs}} \tag{4.1}$$

where Pr_B is the probability of background noise, N_{BN} represents number of background noise occurrences, N_f represents the number of A-band frequency sub-channels, and N_{obs} represent the number of observations made.

Likewise, the probability of impulse noise is represented mathematically by the equation below.

$$Pr_{imp} = \frac{\sum N_{imp}}{N_{obs}} \tag{4.2}$$

Where Pr_{imp} is the probability of impulse noise, N_{imp} represents number of impulse noise occurrences, N_{obs} represent the number of observations made.

Note, from Table 4.5 and 4.7, a comparison of the probability of impulse noise on the average measured in 2011 at the residential in-house site is quite higher than that recorded at the laboratory in the same year. This can be attributed to the presence of more electrical loads which constitute sources of impulse noise present at the residential site.

Likewise a comparison of the probability of impulse noise on the average measured in 2012 at the residential in-house site is higher than that recorded for the laboratory in-house site in the same year. On the average, little changes were recorded in the probability of impulse noise measure at the residential site in 2011 and 2012 with higher probabilities measured in 2011. Also for the laboratory site the probability of impulse noise measured was higher in 2011 than 2012 but with little changes.

Time (Hours)	Impulse Noise (Probability) for 2011	Impulse Noise (Probability) for 2012
8-9am	0.15	0.13
9-10am	0.07	0.05
10-11am	0.12	0.10
11-12pm	0.23	0.19
12-1pm	0.15	0.11
1-2pm	0.07	0.03
2-3pm	0.01	0.03
3-4pm	0.09	0.06
4-5pm	0.05	0.03
5-6pm	0.06	0.04
6-7pm	0.01	0.03
7-8pm	0.05	0.06
8-9pm	0.06	0.04
9-10pm	0.08	0.07
10-11pm	0.11	0.15
11-12am	0.03	0.01
12-1am	0.01	0.02
1-2am	0.01	0.02
2-3am	0.03	0.02
3-4am	0.09	0.08
4-5am	0.04	0.05
5-6am	0.07	0.06
6-7am	0.15	0.12
7-8am	0.12	0.09

Table 4.5: Laboratory In-House Impulse Noise for 2011 and 2012.

Note also, from Table 4.6 and 4.8, a comparison of the probability of background noise on the average measured in 2011 at the residential in-house site is quite lesser than that recorded at the laboratory in the same year. This can be attributed to the presence of several unknown low power

noise sources at the laboratory site. The probability of background noise on the average measured in 2012 at the laboratory in-house site is quite higher than that recorded for the residential in-house site in the same year. On the average, the probability of background noise measured at the residential site in 2011 is slightly higher than that in 2012. While for the laboratory site the probability of background noise measured was slightly higher in 2011 than 2012.

Time (Hours)	Background Noise (Probability) for 2011	Background Noise (Probability) for 2012
8-9am	0.052	0.048
9-10am	0.035	0.033
10-11am	0.01	0.009
11-12pm	0.021	0.023
12-1pm	0.071	0.067
1-2pm	0.031	0.027
2-3pm	0.052	0.049
3-4pm	0.016	0.011
4-5pm	0.042	0.035
5-6pm	0.019	0.012
6-7pm	0.013	0.010
7-8pm	0.008	0.006
8-9pm	0.019	0.012
9-10pm	0.012	0.012
10-11pm	0.002	0.004
11-12am	0.001	0.001
12-1am	0.002	0.001
1-2am	0.003	0.001
2-3am	0.002	0.004
3-4am	0.003	0.002
4-5am	0.003	0.005
5-6am	0.002	0.023
6-7am	0.033	0.053
7-8am	0.023	0.020

Table 4.6: Laboratory In-House Background Noise for 2011 and 2012.

Some of the background noises recorded were discovered to originate from electrical appliances such as mixers, hair dryer, fans and other low power noise sources present on the power line

network at the two different locations of where measurement was carried out. On the other hand, impulse noise recorded has been discovered to originate from light dimmers, transient switching that occurs in power supplies present on the network.

Time (Hours)	Impulse Noise (Probability) for 2011	Impulse Noise (Probability) for 2012
8-9am	0.25	0.22
9-10am	0.1	0.09
10-11am	0.13	0.10
11-12pm	0.15	0.14
12-1pm	0.07	0.05
1-2pm	0.06	0.03
2-3pm	0.04	0.05
3-4pm	0.2	0.3
4-5pm	0.13	0.12
5-6pm	0.07	0.05
6-7pm	0.22	0.19
7-8pm	0.18	0.15
8-9pm	0.21	0.20
9-10pm	0.2	0.19
10-11pm	0.22	0.17
11-12am	0.22	0.23
12-1am	0.09	0.07
1-2am	0.08	0.06
2-3am	0.09	0.06
3-4am	0.08	0.09
4-5am	0.06	0.05
5-6am	0.09	0.09
6-7am	0.1	0.13
7-8am	0.1	0.11

Table 4.7: Residential In-House Impulse Noise for 2011 and 2012.

Time (Hours)	Background Noise Probability for 2011	Background Noise Probability for 2012
8-9am	0.009	0.005
9-10am	0.05	0.07
10-11am	0.03	0.03
11-12pm	0.02	0.04
12-1pm	0.03	0.03
1-2pm	0.03	0.03
2-3pm	0.005	0.011
3-4pm	0.02	0.022
4-5pm	0.02	0.01
5-6pm	0.02	0.04
6-7pm	0.022	0.024
7-8pm	0.05	0.032
8-9pm	0.04	0.03
9-10pm	0.02	0.022
10-11pm	0.002	0.001
11-12am	0.002	0.005
12-1am	0.003	0.004
1-2am	0.006	0.008
2-3am	0.006	0.011
3-4am	0.005	0.006
4-5am	0.008	0.012
5-6am	0.009	0.007
6-7am	0.003	0.006
7-8am	0.003	0.008

Table 4.8: Residential In-House Background Noise for 2011 and 2012.

Noise types	Measurement Location	No. of Occurrences (24 hours)
Narrow band noise	Residential	74
Narrow band noise	Laboratory	32
Background noise	Residential	69
Background noise	Laboratory	38
Impulse noise	Residential	56
Impulse noise	Laboratory	19

Table 4.9: Noise Occurrences taken in 2011 (renovation going on at the Laboratory site)

Noise types	Measurement Location	No. of Occurrences (24 hours)
Narrow band noise	Residential	46
Narrow band noise	Laboratory	68
Background noise	Residential	25
Background noise	Laboratory	50
Impulse noise	Residential	30
Impulse noise	Laboratory	66

Table 4.10: Noise occurrences taken in 2012

Note that Table 4.9 and 4.10 show the noise occurrences recorded in 2011 and 2012 respectively.

Furthermore, the results of measurement taken in 2011 and 2012 are also presented in the bar chart format. Figure 4.5 shows the probability of impulse noise for both residential and laboratory site taken in 2011. It can be observed that the probability of impulse noise is high at 8am, 3pm, and right through from 18 hours to 23 hours. This is as a result of having more impulse noise sources active on the network at this time of the day. The probability of impulse recorded at the laboratory peaks at 11 am, and is generally lower than for the residential site.

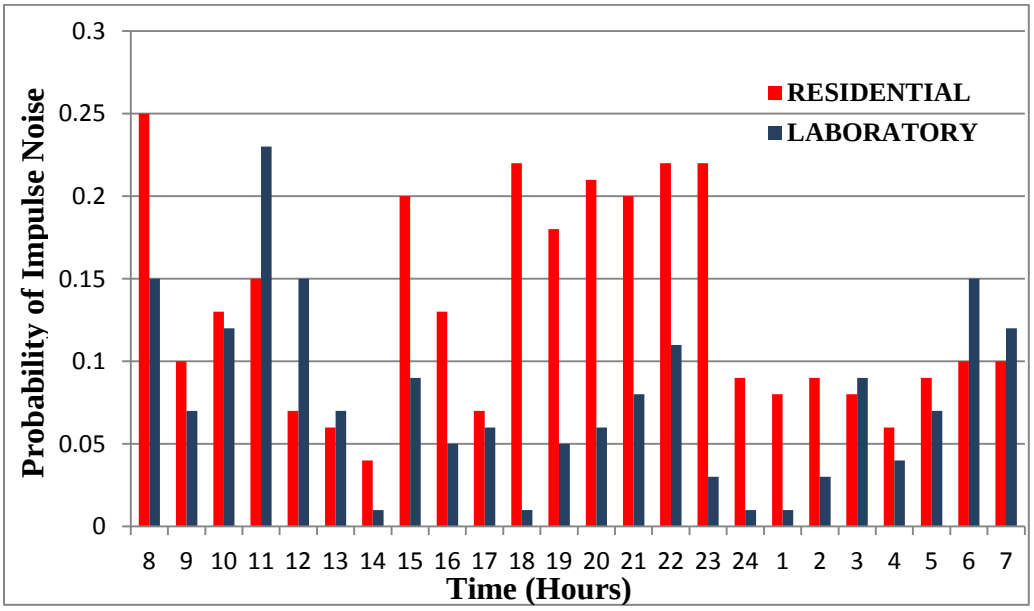

Figure 4.5: Probability of Impulse noise vs. Time (Hours) for 2011.

Figure 4.6 shows the probability of impulse noise measured for both residential and laboratory site in 2012. For the residential site the probability of impulse observed was high at 8 am, and

right through from 15 hours to 23 hours similar to that recorded in 2011 but with lesser magnitude. Note that for the laboratory site probability of impulse only peaks at 8 am, 11 am, 22 hours and also at 6 and 7 am but with lower magnitude when compared to the residential site.

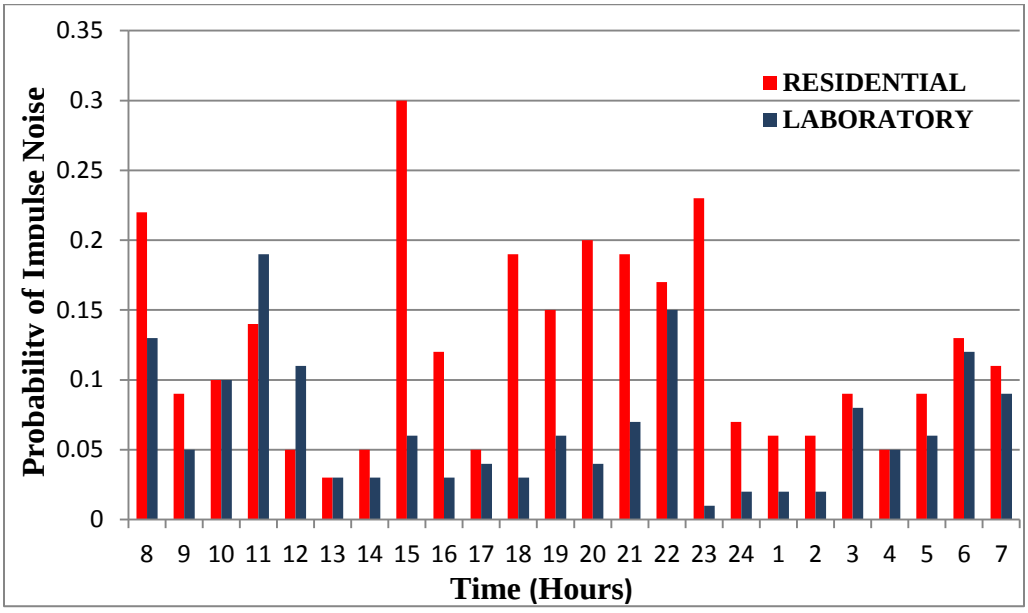

Figure 4.6: Probability of Impulse noise vs. Time (Hours) for 2012.

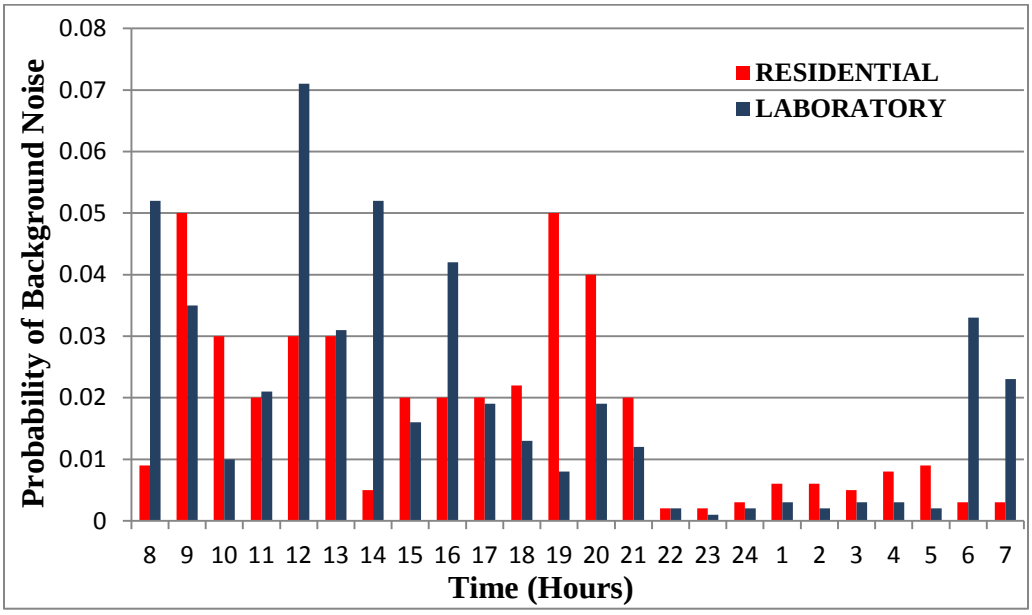

Figure 4.7: Probability of Background noise vs. Time (Hours) for 2011.

Figure 4.7 above shows the probability of background noise recorded for both residential and laboratory sites in 2011. For the residential site the probability of background noise was

observed to peak at 9 am, 19 hours and 20 hours with lower magnitude of background noise recorded at other period of the day except for except for those observed at 10 am, 11 am through to 13 hours, and 15 hours through to 18 hours. For the laboratory site, probability of background noise observed peaked at 8 am, 9 am and 12 noon through to 16 hours, some peak magnitudes were also observed at 6 and 7 am.

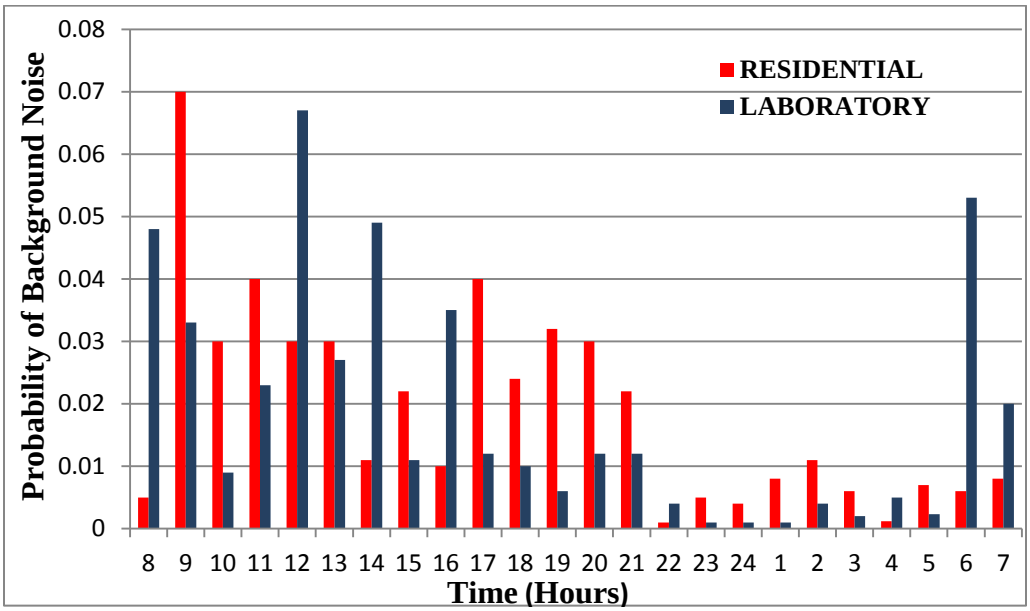

Figure 4.8: Probability of Background noise vs. Time (Hours) for 2012.

Figure 4.8 shows a comparison of the probability of background noise measured at both the residential and laboratory site in 2012. Certain peak values of probability were observed for the residential site at 9, 10, 11, 12 am and 13, 15, 17, 18, 19, 20, 21 hour, while low probability of background noise was observed at other time of the day (8 am, 14, 16, 22-24 hour, and 1-7 am). A number of peak values of probability were also observed for the laboratory site at 8, 9, 11 am, 12 noon, 13, 14,16 hour and around 6,7 am., while low background noise probability were recorded at 10am, 15, 17, 18 hour till 5 am.

Note that Figure 4.9 shows the probability of occurrences of narrowband noise measured at both residential and laboratory locations in 2011. It can be observed that more narrowband noise occurred at the residential site when compared to the laboratory site. Frequent observation of three narrowband noise was observed for the residential site, while frequent observation of two narrowband noise was also observed at the laboratory site.

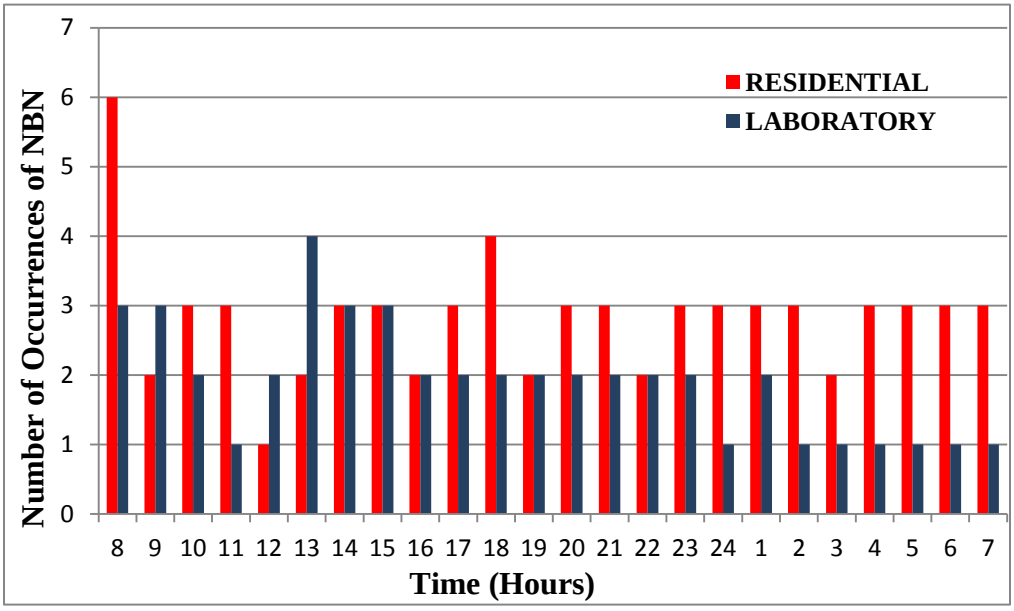

Figure 4.9: Number of occurrences of narrow band noise vs. Time (Hours) for 2011.

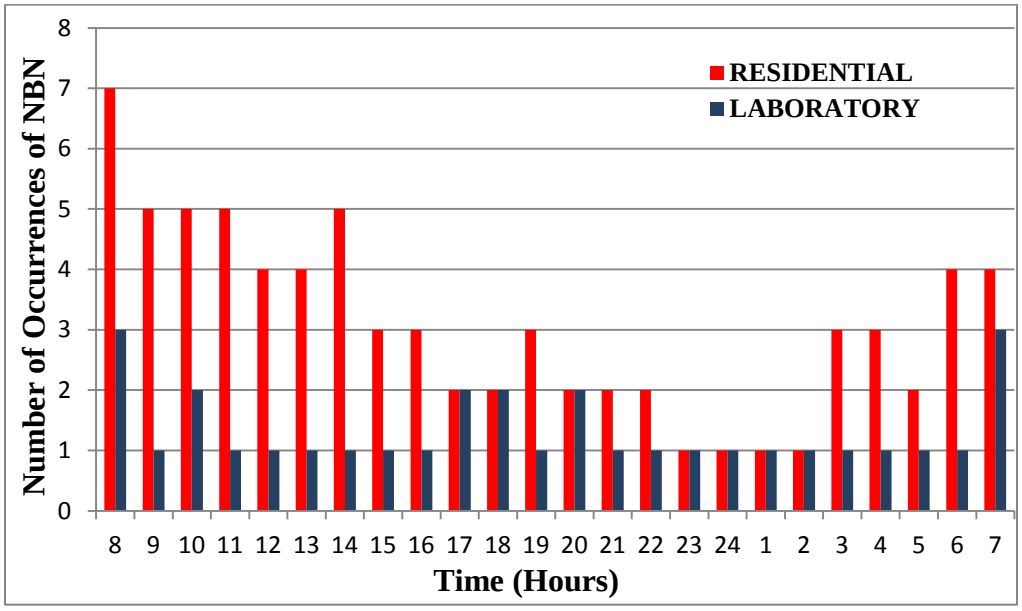

Figure 4.10: Number of occurrences of narrow band noise vs. Time (Hours) for 2012.

Figure 4.10 shows the probability of occurrences of narrowband noise measured at both residential and laboratory locations in 2012. It can be observed that the number of narrowband noise observed at the residential site was on the high side (6 been the highest) when compared to that measured in 2011, while the occurrence of narrowband noise observed at the laboratory site is low (3 been the maximum) when compared to the residential site.

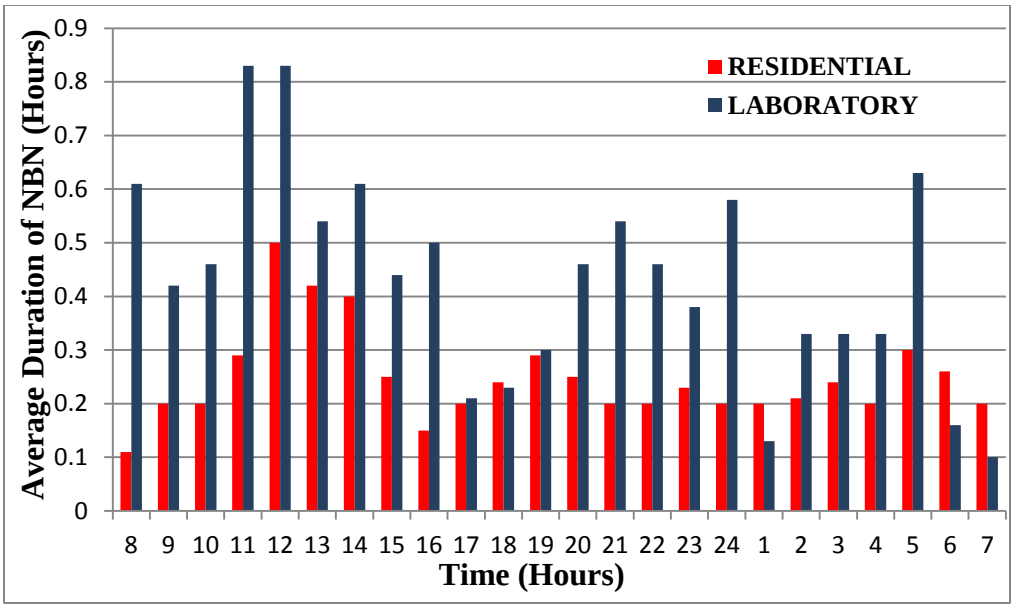

Figure 4.11: Average duration of narrow band noise vs. Time (Hours) for 2011.

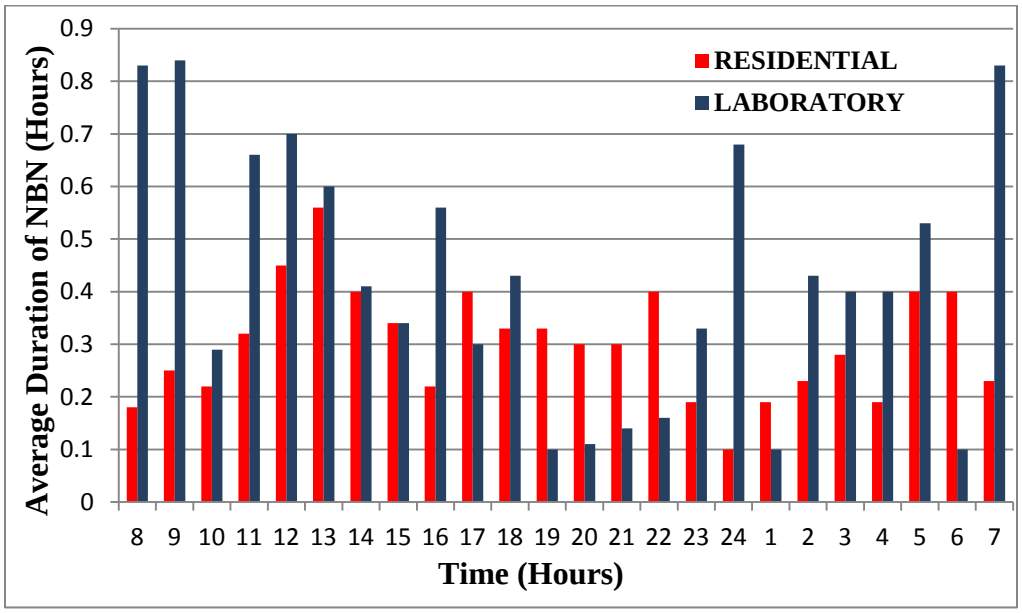

Figure 4.12: Average duration of narrow band noise vs. Time (Hours) for 2012.

Figure 4.11 and 4.12 above shows the average duration of narrowband noise for 2011 and 2012 respectively. For both 2011 and 2012, the occurrence of narrowband noise lasted for a longer duration at the laboratory site when compared to the residential site. The peak average duration for the laboratory site in 2011 is 0.83, while that of 2012 is 0.84. Likewise for the residential site, the peak average duration for narrowband noise measured in 2011 is 0.42, while that of 2012 is

0.56. This shows that narrowband noise sources were active for a longer duration in the laboratory when compared with the residential site.

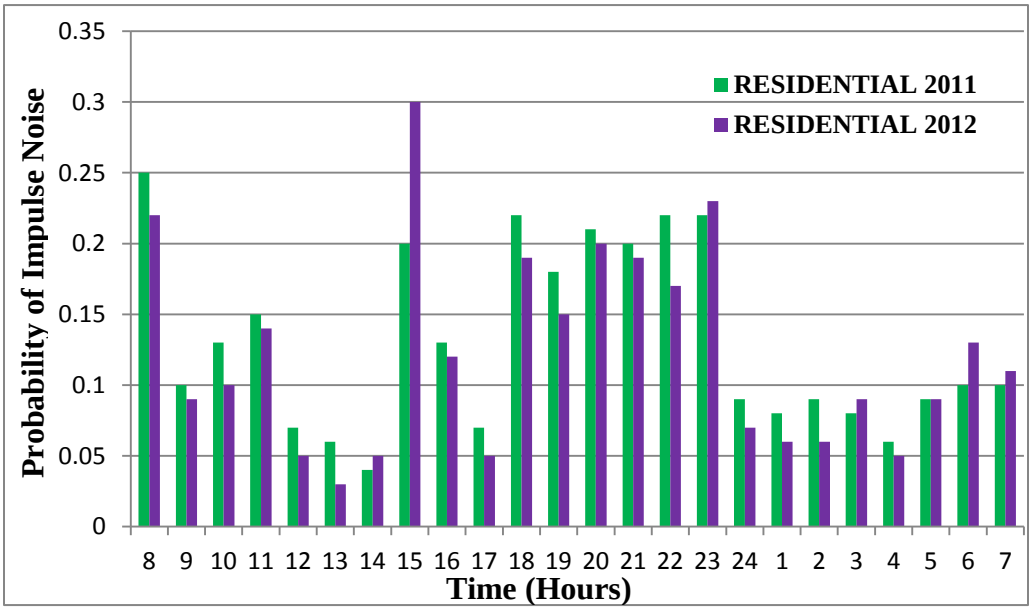

Figure 4.13: Residential Impulse noise probability of occurrence for 2011 vs. 2012.

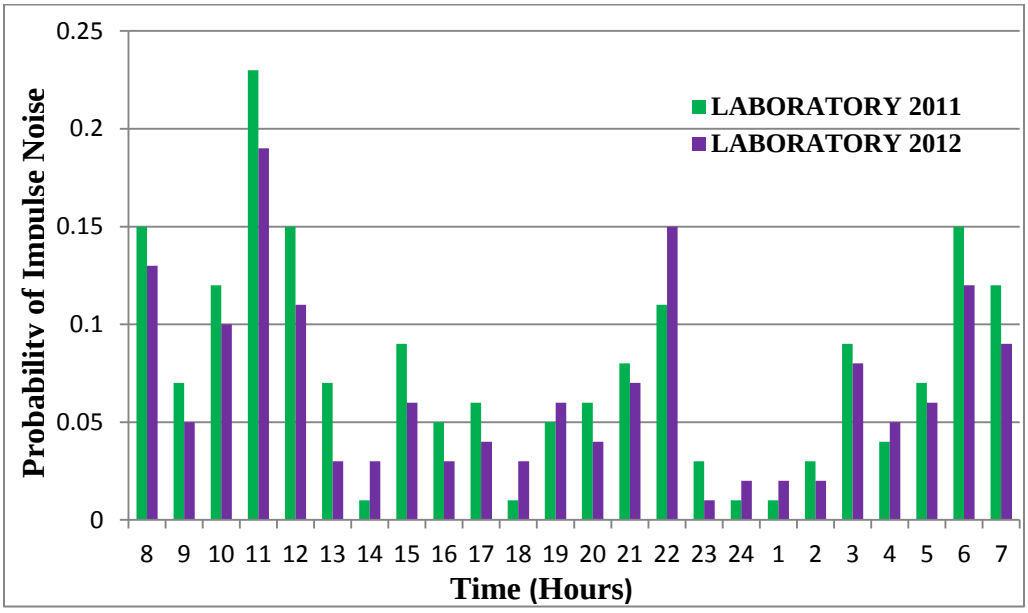

Figure 4.14: Laboratory Impulse noise probability of occurrence for 2011 vs. 2012.

Figure 4.13 and 4.14 shows the residential impulse noise probability of occurrence for 2011 vs. 2012 and laboratory impulse noise probability of occurrence for 2011 vs. 2012 respectively. From Figure 4.13, it can be observed that the probability of impulse noise recorded at the

residential site was higher in 2011 than in 2012, while on the other hand, Figure 4.14 shows that on the average the probability of impulse noise observed was higher in 2011 than in 2012.

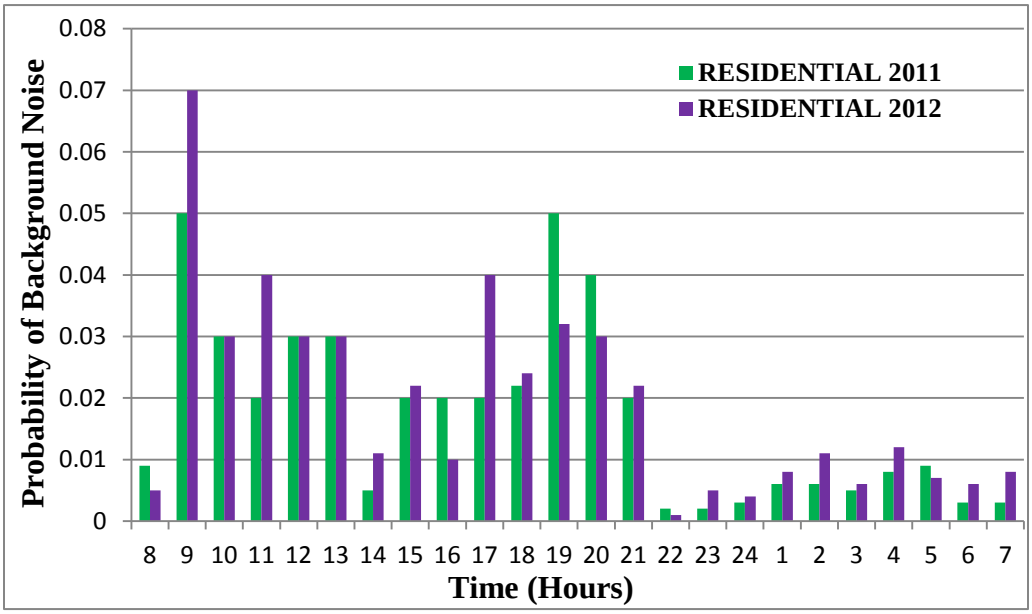

Figure 4.15: Residential Background noise probability of occurrence for 2011 vs. 2012.

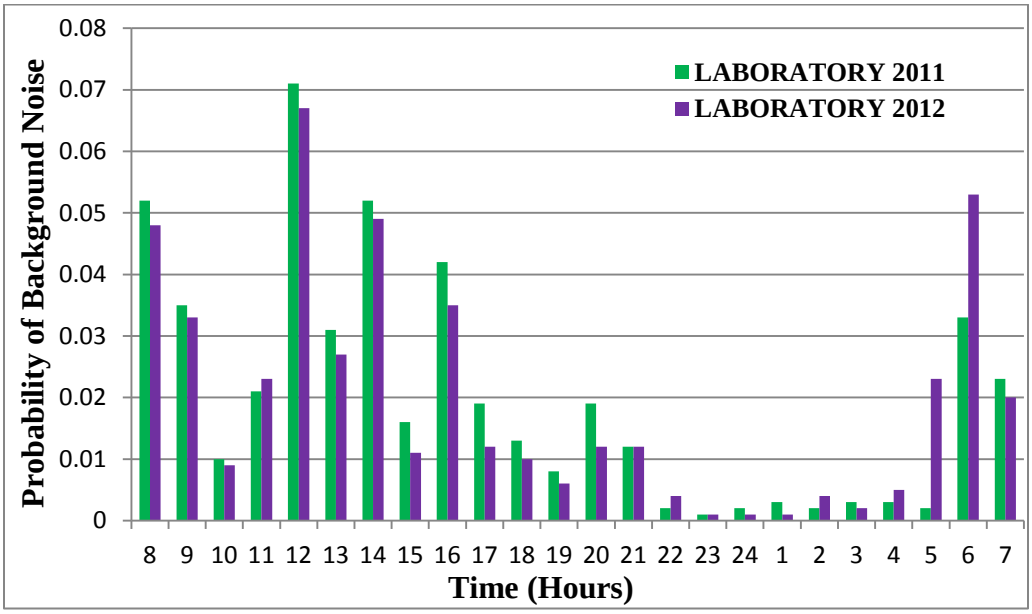

Figure 4.16: Laboratory Background noise probability of occurrence for 2011 vs. 2012.

Figure 4.15 and 4.16 shows the residential background noise probability of occurrence for 2011 vs. 2012 and laboratory background noise probability of occurrence for 2011 vs. 2012 respectively. In Figure 4.15, it can be observed that the probability of background noise

recorded at the residential site was higher in 2012 than in 2011, while on the other hand, Figure 4.16 shows that on the average the probability of background noise observed was higher in 2011 than in 2012.

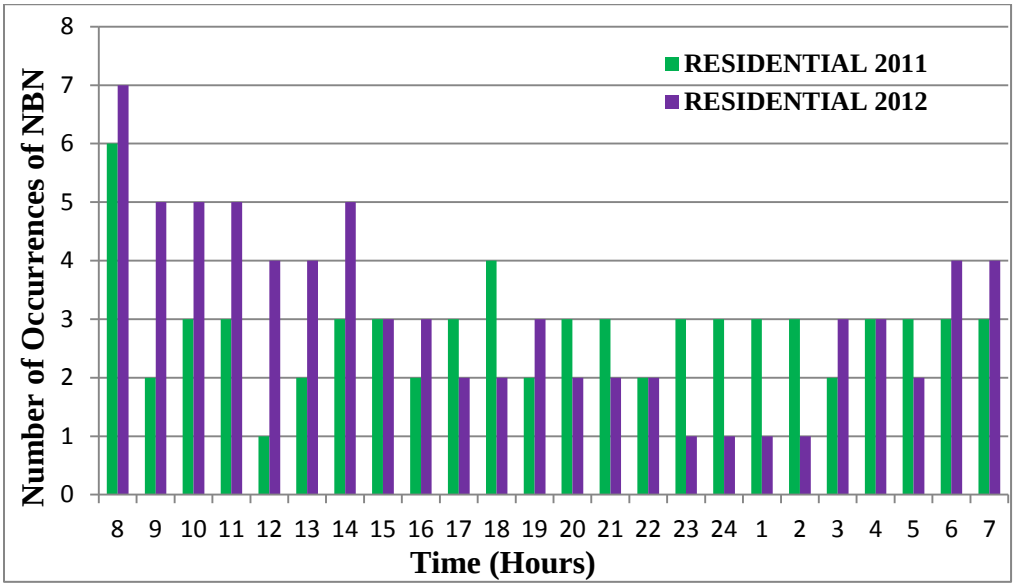

Figure 4.17: Residential narrow band noise number of occurrences for 2011 vs. 2012.

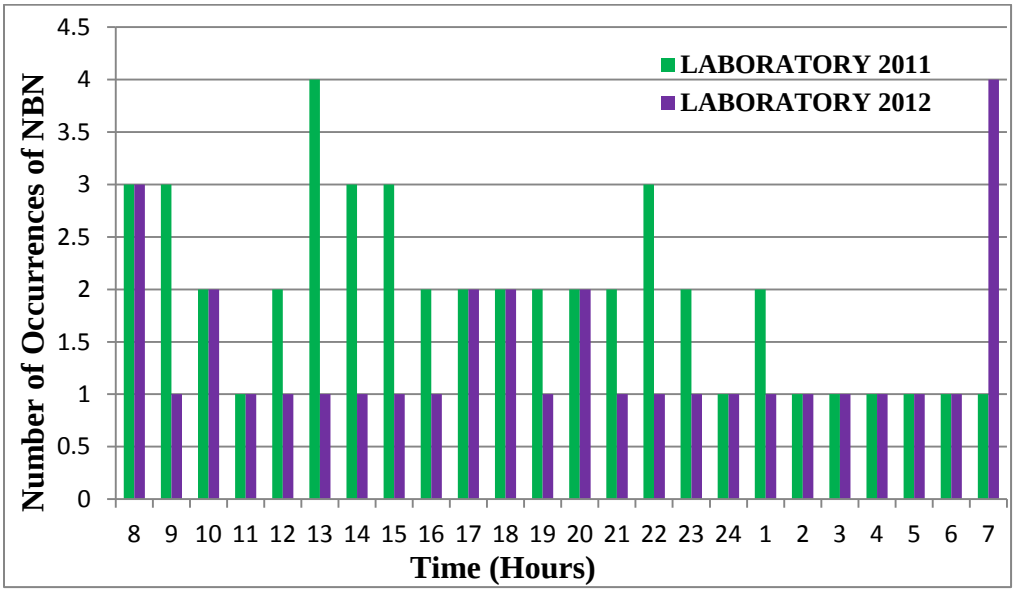

Figure 4.18: Laboratory narrow band noise number of occurrences for 2011 vs. 2012.

Figure 4.17 and 4.18 shows the residential narrow band noise number of occurrences for 2011 vs. 2012 and laboratory narrow band noise number of occurrences for 2011 vs. 2012. From

Figure 4.17, it can be observed that the number of occurrences of residential narrow band noise was higher in 2011 than in 2012, while on the other hand, Figure 4.18 shows that number of occurrences of laboratory narrow band noise was higher in 2012 than in 2011.

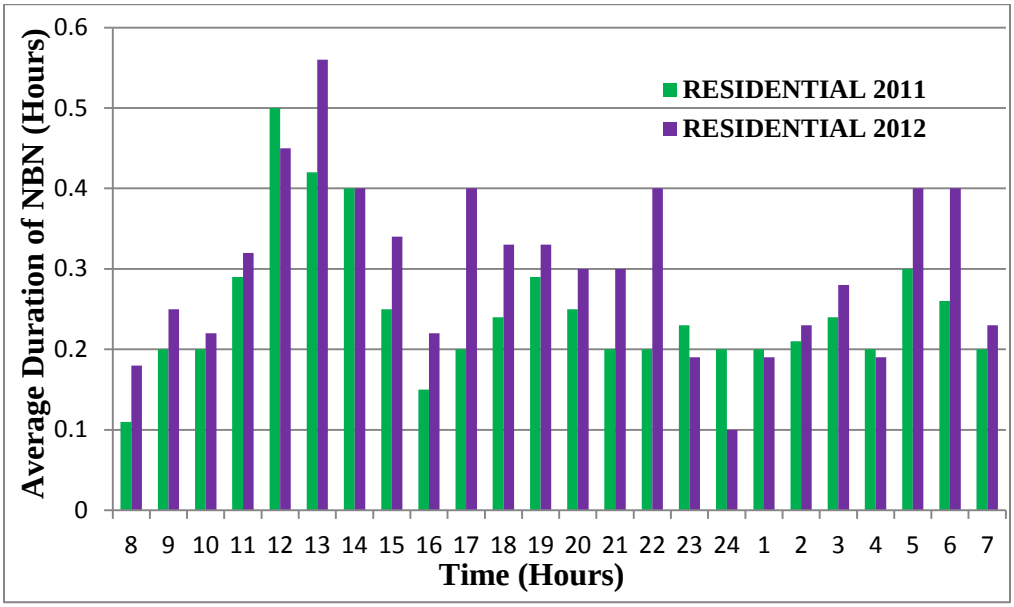

Figure 4.19: Residential narrow band noise average duration for 2011 vs. 2012.

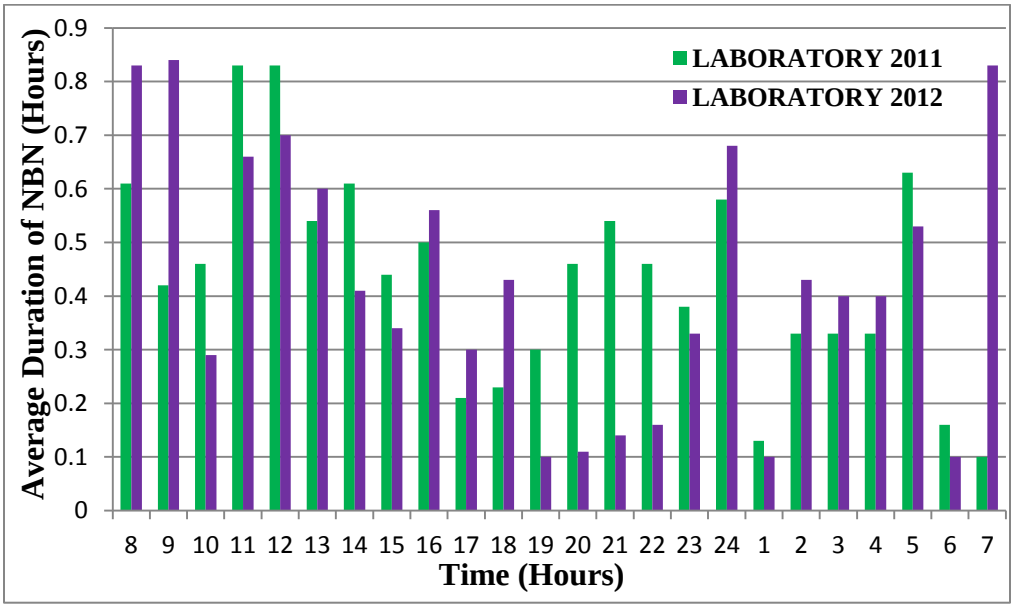

Figure 4.20: Laboratory narrow band noise average duration for 2011 vs. 2012.

Figure 4.19 and 4.20 shows the residential narrow band noise average duration for 2011 vs. 2012 and laboratory narrow band noise average duration for 2011 vs. 2012. It can be observed from

Figure 4.19 that the residential narrow band noise average duration is quite higher in 2012 than in 2011, while on the other hand, the laboratory narrowband noise average duration was quite higher in 2011 than in 2012.

In the next chapter, the error observation sequence generated from the measurement result is used as a training data to the Baum-Welch iterative algorithm for estimation of the Fritchman model parameters.

Chapter 5: Baum-Welch Algorithm Parameter Estimation of the Fritchman Model

5.0 Introduction

This section presents the modeling of the three noise types measured using the Baum-Welch algorithm iterative technique to estimate the Fritchman model parameters. Section 5.1 introduces the training data utilized as input to the Baum-Welch algorithm, while Section 5.2 describes the error observation sequences for the three types of noise generated from experimental measurements. Section 5.3 concludes with the modeling results for 2011 and 2012 noise model.

5.1 Fritchman Model Parameters for the Model

The training data for the Baum-Welch algorithm is given as follows. The state transition matrix A is given by the following.

$$\boldsymbol{A} = \begin{bmatrix} 0.9 & 0 & 0.1 \\ 0 & 0.8 & 0.2 \\ 0.1 & 0.2 & 0.7 \end{bmatrix}$$

As observed in the *A* matrix he values of a_{12} and a_{21} are zeros because for this unique case no transmission is allowed between the same groups of states i.e. transitions do not occur from good state to another good state. This unique condition makes it suitable to model real communication channels like the power line communications channels as it permits the existence of multiple degree of memory in the model [5]. The *A* matrix is assumed for the models, but note that the diagonal elements of the state transition probability *A* assumed is uniquely chosen to make sure that upon transitioning to a new state, there is high probability that the channel stays in the same state before transitioning to another one [5].

The *B* matrix is represented in matrix form as follows for the three-state Fritchman model.

$$\boldsymbol{B} = \begin{bmatrix} \Pr\{C|g\} & \Pr\{C|g\} & \Pr\{C|b\} \\ \Pr\{E|g\} & \Pr\{E|g\} & \Pr\{E|b\} \end{bmatrix}$$

Pr {C|g} denotes the probability of correct decision in the good state, while Pr {C|b} represents the probability of correct decision in bad state. Likewise, Pr {E|g} denotes the probability of error in the good state, while Pr {E|b} represents the probability of error in the bad state. Since it is assumed for the three-state model that errors only occur in the bad state hence the B matrix is represented in binary form below.

$$\boldsymbol{B} = \begin{bmatrix} 1 & 1 & 0 \\ 0 & 0 & 1 \end{bmatrix}$$

The first two columns represent the two good states while the last column represents the bad state. 1 denotes the probability that a correct decision or error will definitely happen, while 0 denotes the probability that a correct decision or error does not occur

Lastly, the initial state distribution $\boldsymbol{\pi}$ is represented below.

$$\boldsymbol{\pi} = [0.3 \quad 0.3 \quad 0.4]$$

Note that the error sequence generated for each type of noise measured on the power line is also fed as input to the Baum-Welch algorithm as these noises are modeled separately because of their different effect on signal propagation on the power line. This error observation sequence is 3072 in length so is not included in this section. Section 5.2 refers us to the error observation sequence data.

Also the number of state chosen for The Fritchman model is 3-states (two good states and a bad state), where the good states represent the error-free transmission while the bad state represents error transmission. The choice of one single error-state being sufficient for the model is based on the fact that it makes it possible for the error-free distribution to uniquely specify the single error state in other words this means that the model parameters can be derived from the error-free run distributions and vice versa [8].

Furthermore, the number of iteration at which the model parameters reach convergence is at the 20th iteration. With all the input parameters set, the inputs are fed in into the Baum-Welch algorithm for computation of the model parameters. Execution of the Baum-Welch algorithm with the three different error sequences generated for each type of noise results in three estimated channel model for the three noise types being modeled. The error-free run distribution and the probability of error resulting from these three noise models are also determined. Finally, the log-

likelihood function plot shows when the model attains convergence, this convergence is to a local maximum (an attribute of the Baum-Welch algorithm).

5.2 Error Observation Sequence for the Three Noise Types

For the generation of the error observation sequences for the three types of error, the threshold set for categorization of the noise type is used to generate the error sequence. Any noise impulse that is above the set threshold is regarded as an error and is denoted with binary '1' while any noise impulse below the set threshold is regarded as error-free and denoted with '0'. Based on the fact that the length of the noise observation is 3072 samples, which implies that the error observation sequence for the three noise type recorded has the same length T= 3072. Hence the error observation sequence cannot be included in this report but copied unto the CD accompanying this report.

5.3 Modeling Results for 2011 and 2012 Observation Sequences

This section analyzes the modeling results generated by the Baum-Welch algorithm. The estimated state transition matrix *A* for both 2011 and 2012 noise model is presented in Section 5.3.1, while the corresponding error probabilities of the model are presented in Section 5.3.2. In Section 5.3.3, the log-likelihood plot shows at what iteration the model parameter starts to converge. Finally, in Section 5.3.4, the error-free run distribution plot shows the probability of having *m* consecutive error-free states after the occurrence of an error.

5.3.1 Estimated State Transition Matrix

A	**NBN (r)**	**BN (r)**	**IN (r)**	**NBN (l)**	**BN (l)**	**IN (l)**
a_{11}	0.9851	0.9947	0.9947	0.9868	0.9962	0.9969
a_{13}	0.0149	0.0053	0.0030	0.0132	0.0038	0.0031
a_{22}	0.8050	0.8657	0.8679	0.7944	0.9595	0.7836
a_{23}	0.1950	0.1343	0.1321	0.2056	0.0405	0.2164
a_{31}	0.6676	0.2817	0.1762	0.7956	0.1867	0.4657
a_{32}	0.2090	0.5710	0.4968	0.0384	0.7252	0.2013
a_{33}	0.1235	0.1473	0.3270	0.1660	0.0881	0.3330

Table 5.1: Estimated state transition matrix for the 2011 noise sequence.

Table 5.1 above and Table 5.2 below show the estimated state transition matrix vectors realized from the three noise model for 2011 and 2012. Note that NBN (r) stands for narrowband noise captured at the residence, BN (r) stands for background noise captured at the residence, IN (r) stands for impulse noise measured at the residence, NBN (l) stands for narrowband noise captured at the laboratory, BN (l) stands for background noise captured at the laboratory and IN (l) stands for impulse noise captured at the laboratory.

Observing Table 5.1, note that for the two measurement environment that the transition matrices under the BN (r) and IN (r) are the most similar, while for Table 5.2 below, the transition matrices under NBN (l) and BN (l) are also the most similar. Drawing an inference from this, it implies that the PLC channel characteristics are of most similarity under these two scenarios. On the contrary, the difference in channel characteristics among other noise scenario is large.

A	**NBN (r)**	**BN (r)**	**IN (r)**	**NBN (l)**	**BN (l)**	**IN (l)**
a_{11}	0.9928	0.9900	0.9933	0.9955	0.9959	0.9988
a_{13}	0.0072	0.0100	0.0067	0.0045	0.0041	0.0012
a_{22}	0.8938	0.8703	0.8948	0.8918	0.8258	0.9785
a_{23}	0.1062	0.1297	0.1052	0.1082	0.1742	0.0215
a_{31}	0.2594	0.4737	0.3913	0.3923	0.4298	0.0424
a_{32}	0.5973	0.2801	0.3408	0.3378	0.2976	0.6660
a_{33}	0.1433	0.2463	0.2679	0.2700	0.2726	0.2915

Table 5.2: Estimated state transition matrix for the 2012 noise sequence.

5.3.2 Error Probabilities of the Model

Table 5.3 and Table 5.4 indicate error probabilities of the noise model for 2011 and 2012 respectively. Note that it can be observed from both tables that the three noise models possess low error probability with the IN (l) showing the lowest error probability for both 2011 and 2012 noise models.

	NBN (r)	**BN (r)**	**IN (r)**	**NBN (l)**	**BN (l)**	**IN (l)**
Pe	0.0221	0.0215	0.0163	0.0150	0.0098	0.0081

Table 5.3: Error Probabilities (P_e) for the different Noise models (2011 error sequence).

	NBN (r)	BN (r)	IN (r)	NBN (l)	BN (l)	IN (l)
Pe	0.0241	0.0225	0.0182	0.0104	0.0124	0.0062

Table 5.4: Error Probabilities (P_e) for the different Noise models (2012 error sequence).

5.3.3 The Log-likelihood Ratio Plots

For large data size, the computation of the forward and backward variables tends to zero exponentially, hence, the need for proper scaling so as to prevent numerical underflow. The scaling constant used and implemented for the Baum-Welch algorithm Matlab code is represented with the mathematical notation as follows [142].

$$C_t = \sum_{i=1}^{N} \alpha_t\,(i) \tag{5.1}$$

For example the scaled value of $\alpha_t\,(j)$ is denoted by $\overline{\alpha_t}\,(j)$ and is represented by the mathematical notation shown as follows.

$$\overline{\alpha_t}\,(j) = {\alpha_t\,(j)}/{C_t} \tag{5.2}$$

Which invariably that

$$\sum_{i=1}^{N} \overline{\alpha_t}\,(i) = 1 \tag{5.3}$$

The values of the scaling constant C_t are then saved and used in the scaling of the backward variables. Hence, the scaled values of the backward variables $\beta_t(i)$ are denoted by $\overline{\beta_t}$ and are mathematically represented as follows [142].

$$\overline{\beta_i}(i) = {\beta_i(i)}/{C_t} \tag{5.4}$$

The initialization is mathematically represented as

$$\overline{\beta_T} = \frac{1}{C_T} \tag{5.5}$$

In the equation above, the 1 refers to column vector containing all ones. Normalization of the gamma variables is also possible if desired but not essential. A more detailed discussion on scaling can be found in [150].

Because Baum-Welch algorithm is an iterative algorithm, to achieve a required level of model accuracy, there is need to determine the number of iterations that must be executed. Possibly one of the best ways to achieve this accuracy is to display the estimated values of *A* and *B* while the Baum-Welch algorithm is executing until the desired level of accuracy is reached.

Take for example, the desire to have the values of *A* and *B* to a given number of significant figures (a four decimal place was assumed in this project), execution of the Baum-Welch algorithm is therefore allowed to run until no changes in the value of *A* and *B* is experienced within the desired accuracy, thence the algorithm terminated manually [142]. Another best method of convergence determination is to allow the algorithm to run until consecutive values of $Pr\ [\bar{O}\ |\Gamma]$ differ very little as the Baum-Welch algorithm has been confirmed to converge to a maximum likelihood result [150].

$Pr\ [\bar{O}\ |\Gamma]$ is mathematically determined in terms of the earlier defined scaling constant C_t represented as follows [142].

$$Pr\ [\bar{O}\ |\Gamma] = \prod_{t=1}^{T} C_t \tag{5.6}$$

For error sequence where *T* is large, the value is very small and is commonly expressed mathematically as follows

$$log_{10}\, Pr\ [\bar{O}\ |\Gamma] = \sum_{t=1}^{T} log_{10} C_t \tag{5.7}$$

The above equation is referred to as the log-likelihood ratio and the plot for the different noise model is as shown in Figure 5.1 and 5.2.

It can be ascertained that the derived model yields acceptable performance because the Baum-Welch algorithm converges to a local maximum likelihood evident in the log-likelihood ratio plot shown in Figure 5.1 and 5.2, showing a desired level of convergence and accuracy.

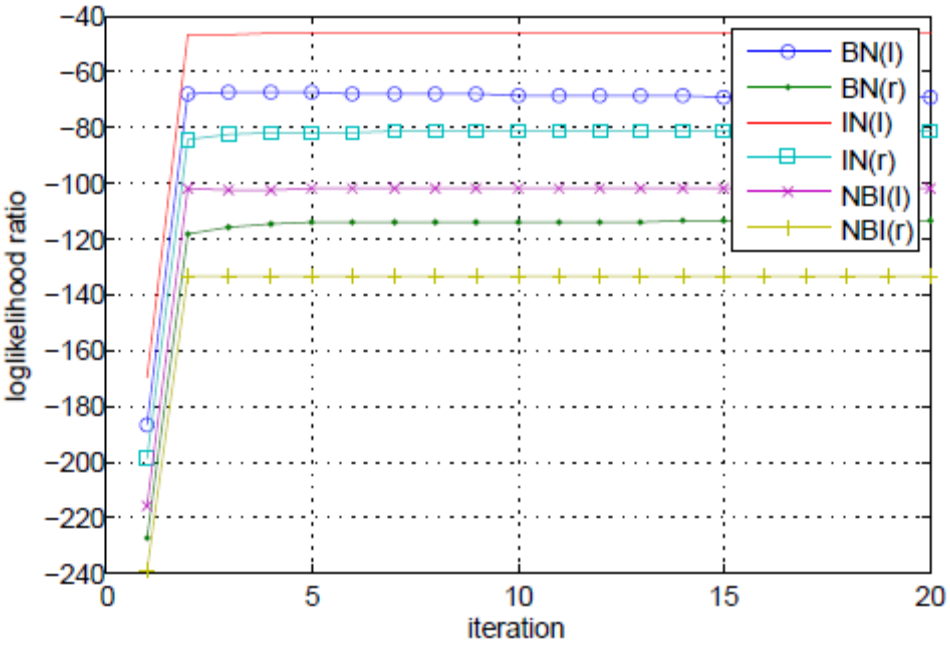

Figure 5.1: Log-likelihood ratio vs. iteration for 2011.

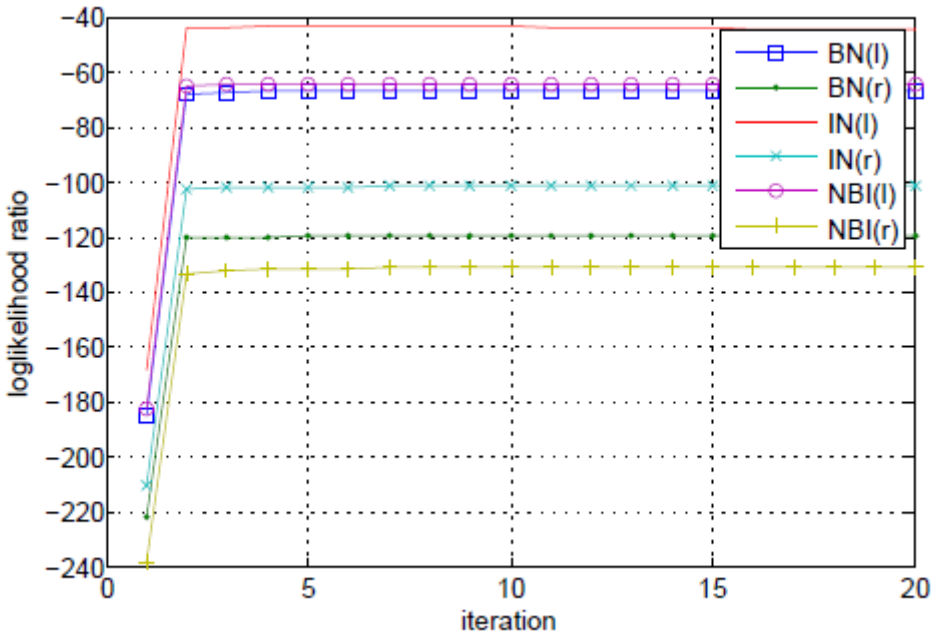

Figure 5.2: Log-likelihood ratio vs. iteration for 2012.

Figure 5.1 and 5.2 above shows the log-likelihood ratio plot for 2011 and 2012 respectively. This plot shows similar level of convergence point between the different noise models. And it was

discovered that the model parameters converges quickly and the point of accuracy chosen was the 20th iteration where the model parameter value remained constant with no changes.

5.3.4 Error-free run Distribution Plot

Figure 5.3 and 5.4 below show the error-free run distribution plot $Pr(0^m|1)$, for the 2011 and 2012 noise model respectively. This error-free run plot shows the probability of transitioning to *m*-consecutive error-free state after the occurrence of an error. For Figure 5.3, the length of *m*-consecutive error-free intervals obtained for the 2011 noise model are given as follows for the individual noise models: BN (l) = 719, BN (r) = 901, IN (l) = 1025, IN (r)= 1365, NBI (l) =379 and NBI (r) = 182. On the other hand, from Figure 5.4, the corresponding length of *m*-consecutive error-free intervals obtained for the 2012 noise model are given as follows for the individual noise models: BN (l)=793, BN (r)=544, IN (l)=1254, IN (r)=586, NBI (l)=790 and NBI (r)=493. A comparison between Figure 5.3 and 5.4 shows that both BN (l) and IN (l) show considerably similar length of error-free runs which can also be attributed to similar channel characteristics at both instances, while others show large deviation in the length of intervals obtained due to different channel characteristics.

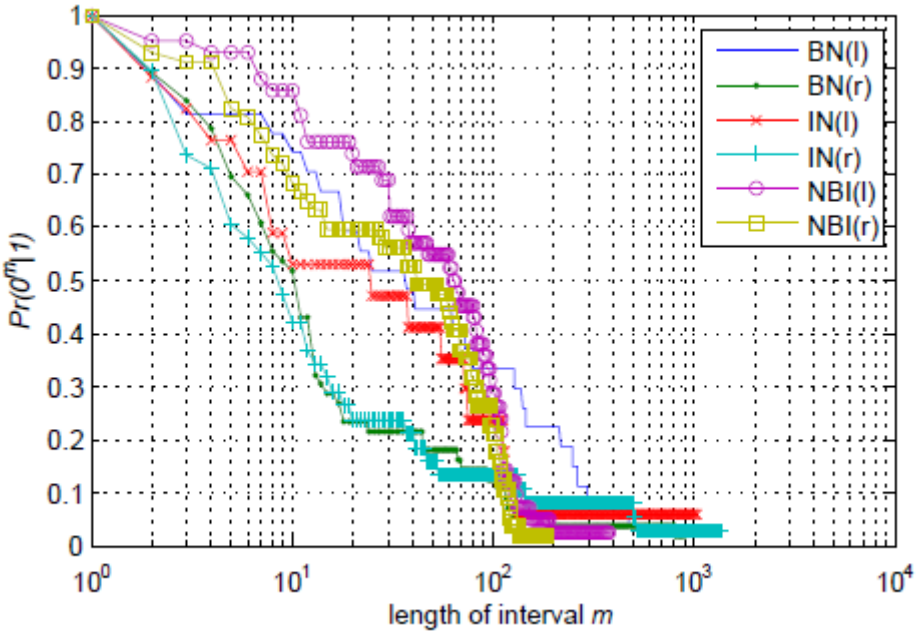

Figure 5.3: Pr (0^m|1) vs. interval *m* for 2011.

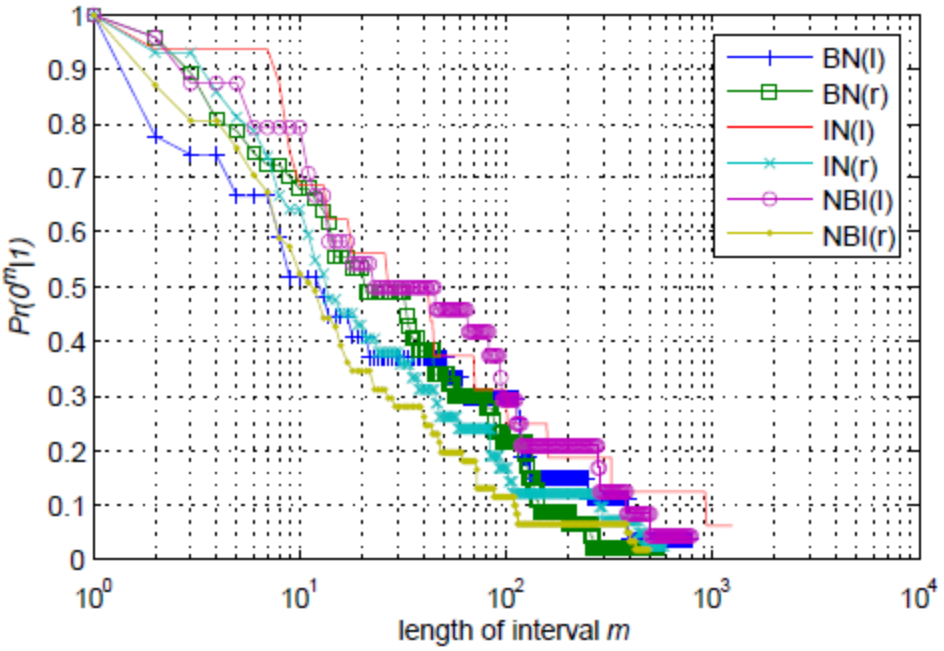

Figure 5.4: Pr (0^m|1) vs. interval *m* for 2012.

Chapter 6: Research Summary and Conclusion

6.0 Introduction

This chapter concludes this research report with a brief summary of each chapter of this research report in Section 6.1. Section 6.2 presents a conclusion of this research report. This chapter ends with recommendations and proposed future works in Section 6.3.

6.1 Research Summary

This section presents a brief highlight of what is covered in this research project:

In this research report, firstly, a contextualization of the research study was carried out, defining the problem statement, the motivation for this project and the scope and objectives of the research.

In Chapter 2, a literature review of related works was presented under the following headings: PLC historical overview, PLC channel and noise modeling, Fritchman model and the Baum-Welch algorithm.

In Chapter 3, PLC techniques related to work carried out in this research was presented. First, an overview of PLC technology studied, followed by the overview of PLC standardization landscape. PLC channel characteristics, noise classification and coupling circuit were also discussed. An in-depth study of the hidden Markov model was carried out, while the study of the Baum-Welch algorithm concludes this chapter.

In Chapter 4, the measurement methodology utilized for noise classification and measurement was the subject of this chapter. Moreover, the measurement site was also described, while the experimental setup used for noise data capture was shown. Presentation and discussion of measurement results concludes this chapter.

In Chapter 5, the modeling results were presented. First, the Fritchman model parameter assumed for the model was presented, while the training data (the error observation sequence) was

introduced. The estimated state transition matrix and error probabilities resulting from the model for each noise type were discussed. The log-likelihood ratio plot was shown for a clear view of how the model parameter converges and the number of iteration carried out before the parameters start to converge. Conclusively, this chapter ends with a discussion of the error-free distribution plot showing the probability of transitioning to error-free states after the occurrence of an error.

6.2 Conclusion

PLC is fast becoming an alternative for home automation and in-home networking, because of the advantage it offers over other medium of communication as a result of the already existing ubiquitous network it uses as a medium for communication, hence reducing the cost of having to lay new cables for data communication and home automation and networking. Despite the advantages PLC offers over other communication media, it still faces several challenges in its quest to realize its full potential and offer reliable data communication media. This challenges are as a result of the fact that the power line network been used by PLC was not originally intended for data communication, therefore it inherits the harsh intrinsic attribute of the power line which are unfriendly to data communication. One of this intrinsic attributes is the noise present on this network. Hence, there is a need to understand the PLC channel attributes, and there is need for a meaningful channel modeling.

Furthermore, understanding of the channel attributes and characteristics can only be realized through measurement and modeling of the channel impairment that are present on the PLC channel, hence the motivation behind the measurement and modeling of noise on the PLC channel.

An experimental measurement of noise was carried out on the CENELEC A-band at two metropolitan locations of South Africa (a residential detached building with several major household electrical and electronic appliances which are sources of noise and the electric circuits and electronics laboratory of the school of Electrical and Information Engineering department of the University of Witwatersrand, Johannesburg, South Africa). The measurement of noise was carried out over a complete day within a two year span. The analysis of the three major types of noise captured shows the statistical properties of noise on the CENELEC A-band.

Furthermore, a first-order modeling of the three noise types measured was carried out using the Fritchman hidden Markov model whose parameters were estimated with the use of an iterative algorithm referred to as Baum-Welch algorithm. These three noise type were modeled separately because each has its own characteristics and distinguishing effects on data communication on the PLC channel. The corresponding state transition matrix A for the three types of noise was computed and the error free-run distribution plots shown accordingly. The noise measurement and modeling results apart from showing the statistical properties of the noise type (error-free distribution) show the error patterns and behavior of noise on the CENELEC A-band, hence this information becomes useful when transmitting on the PLC channel. The results are useful and are essential in the evaluation of the performance of coding techniques and modulation schemes on the PLC channel. Hence, these evaluations can then be used for the optimization of PLC system design to achieve reliable data communication on the harsh PLC channel.

6.3 Recommendation and Proposed Future Work

This resulting model from this work can be used in the design and evaluation of modulation schemes and coding/decoding techniques used on the PLC channel. It is also useful in optimizing the design of PLC system designs.

Below are recommended works which are beyond the scope of this research so as to enhance a better understanding of the PLC channel attributes and further modeling:

Measurement of power line impedance and analysis.

A second-order description of the channel (investigating the correlation properties of the Markov chains).

A novel approach for noise measurement on the PLC channel.

Evaluation of different modulation schemes on PLC channel.

References

[1] B. S. I. Staff, “Signalling on Low-voltage Electrical Installations in the Frequency Range 3 KHz to 148.5 KHz. Immunity Requirements for Mains Communications Equipment and Systems Operating in the Range of Frequencies 3 KHz to 95 KHz and Intended for Use by Electricity Suppliers and Distributors”. *B. S. I. Standards*, 2003.

[2] M. Katayama, T. Yamazato, and H. Okada, “A mathematical model of noise in narrowband power line communication systems,” *Selected Areas in Communications, IEEE Journal on*, vol. 24, no. 7, pp. 1267 – 1276, July 2006.

[3] G. Bumiller and N. Pirschel, “Airfield ground lighting automation system realized with power line communication,” *in Proc. 8th International Symposium Power Line Communications and Its Application*, pp. 16–20, 2003.

[4] G. Griepentrog, “Power line communication on 750V DC networks,” *in 5th International Symposium on Power-Line Communications and Its Applications*, pp. 259–265, Malmö, Sweden, April 4-6, 2001.

[5] B. Fritchman, “A binary channel characterization using partitioned Markov chains,” Information Theory, IEEE Transactions on, vol. 13, no. 2, pp. 221 –227, April 1967.

[6] E.N. Gilbert, “Capacity of burst-noise channel”, Bell System Technical Journal, vol. 39, no. 9, pp. 1253-1265, 1960.

[7] L. E. Baum, T. Petrie, G. Soules, and N. Weiss, “A maximization technique occurring in the statistical analysis of probabilistic functions of Markov chains,” *The Annals of Mathematical Statistics*, vol. 41, no. 1, pp. 164–171, 1970.

[8] M. Schwartz, “History of communications-Carrier-wave telephony over power lines: Early history,” *IEEE Communication Magazine*, vol. 47, no. 1, pp. 14–18, Jan. 2009.

[9] K. Dostert, Power Line Communications. Upper Saddle River, NJ: Prentice Hall, 2001.

[10] H. Ferreira, L. Lampe, J. Newbury, and T. Swart, Eds., "Power Line Communications," 1st ed. New York: Wiley, 2010.

[11] T. Waldeck, T, M. Busser, and K. Dostert, "Telecommunication applications over the low voltage power distribution grid," *Spread Spectrum Techniques and Applications, IEEE 5th International Symposium on,* pp.73-77, Sep 2-4, 1998.

[12] R. Broadbridge, "Power line modems and networks," *Telecommunications, Second IEE National Conference on,* pp.294-296, 2-5 Apr. 1989.

[13] B. E. Eyre, "Results of A Comprehensive Field Trial of A United Kingdom Customer Telemetry System Using Mains Borne Signaling", *Proceedings of the Sixth International Conference on Metering Apparatus and Tariffs for Electricity Supply*, IEE Conference Publication no. 317, pp. *252-256***,** 1990.

[14] M. Hosono, "Improved Automatic meter reading and load control system and its operational achievement," *4th International Conference on metering, apparatus and tariffs for electricity supply*, pp.26-28, October 1982.

[15] Jean-Pierre Auffret, and Jeffrey H. Matsuura, "Technological Change, Telecommunications Deregulation, Telecommunications Economics, and Internet Globalization" *Proc. in Institute for New Economic Thinking (INET)*, Online [Available]: http://www.isoc.org/inet98/proceedings/5c/5c_3.htm. Accessed on 15 February, 2013.

[16] D. Hong, J. Lee, and J. Choi, "Power Quality Monitoring System Using Power Line Communication," *Information, Communications and Signal Processing, Fifth International Conference on,* pp.931-935, 2005.

[17] I.H. Cavdar, "A solution to remote detection of illegal electricity usage via power line communications," *Power Delivery, IEEE Transactions on*, vol.19, no.4, pp. 1663-1667, Oct. 2004.

[18] D.E. Nordell, "Communication systems for Distribution Automation," *Transmission and Distribution Conference and Exposition, T&D. IEEE/PES*, pp.1-14, 21-24 April 2008.

[19] D. Rieken and M. Walker, "Distance effects in low-frequency power line communications," *in Proc. IEEE International Symposium on Power Line Communications and Its Applications,* Rio de Janeiro, Brazil, Mar. 28–31, 2010.

[20] D. Clark, D, "Power line communications: finally ready for prime time?," *Internet Computing, IEEE*, vol.2, no.1, pp.10-11, Jan. 1998.

[21] The Open PLC European Research Alliance (OPERA). Online [Available]: http://www.ist-opera.org. Accessed on 18 February, 2013.

[22] E. Biglieri, "Coding and modulation for a horrible channel," *Communications Magazine, IEEE*, vol.41, no.5, pp. 92-98, May 2003.

[23] M. Gotz, M. Rapp, and K. Dostert, "Power line channel characteristics and their effect on communication system design," *IEEE Communication Magazine*, vol. 42, no. 4, pp. 78-86, Apr. 2004.

[24] S. Galli and A. Scaglione, "Discrete-time block models for transmission line channels: Static and doubly selective cases," *arXiv preprint arXiv: 1109.5382* (2011).

[25] P. Amirshahi, F. Canete, K. Dostert, S. Galli, M. Katayama, and M. Kavehrad, "Channel characterization," *in Power Line Communications*, H. Ferreira, L. Lampe, J. Newbury, and T. Swart, Eds., 1st ed. New York: Wiley, 2010.

[26] S. Galli and T. Banwell, "A novel approach to the modeling of the indoor power line channel -Part II: Transfer function and its properties," *IEEE Trans. Power Del*., vol. 20, no. 3, pp. 1869–1878, Jul. 2005.

[27] M. Zimmermann and K. Dostert, "A multipath model for the power line channel," *IEEE Transaction on Communication*, vol. 50, no. 4, pp. 553–559, Apr. 2002.

[28] S. Galli, "A simplified model for the indoor power line channel," *in Proc. IEEE International Symposium on Power Line Communications and Its Application*, Dresden, Germany, Mar. 29–Apr. 1, 2009.

[29] S. Galli and T. Banwell, "A deterministic frequency-domain models for the indoor power line transfer function," *IEEE Journal on Selected Areas in Communication*., vol. 24, no. 7, pp. 1304–1316, Jul. 2006.

[30] F. Canete, J. Corte´s, L. Dıez, and J. Entrambasaguas, "Analysis of the cyclic short-term variation of indoor power line channels," *IEEE Journal Selected Areas in Communications*, vol. 24, no. 7, pp. 1327–1338, Jul. 2006.

[31] H. Meng, S. Chen, Y.L. Guan, C.L. Law, P.L. So, E. Gunawan, and T.T. Lie, "Modeling of transfer Characteristics for the broadband power line communication channel," *Power Delivery, IEEE Transactions on* , vol.19, no.3, pp. 1057- 1064, July 2004.

[32] H. Philipps, "Modeling of power line communications channels," *in Proceedings International Symposium on Power Line Communications and Its Application,* Lancaster, U.K., Mar. 30–Apr. 1, 1999.

[33] L.T. Tang, P.L. So, E. Gunawan, Y.L. Guan, S. Chen, and T.T. Lie, "Characterization and modeling of in-building power lines for high-speed data transmission," *Power Delivery, IEEE Transactions on* , vol.18, no.1, pp. 69- 77, Jan 2003.

[34] D. Anastasiadou and T. Antonakopoulos, "An Experimental Setup for Characterizing the Residential Power Grid Variable Behavior," *in Proc. IEEE International Symposium on Power Line Communications and Its Applications,* Athens, Greece, March 2002.

[35] T. Esmailian, F. R. Kschischang, and P.G. Gulak, "An in-building power line channel simulator," *in IEEE International Symposium on Power Line Communications and Its Applications*, Apr. 2000.

[36] D. Sabolic, A. Bazant, and R. Malaric, "Signal propagation modeling in power-line communication networks," *Power Delivery, IEEE Transactions on* , vol.20, no.4, pp. 2429-2436, Oct. 2005.

[37] J. Barnes, “A physical multi-path model for power distribution network propagation,” *in Proc. IEEE International Symposium on Power Line Communications and Its Application,* Tokyo, Japan, Mar. 24–26, 1998.

[38] M. Zimmermann and K. Dostert, “A multi-path signal propagation model for the power line channel in the high frequency range,” *in Proc. IEEE International Symposium on Power Line Communications and Its Application*, Lancaster, UK, Mar. 30–Apr. 1, 1999.

[39] H. Meng, S. Chen, Y.L. Guan, C.L. Law, P.L. So, E. Gunawan, and T.T. Lie, “A transmission line model for high-frequency power line communication channel,” *Power System Technology, Proceedings International Conference on*, vol.2, no., pp. 1290-1295, 2002.

[40] T. Banwell and S. Galli, “A new approach to the modeling of the transfer function of the power line channel,” *in Proc. IEEE International Symposium on Power Line Communications and Its Application*, Malmo, Sweden, Apr. 4–6, 2001.

[41] T. Sartenaer, and P. Delogne, “Power line cables modeling for broadband communications,” *in Proc. IEEE International Symposium on Power Line Communications and Its Application*, Malmo, Sweden, Apr. 4–6, 2001.

[42] T. Esmailian, F. Kschischang, and P. Gulak, “In-building power lines as high-speed communication channels: Channel characterization and a test channel ensemble,” *International Journal on Communication Systems,* vol. 16, pp. 381–400, 2003.

[43] T. Banwell and S. Galli, “A novel approach to the modeling of the indoor power line channel-Part I: Circuit analysis and companion model,” *IEEE Trans. Power Del.*, vol. 20, no. 2, pp. 655–663, Apr. 2005.

[44] M. Tlich, A. Zeddam, F. Moulin, and F. Gauthier, “Indoor power-line communications channel characterization up to 100 MHz- part I: One-parameter deterministic model,” *IEEE Trans. on Power Delivery*, vol. 23, no. 3, pp. 1392-1401, July 2008.

[45] M. Zimmermann, and K. Dostert, "An analysis of the broadband noise scenario in power line networks," *in Proc. IEEE International Symposium on Power line Communications and its Applications*, pp. 131-138, 2000.

[46] H. Meng, Y.L. Guan, and S. Chen, "Modeling and analysis of noise effects on broadband power-line communications," *Power Delivery, IEEE Transactions on* , vol.20, no.2, pp. 630-637, April 2005.

[47] D. Benyoucef, "A new statistical model of the noise power density spectrum for power line communication," *in Proc. IEEE International Symposium on Power Line Communications and Its Applications,* pp. 136–141, 2003.

[48] H. Philipps, "Development of a statistical model for power line communication channels," in *IEEE International Symposium on Power Line Communications and Its Applications ISPLC '2000*, pages 153–159, 2000.

[49] M. Babic, M. Hagenau, K. Dostert, and J. Bausch, "Theoretical postulation of PLC channel model," *IST Integrated Project Deliverable D4v2. 0, The OPERA Consortium* (2005).

[50] A. G. Burr, D.M.W. Reed, and P.A. Brown, "HF Broadcast Interference on LV Mains Distribution Networks," in *Proc. IEEE International Symposium on Power Line Communications and Its Applications*, pp. 253–262, 1998.

[51] M. Arzberger, K. Dostert, T. Waldeck, and M. Zimmermann, "Fundamental properties of the low voltage distribution grid," in *Proc. IEEE International Symposium on Power Line Communications and Its Applications*, pp. 45–50, 1997.

[52] S. Baig and N.D. Gohar, "A discrete multi-tone transceiver at the heart of the PHY layer of an in-home power line communication local-area network," *Communications Magazine, IEEE,* vol.41, no.4, pp. 48-53, April 2003.

[53] M. Katayama, S. Itou, T. Yamazato, and A. Ogawa, "Modeling of cyclo-stationary and frequency dependent power-line channels for communications," in *Proc. IEEE*

International Symposium on Power Line Communications and Its Applications, pp. 123–130, 2000.

[54] G. Laguna, and R. Barron, "Survey on Indoor Power Line Communication Channel Modeling," *Electronics, Robotics and Automotive Mechanics Conference*, pp.163-168, Sept. 30 2008-Oct. 3 2008.

[55] S. Sancha, F.J. Canete, L. Diez, and J.T. Entrambasaguas, "A Channel Simulator for Indoor Power-line Communications," *Power Line Communications and Its Applications, IEEE International Symposium on*, pp.104-109, 26-28 March 2007.

[56] T. Calliacoudas and F. Issa, "Multi-conductor Transmission Lines and Cables Solver, an Efficient Simulation Tool for PLC Networks Development" in *Proc. IEEE International Symposium on Power Line Communications and Its Applications*, 2002.

[57] F. Versolatto, and A.M. Tonello, "Analysis of the PLC channel statistics using a bottom-up random simulator," in *Proc. IEEE International Symposium on Power Line Communications and Its Applications*, pp.236-241, 28-31 March 2010.

[58] J. Yazdani, M. Naderi, and B. Honary, "Power Line Analyzing Tool (plat) for Channel Modeling," in *IEEE International Symposium on Power Line Communications and Its Applications*, pp. 21–28, 2001.

[59] F.J. Canete, J.A. Cortes, L. Diez, J.T. Entrambasaguas, and J.L. Carmona, "Fundamentals of the cyclic short-time variation of indoor power-line channels," in *Proc. IEEE International Symposium on Power Line Communications and Its Applications*, pp. 157-161, 6-8 April 2005.

[60] S. Barmada, A. Musolino, and M. Raugi, "Innovative model for time-varying power line communication channel response evaluation," *Selected Areas in Communications, IEEE Journal on* , vol.24, no.7, pp. 1317-1326, July 2006.

[61] D.R. Oosthuizen, H.C. Ferreira, and F. Swarts, "On renewal inner channels and block code error control outer channels," *Global Telecommunications Conference, and*

Exhibition. Communications Technology for the 1990s and Beyond, IEEE, pp. 1703-1707, vol.3, 27-30 Nov 1989.

[62] A. Drukarev, and K. Yiu, "Performance of Error-Correcting Codes on Channels with Memory," *Communications, IEEE Transactions on*, vol.34, no.6, pp. 513-521, June 1986.

[63] M.D. Knowles, and A.I. Drukarev, "Bit error rate estimation for channels with memory," *Communications, IEEE Transactions on*, vol.36, no.6, pp.767-769, June 1988.

[64] S. Tsai, "Markov Characterization of the HF Channel," *Communication Technology, IEEE Transactions on*, vol.17, no.1, pp.24-32, February 1969.

[65] M. Lotter, P. Van Rooyen, and F. Swarts, "Markov Channel Models for DS-CDMA Communications," *the Transactions of the S.A. Institute of Electrical Engineers*, June 1997.

[66] F. Swarts, and H.C. Ferreira, "Markov characterization of digital fading mobile VHF channels," *Vehicular Technology, IEEE Transactions on*, vol.43, no.4, pp.977-985, Nov 1994.

[67] F. Antoni, *"Statistics of error distribution in data transmission on VHF-channels"*, Signal processing 11: theories and applications (Elsevier, 1983) Schussler, H.W. (Ed.).

[68] J. Garcia-Frias, and P.M. Crespo, "Hidden Markov models for burst error characterization in indoor radio channels," *Vehicular Technology, IEEE Transactions on*, vol.46, no.4, pp.1006-1020, Nov 1997.

[69] A. Van Heerden, H.C. Ferreira, "Modeling of mobile frequency hopped VHF channels and error correction on the channel," *Communications, Discovering a New World of Communications., IEEE International Conference on*, pp.1047-1051, 14-18, June 1992.

[70] D. Dalalah, L. Cheng, and G. Tonkay, "Modeling End-to-End Wireless Lossy Channels: A Finite-State Markov Approach," *Wireless Communications, IEEE Transactions on*, vol.7, no.4, pp.1236-1243, April 2008.

[71] J.A.W. Tina, A.J. Snyders, and H.C. Ferreira, "Implementation of a gap recorder for measuring impulsive noise error distributions in Power Line Communications using the Fritchman model," in *Proc. IEEE International Symposium on Power Line Communications and Its Applications*, pp.374-379, 27-30 March 2012.

[72] X. Zhang, Y. Wang, and Z. Zhao, "A Hybrid Speech Recognition Training Method for HMM Based on Genetic Algorithm and Baum Welch Algorithm," *Innovative Computing, Information and Control, Second International Conference on*, pp.572, 5-7 Sept. 2007.

[73] V. Breuer, and G. Radons, "Baum-Welch re-estimation formula for coupled sequential machines," *Signal Processing, IEEE Transactions on*, vol.43, no.5, pp.1313-1316, May 1995.

[74] S. Kim, and S.B. Wicker, "An exploration of the relationship between the Baum-Welch algorithm and turbo decoding," *Information Theory, Proceedings IEEE International Symposium on*, pp.119, 16-21 Aug 1998.

[75] B. Matuz, F.L. Blasco, G. Liva, "On the Application of the Baum-Welch Algorithm for Modeling the Land Mobile Satellite Channel," *Global Telecommunications Conference, IEEE*, pp.1-5, 5-9 Dec. 2011.

[76] L.A. Johnston, and J.H. Elder, "Efficient Computation of Closed Contours using Modified Baum-Welch Updating," *Computer Vision and Pattern Recognition Workshop, Conference on*, pp. 48, 27-02 June 2004.

[77] S. Cheshomi, S. Rahati-Q, and M.-R. Akbarzadeh-T, "Hybrid of Chaos Optimization and Baum-Welch algorithms for HMM training in Continuous speech recognition," *Intelligent Control and Information Processing, International Conference on*, pp.83-87, 13-15 Aug. 2010.

[78] S. Cheshomi, S. Rahati-Q, and M.-R. Akbarzadeh-T, "HMM training by a hybrid of Chaos Optimization and Baum-Welch algorithms for discrete speech

recognition," *Digital Content, Multimedia Technology and its Applications, 6th International Conference on*, pp.337-341, 16-18 Aug. 2010.

[79] F. Gelgi, H. Davulcu, "Baum-Welch Style EM Approach on Simple Bayesian Models for Web Data Annotation," *Web Intelligence, IEEE/WIC/ACM International Conference on*, pp.736-742, 2-5 Nov. 2007.

[80] H.A. Cirpan, and E. Panayirci, "Blind channel estimation for space-time coding systems with Baum-Welch algorithm," *Communications, IEEE International Conference on*, vol.3, pp. 1579-1583, 2002.

[81] M. Nissila, S. Pasupathy, "Adaptive Baum-Welch algorithms for frequency-selective fading channels," *Communications, IEEE International Conference on*, vol.1, no., pp.79-83, 2002.

[82] R. Hsiao, Yik-Cheung Tam, and T. Schultz, "Generalized Baum-Welch algorithm for discriminative training on large vocabulary continuous speech recognition system," *Acoustics, Speech and Signal Processing, IEEE International Conference on*, pp.3769-3772, 19-24 April 2009.

[83] T.N Sainath, D. Kanevsky, G. Iyengar, "Unsupervised Audio Segmentation using Extended Baum-Welch Transformations," *Acoustics, Speech and Signal Processing, IEEE International Conference on*, pp.I-209-I-212, 15-20 April 2007.

[84] H. Hrasnica, A. Haidine, and R. Lehnert, "Broadband Power line Communications: Network Design," *Dresden University of Technology, Ed. Wiley* (2004).

[85] S. Mak and D. Reed, "TWACS, a new viable two-way automatic communication system for distribution networks. Part I: Outbound communication," *IEEE Trans. Power App. Syst.*, vol. PAS-101, no. 8, pp. 2941-2949, Aug. 1982.

[86] S. Mak and T. Moore, "TWACS, a new viable two-way automatic communication system for distribution networks. Part II: Inbound communication," *IEEE Trans. Power App. Syst.*, vol. PAS-103, no. 8, pp. 2141–2147, Aug. 1984.

[87] S. Galli, A. Scaglione, and Z. Wang, "For the Grid and Through the Grid: The Role of Power Line Communications in the Smart Grid," *Proceedings of the IEEE*, vol.99, no.6, pp.998-1027, June 2011.

[88] Comité Européen de Normalisation Electrotechnique: [Online]: Available on http://www.cenelec.eu

[89] Federal Communications Commission: Online [Available]: http://www.fcc.gov Accessed on 15 February, 2013.

[90] Carcelle Xavier, "*Power line communications in practice*," Artech House Publishers, 2009.

[91] J. García-Hernández, "Análisis de Estándares Aplicables a Sistemas BPL (Broadband over Power Lines)", Internal Technical Report, IIE, March 2007.

[92] International Electrotechnical Commission: Online [Available]: http://www.iec.ch/ Accessed on 15 February, 2013.

[93] International Special Committee on Radio Interference: Online [Available]: http://www.iec.ch Accessed on 15 February, 2013.

[94] International Organization for Standardization. Online [Available]: http://www.iso.ch Accessed on 15 February, 2013.

[95] International Telecommunication Union. Online [Available]: http://www.itu.int Accessed on 15 February, 2013.

[96] American National Standards Institute. Online [Available]: http://www.ansi.org Accessed on 15 February, 2013.

[97] Electronic Industries Alliance: Online [Available]: http://www.eia.orgn Accessed on 15 February, 2013.

[98] Institute of Electrical and Electronics Engineers: Online [Available]: http://www.ieee.org Accessed on 15 February, 2013.

[99] European Telecommunications Standards Institute: Online [Available]: http://www.etsi.org Accessed on 15 February, 2013.

[100] Information and Communications Technologies Standards Board: Online [Available]: http://www.ict.etsi.org Accessed on 15 February, 2013.

[101] S. Galli, M. Koch, H. Latchman, S. Lee, and V. Oksman, "Industrial and international standards on PLC base networking technologies," in *Power Line Communications*., H. Ferreira, L. Lampe, J. Newbury, and T. Swart, Eds., 1st ed. New York: Wiley, 2010.

[102] Open Data Communication in Building Automation, Controls and Building Management-Control Network Protocol, ISO/IEC Std. DIS 14908, 2008.

[103] LonWorks: Online [Available]: https://www.echelon.com/technology/lonworks/ Accessed on 15 February, 2013.

[104] Power line Related Intelligent Metering Evolution (PRIME). Online [Available]: http://www.prime-alliance.org/ Accessed on 15 February, 2013.

[105] G3-PLC: *Open Standard for Smart Grid Implementation.* Online [Available]: http://www.maxim-ic.com/products/powerline/g3-plc/ Accessed on 15 February, 2013.

[106] M. Hoch, "Comparison of PLC G3 and PRIME," *Proc. IEEE International Symposium on Power Line Communications and Its Applications*, pp.165-169, 2011.

[107] I. H. Kim, B. Varadarajan, and A. Dabak, "Performance analysis and enhancements of narrowband OFDM power line communication systems," in *Proceedings IEEE International Conference on Smart Grid Communication*, pp. 362-367, 2010.

[108] V. Oksman and J. Zhang, "G.HNEM: the new ITU-T standard on narrowband PLC technology," *IEEE Communication Magazine,* vol. 49, no. 12, pp. 36-44, 2011.

[109] --, *Channel and Noise measurements,* IEEE P1901.2 Std., April 2011, doc: 2wg-11-0124-00-PHM5.

[110] D. Umehara, M. Kawai, and Y. Morihiro, "Performance analysis of non-coherent coded modulation for power line communications," *Proceedings International Symposium on Power Line Communications and Its Applications,* pp. 291-298, 2001.

[111] CENELEC - European Committee for Electro-technical Standardization: Online [Available]: http://www.ictsb.org/about/about_CENELEC.htm Accessed on 15 February, 2013.

[112] *Signaling on Low-Voltage Electrical Installations in the Frequency Range 3 kHz to 148.5 kHz—Part1: General Requirements, Frequency Bands and Electromagnetic Disturbances,* EN 50065-1, 2001.

[113] P. A. Janse van Rensburg and H. C. Ferreira, "Design of a bidirectional impedance-adapting transformer coupling circuit for low-voltage power line communications," *IEEE Transactions on Power Delivery*, vol. 20, no. 1, pp. 64-70, 2005.

[114] R. M. Vines, H. J. Trussel, K. C. Shuey, and J. B. O'Neal, "Impedance of the residential power-distribution circuit." *IEEE Transaction Electromagnetic Compatibility*, vol. EMC-27, no. 1, pp. 6-12, 1985.

[115] C.N. Krishnan, P.V. Ramakrishna, T.V. Prasad, and S. Karthikeyan, "Power-line As Access Medium- A Survey," *International Millennium Conference on Affordable Telecom and IT Solutions for Developing Countries*, pp. 1-10, 2000.

[116] H.C. Ferreira, H.M. Grové, O. Hooijen, and A. J. Han Vinck, "Power line communication," *Wiley Encyclopedia of Electrical and Electronics Engineering* , pp. 706-716, 1999.

[117] ABB ETL, "Power line carrier system- The best of a long line," ABB Netcom Ltd, Power System Communications, CH-5300 Turgi, Switzerland.

[118] M.E. Hardy, S. Ardalan, J.B. O'Neal, Jr., K.C. Shuey, and L.J. Gale, "Measurements of communication signal propagation on three phase power distribution lines," *IEEE Transaction on Power Delivery,* pp. 945-951, Jul. 1991.

[119] M.H.L. Chan and R.W. Donaldson, “Attenuation of communication signals on residential and commercial intra-building power-distribution circuits,” *IEEE Transaction on Electromagnetic. Compatibility*, vol. 28, no. 4, pp.220-230, 1986.

[120] K.M. Dostert, “Datenubertragung auf Stromnetze; Stand der Technik in Europea”, *Proceedings Workshop Communication Power lines*, Essen, Germany, Part IV., 1994.

[121] N. Pavlidou, A.J. Han Vinck, J. Yazdani and B. Honary, “Power line communications: state of the art and future trends,” *Communications Magazine, IEEE*, vol.41, no.4, pp. 34-40, April 2003.

[122] Van den Keybus, J., Bolsens, B., Driesen, J., Belmans, R., "Power line communication front-ends based on ADSL technology," *Circuits and Systems, IEEE International Symposium on*, vol.5, pp. 425-428, 2002.

[123] Vines, R.M., Trissell, H.J., Gale, L.J., and Ben O'neal, J., "Noise on Residential Power Distribution Circuits," *Electromagnetic Compatibility, IEEE Transactions on*, vol.EMC-26, no.4, pp.161-168, Nov. 1984.

[124] W.N. Sado, and J.S. Kunicki, “Personal communication on residential power lines-assessment of channel parameters,” *Universal Personal Communications, Fourth IEEE International Conference on*, pp. 532-537, 6-10 Nov 1995.

[125] Hooijen, O.G., "A channel model for the residential power circuit used as a digital communications medium," *Electromagnetic Compatibility, IEEE Transactions on*, vol.40, no.4, pp.331-336, Nov 1998.

[126] M. Zimmermann, and K. Dostert, “Analysis and modeling of impulsive noise in broad-band power line communications,” *Electromagnetic Compatibility, IEEE Transactions on*, vol.44, no.1, pp.249-258, Feb 2002.

[127] J. Misurec, “Interference in data communication over narrow-band PLC,” *Internal Journal of Computer Science and Network Security IJCSN*, vol. 8, no. 11, pp. 281-285, November, 2008.

[128] H.C. Ferreira, L. Lampe, J. Newbury and T.G. Swart, "Power Line Communications: Theory and Applications for Narrowband and Broadband Communications over Power lines," Wiley, 2010.

[129] A.D. Familua, A.O. Qatarey, P.A.J. Van Rensburg, and Ling Cheng, "Error pattern/behavior of noise in in-house CENELEC A-Band PLC channel," in *Proc. IEEE International Symposium on Power Line Communications and Its Applications*, pp.114-119, 27-30 March 2012.

[130] M. Tlich, H. Chaouche, A. Zeddam, and P. Pagani, "Novel approach for PLC impulsive noise modeling," in *Proc. IEEE International Symposium on Power Line Communications and Its Applications*, pp.20-25, March 29 2009-April 1 2009.

[131] H.C. Ferreira, H.M Grove, O. Hooijen, and A.J Han Vinck, "Power line Communications: an Overview," *4th IEEE Africon*, Stellenbosch, pp. 558-563, 24-27 Sep. 1996.

[132] Osama Bilal, Er Liu, Yangpo Gao and Timo O. Korhonen, "Design of Broadband Coupling Circuits for Power-Line Communication," in *Proc. IEEE International Symposium on Power Line Communications and Its Applications*, March 2004.

[133] Petrus A.J. V. Rensburg and H.C. Ferreira, "Practical Aspects of Component Selection and Circuit Layout for Modem and Coupling Circuitry," in *Proc. 7th IEEE International Symposium on Power Line Communications and Its Applications*, Kyoto, Japan, pp. 197-203, March 26-28, 2003.

[134] Janse Van Rensburg, "Effective Coupling for Power-Line Communication", *Research dissertation, University of Johannesburg*, January 2008.

[135] H.K. Podszeck, "Carrier communication over power lines" 4th Edition, New York: Springer-Verlag, 1963.

[136] IEEE Guide for power-line carrier Applications, IEEE Standard 643-1980.

[137] ANSI C93.1-1972, Requirements for Power Line Coupling Capacitors

[138] Petrus A.J. V. Rensburg and H.C. Ferreira, "Coupling Circuitry: Understanding the Functions of Different Components," *Proc. of 7th IEEE International Symposium on Power Line Communications and Its Applications,*, Kyoto, Japan, pp. 26-28, March 26-28, 2003.

[139] Petrus A. J. V. Rensburg and H.C. Ferreira, "Step-by-step design of a coupling circuit with bi-directional transmission capabilities," *Proc. of 8th IEEE International Symposium on Power Line Communications and Its Applications, Zaragoza, Spain*, pp. 238-243, 2004.

[140] L. Rabiner, and B. Juang, "An introduction to hidden Markov models," *ASSP Magazine, IEEE*, vol.3, no.1, pp.4-16, Jan 1986.

[141] Lawrence R. Rabiner, "A Tutorial on Hidden Markov Models and Selected Applications in Speech Recognition," *Proceedings of IEEE,* vol. 77, no. 2, pp. 257-286, February 1989.

[142] W. Tranter, K. Shanmugan, T. Rappaport, and K. Kosbar, "*Principles of communication systems simulation with wireless applications"*, First. Upper Saddle River, NJ, USA: Prentice Hall Press, 2003.

[143] B. D. Fritchman, "A binary channel characterization using partitioned Markov chains," *Information Theory, IEEE Transactions on*, vol.13, no.2, pp.221-227, April 1967.

[144] M.C. Jeruchim, P. Balaban and K.S. Shanmugan, "Simulations of Communication Systems Modeling, Methodology and Techniques," Kluwer Academic Publishers, New York, 2000.

[145] L. Cheng, T. G. Swart, and H. C. Ferreira, "Synchronization using insertion/deletion correcting permutation codes," in International Symposium on Power-Line Communications and its Applications, Jeju Island, Korea, Apr. 2-4 2008, pp. 135–140.

[146] L. Cheng, H. C. Ferreira, and K. Ouahada, "Re-synchronization of permutation codes with Viterbi-like decoding." in International Symposium on Power-Line Communications and its Applications, Dresden, Germany, 2009, pp. 36–40.

[147] L. Cheng and H. C. Ferreira, "Time-diversity permutation coding scheme for narrow-band power-line channels," in International Symposium on Power-Line Communications and its Applications, Beijing, China, Mar. 27-30, 2012.

[148] S.E Levinson, L.R. Rabiner, and M.M. Sondhi, "An Introduction to the Application of the Theory of Probabilistic Functions of a Markov Process to Automatic Speech Recognition," *B.S.T.J.*, vol. 62, no. 4, pp.1035-1074, April 1983.

[149] J.Y. Chouinard, M. Lecours, and G. Delisle, "Estimation of Gilbert's and Fritchman's Models Parameters Using the Gradient Method for Digital Mobile Radio Channels," *IEEE Trans. on Vehicular Technology*, vol. 37, no. 3, pp. 158-166, August 1988.

[150] W. Turin, *Digital Transmission Systems: Performance, Analysis and Modeling*, 2nd edition, New York: McGraw-Hill, 1999.

APPENDIX A: BAUM WELCH ALGORITHM EQUATION FOR AN ERROR SEQUENCE OF LENGTH T=4.

A three-state Fritchman model is assumed.

Forward Variables Computation

$$\alpha_t(i) = \Pr[O_1\ , O_2\ , \dots , O_t\ ]$$

$$\alpha_t(i) = \pi_i\ b_i\ (O_t\ )$$

The computation of the forward variables is executed in three steps: initialization, induction and termination.

Initialization Step: (t =1)

$$\alpha_1(1) = \pi_1\ b_1\ (O_1\ )$$

$$\alpha_t(2) = \pi_2\ b_2\ (O_1\ )$$

$$\alpha_t(3) = \pi_3\ b_3\ (O_1\ )$$

Induction Step:

$$\alpha_{t+1}(\mathrm{j}) = \left[\sum_{i=1}^{\mathrm{N}} \alpha_t(i)\ a_{ij}\right] \mathrm{b_j}\ (\mathrm{O_{t+1}}) \qquad 1 \le \mathrm{t}\ \le \mathrm{T} - 1, 1\ \le \mathrm{j} \le \mathrm{N}$$

(For t=1; j=1)

$$\alpha_2(1) = [\alpha_1(1)\ a_{11} +\ \alpha_1(2)\ a_{21} +\ \alpha_1(3)\ a_{31}]\ \mathrm{b_1}\ (\mathrm{O_2})$$

$$\alpha_2(2) = [\alpha_1(1)\ a_{12} +\ \alpha_1(2)\ a_{22} +\ \alpha_1(3)\ a_{32}]\ \mathrm{b_2}\ (\mathrm{O_2})$$

$$\alpha_2(3) = [\alpha_1(1)\ a_{13} +\ \alpha_1(2)\ a_{23} +\ \alpha_1(3)\ a_{33}]\ \mathrm{b_3}\ (\mathrm{O_2})$$

$$\alpha_3(1) = [\alpha_2(1)\ a_{11} +\ \alpha_2(2)\ a_{21} +\ \alpha_2(3)\ a_{31}]\ \mathrm{b_1}\ (\mathrm{O_3})$$

$$\alpha_3(2) = [\alpha_2(1)\ a_{12} +\ \alpha_2(2)\ a_{22} +\ \alpha_2(3)\ a_{32}]\ \mathrm{b_1}\ (\mathrm{O_3})$$

$$\alpha_3(3) = [\alpha_2(1)\ a_{13} +\ \alpha_2(2)\ a_{23} +\ \alpha_2(3)\ a_{33}]\ \mathrm{b_1}\ (\mathrm{O_3})$$

Termination Step: (t = T)

$$\alpha_T(i) = \Pr\ [O_1\ , O_2\ , \dots , O_T\ , \mathrm{S_T} = i \mid \Gamma]$$

$$\sum_{i=1}^{\mathrm{N}} \alpha_T(i) = \sum_{i=1}^{\mathrm{N}} \Pr\ [O_1\ , O_2\ , \dots , O_T\ , \mathrm{S_T} = i \mid \Gamma] = \Pr\ [\overline{\mathrm{O}} \mid \Gamma]$$

$$\Pr\ [\overline{\mathrm{O}} \mid \Gamma] = \sum_{i=1}^{\mathrm{N}} \alpha_T(i)\, \beta_{\mathrm{T}}\,(i)$$

Since$\beta_{\mathrm{T}}(i) = 1$, Therefore for ($i$ = 1, 2,…, N and N=3 for the case considered)

$$\beta_4(1) = 1$$

$$\beta_4(2) = 1$$

$$\beta_4(3) = 1$$

Hence,

$$\Pr\ [\overline{\mathrm{O}} \mid \Gamma] = \sum_{i=1}^{\mathrm{N}} \alpha_T(i)\ = \sum_{\mathrm{i}=1}^{\mathrm{N}} \pi_i\, b_i(O_{\mathrm{T}})$$

For (t= T)

$$\alpha_4(1) = \pi_1\ b_1\,(O_4\,)$$

$$\alpha_4(2) = \pi_2\ b_2\,(O_4\,)$$

$$\alpha_4(3) = \pi_3\ b_3\,(O_4\,)$$

Therefore,

$$\Pr\ [\overline{\mathrm{O}} \mid \Gamma] = \alpha_4(1) + \ \alpha_4(2) + \ \alpha_4(3)$$

Backward Variables Computation

The computation of the backward variables unlike the forward variable is executed in two steps: initialization and induction.

Initialization: $\beta_{\mathrm{T}}(i) = 1$,

Therefore,

$$\beta_4(1) = 1$$

$$\beta_4(2) = 1$$

$$\beta_4(3) = 1$$

Induction:

$$\beta_t(i) = \sum_{j=1}^{N} \beta_{t+1}(j) b_j(O_{t+1}) a_{ij} \quad , \qquad 1 \le t \le T-1, 1 \le j \le N$$

$$\beta_3(1) = \beta_4(1) b_1(O_4) a_{11} + \beta_4(2) b_2(O_4) a_{12} + \beta_4(3) b_3(O_4) a_{13}$$

$$\beta_3(2) = \beta_4(1) b_1(O_4) a_{21} + \beta_4(2) b_2(O_4) a_{22} + \beta_4(3) b_3(O_4) a_{23}$$

$$\beta_3(3) = \beta_4(1) b_1(O_4) a_{31} + \beta_4(2) b_2(O_4) a_{32} + \beta_4(3) b_3(O_4) a_{33}$$

$$\beta_2(1) = \beta_3(1) b_1(O_3) a_{11} + \beta_3(2) b_2(O_3) a_{12} + \beta_3(3) b_3(O_3) a_{13}$$

$$\beta_2(2) = \beta_3(1) b_1(O_3) a_{21} + \beta_3(2) b_2(O_3) a_{22} + \beta_3(3) b_3(O_3) a_{23}$$

$$\beta_2(3) = \beta_3(1) b_1(O_3) a_{31} + \beta_3(2) b_2(O_3) a_{32} + \beta_3(3) b_3(O_3) a_{33}$$

$$\beta_1(1) = \beta_2(1) b_1(O_2) a_{11} + \beta_2(2) b_2(O_2) a_{12} + \beta_2(3) b_3(O_2) a_{13}$$

$$\beta_1(2) = \beta_2(1) b_1(O_2) a_{21} + \beta_2(2) b_2(O_2) a_{22} + \beta_2(3) b_3(O_2) a_{23}$$

$$\beta_1(3) = \beta_2(1) b_1(O_2) a_{31} + \beta_2(2) b_2(O_2) a_{32} + \beta_2(3) b_3(O_2) a_{33}$$

Computation of the Expected Frequencies

$$\gamma_t(i) = \Pr[s_t = i \,|\overline{O}, \Gamma] \quad = \frac{\alpha_t(i)\beta_t(i)}{P[\overline{O}\,|\Gamma]} \; ; \quad i = 1,2,\dots,N$$

$$\gamma_1(1) = \frac{\alpha_1(1)\beta_1(1)}{\alpha_1(1)\,\beta_1(1) + \alpha_1(2)\,\beta_1(2) + \alpha_1(3)\,\beta_1(3)}$$

$$\gamma_1(2) = \frac{\alpha_1(2)\beta_1(2)}{\alpha_1(1)\,\beta_1(1) + \alpha_1(2)\,\beta_1(2) + \alpha_1(3)\,\beta_1(3)}$$

$$\gamma_1(3) = \frac{\alpha_1(3)\beta_1(3)}{\alpha_1(1)\,\beta_1(1) + \alpha_1(2)\,\beta_1(2) + \alpha_1(3)\,\beta_1(3)}$$

$$\gamma_2(1) = \frac{\alpha_2(1)\beta_2(1)}{\alpha_2(1)\,\beta_2(1) + \alpha_2(2)\,\beta_2(2) + \alpha_2(3)\,\beta_2(3)}$$

$$\gamma_2(2) = \frac{\alpha_2(2)\beta_2(2)}{\alpha_2(1)\,\beta_2(1) + \alpha_2(2)\,\beta_2(2) + \alpha_2(3)\,\beta_2(3)}$$

$$\gamma_2(3) = \frac{\alpha_2(3)\beta_2(3)}{\alpha_2(1)\,\beta_2(1) + \alpha_2(2)\,\beta_2(2) + \alpha_2(3)\,\beta_2(3)}$$

$$\gamma_3(1) = \frac{\alpha_3(1)\beta_3(1)}{\alpha_3(1)\,\beta_3(1) + \alpha_3(2)\,\beta_3(2) + \alpha_3(3)\,\beta_3(3)}$$

$$\gamma_3(2) = \frac{\alpha_3(2)\beta_3(2)}{\alpha_3(1)\,\beta_3(1) + \alpha_3(2)\,\beta_3(2) + \alpha_3(3)\,\beta_3(3)}$$

$$\gamma_3(3) = \frac{\alpha_3(3)\beta_3(3)}{\alpha_3(1)\,\beta_3(1) + \alpha_3(2)\,\beta_3(2) + \alpha_3(3)\,\beta_3(3)}$$

$$\gamma_4(1) = \frac{\alpha_4(1)\beta_4(1)}{\alpha_4(1)\,\beta_4(1) + \alpha_4(2)\,\beta_4(2) + \alpha_4(3)\,\beta_4(3)}$$

$$\gamma_4(2) = \frac{\alpha_4(2)\beta_4(2)}{\alpha_4(1)\,\beta_4(1) + \alpha_4(2)\,\beta_4(2) + \alpha_4(3)\,\beta_4(3)}$$

$$\gamma_4(3) = \frac{\alpha_4(3)\beta_4(3)}{\alpha_4(1)\,\beta_4(1) + \alpha_4(2)\,\beta_4(2) + \alpha_4(3)\,\beta_4(3)}$$

$$\xi_t(i,j) = \Pr\left[s_t = i\,, s_{t+1} = j \,|\overline{O}\,|\Gamma\right]$$

$\xi_t(i,j)$, denotes the probability of being in state *i* at time *t*, and state *j* at time *t+1*, given the model Γ and the observation sequence $\bar{O}$.

$$\xi_t(i,j) = \frac{\Pr\left[s_t = i\,, s_{t+1} = j \,|\overline{O}\,|\Gamma\right]}{\mathrm{P}[\overline{O}\,|\Gamma]}$$

$$\xi_t(i,j) = \frac{\alpha_t(i)\, a_{ij}\, b_j(O_{t+1})\, \beta_{t+1}(j)}{\sum_{i=1}^{N}\sum_{j=1}^{N}\ \alpha_t(i)\, a_{ij}\, b_j(O_{t+1})\, \beta_{t+1}(j)}$$

$$\xi_1(1,1) = \frac{\alpha_1(1)\, a_{11}\, b_1(O_2)\, \beta_2(1)}{\alpha_1(1)\, a_{11}\, b_1(O_2)\, \beta_2(1) + \ \alpha_1(2)\, a_{22}\, b_2(O_2)\, \beta_2(2) + \ \alpha_1(3)\, a_{33}\, b_3(O_2)\, \beta_2(3)}$$

$$\xi_1(1,2) = \frac{\alpha_1(1)\, a_{12}\, b_2(O_2)\, \beta_2(2)}{\alpha_1(1)\, a_{11}\, b_1(O_2)\, \beta_2(1) + \ \alpha_1(2)\, a_{22}\, b_2(O_2)\, \beta_2(2) + \ \alpha_1(3)\, a_{33}\, b_3(O_2)\, \beta_2(3)}$$

$$\xi_1(1,3) = \frac{\alpha_1(1)\, a_{13}\, b_3(O_2)\, \beta_2(3)}{\alpha_1(1)\, a_{11}\, b_1(O_2)\, \beta_2(1) + \ \alpha_1(2)\, a_{22}\, b_2(O_2)\, \beta_2(2) + \ \alpha_1(3)\, a_{33}\, b_3(O_2)\, \beta_2(3)}$$

$$\xi_1(2,1) = \frac{\alpha_1(2)\, a_{21}\, b_1(O_2)\, \beta_2(1)}{\alpha_1(1)\, a_{11}\, b_1(O_2)\, \beta_2(1) + \ \alpha_1(2)\, a_{22}\, b_2(O_2)\, \beta_2(2) + \ \alpha_1(3)\, a_{33}\, b_3(O_2)\, \beta_2(3)}$$

$$\xi_1(2,2) = \frac{\alpha_1(2)\, a_{22}\, b_2(O_2)\, \beta_2(2)}{\alpha_1(1)\, a_{11}\, b_1(O_2)\, \beta_2(1) + \ \alpha_1(2)\, a_{22}\, b_2(O_2)\, \beta_2(2) + \ \alpha_1(3)\, a_{33}\, b_3(O_2)\, \beta_2(3)}$$

$$\xi_1(2,3) = \frac{\alpha_1(2)\, a_{23}\, b_3(O_2)\, \beta_2(3)}{\alpha_1(1)\, a_{11}\, b_1(O_2)\, \beta_2(1) + \ \alpha_1(2)\, a_{22}\, b_2(O_2)\, \beta_2(2) + \ \alpha_1(3)\, a_{33}\, b_3(O_2)\, \beta_2(3)}$$

$$\xi_1(3,1) = \frac{\alpha_1(3)\, a_{31}\, b_1(O_2)\, \beta_2(1)}{\alpha_1(1)\, a_{11}\, b_1(O_2)\, \beta_2(1) + \ \alpha_1(2)\, a_{22}\, b_2(O_2)\, \beta_2(2) + \ \alpha_1(3)\, a_{33}\, b_3(O_2)\, \beta_2(3)}$$

$$\xi_1(3,2) = \frac{\alpha_1(3)\, a_{32}\, b_2(O_2)\, \beta_2(2)}{\alpha_1(1)\, a_{11}\, b_1(O_2)\, \beta_2(1) + \ \alpha_1(2)\, a_{22}\, b_2(O_2)\, \beta_2(2) + \ \alpha_1(3)\, a_{33}\, b_3(O_2)\, \beta_2(3)}$$

$$\xi_1(3,3) = \frac{\alpha_1(3)\, a_{33}\, b_3(O_2)\, \beta_2(3)}{\alpha_1(1)\, a_{11}\, b_1(O_2)\, \beta_2(1) + \ \alpha_1(2)\, a_{22}\, b_2(O_2)\, \beta_2(2) + \ \alpha_1(3)\, a_{33}\, b_3(O_2)\, \beta_2(3)}$$

$$\xi_2(1,1) = \frac{\alpha_2(1)\, a_{11}\, b_1(O_3)\, \beta_3(1)}{\alpha_2(1)\, a_{11}\, b_1(O_3)\, \beta_3(1) + \ \alpha_2(2)\, a_{22}\, b_2(O_3)\, \beta_3(2) + \ \alpha_2(3)\, a_{33}\, b_3(O_3)\, \beta_3(3)}$$

$$\xi_2(1,2) = \frac{\alpha_2(1)\, a_{12}\, b_2(O_3)\, \beta_3(2)}{\alpha_2(1)\, a_{11}\, b_1(O_3)\, \beta_3(1) + \ \alpha_2(2)\, a_{22}\, b_2(O_3)\, \beta_3(2) + \ \alpha_2(3)\, a_{33}\, b_3(O_3)\, \beta_3(3)}$$

$$\xi_2(1,3) = \frac{\alpha_2(1)\, a_{13}\, b_3(O_3)\, \beta_3(3)}{\alpha_2(1)\, a_{11}\, b_1(O_3)\, \beta_3(1) + \ \alpha_2(2)\, a_{22}\, b_2(O_3)\, \beta_3(2) + \ \alpha_2(3)\, a_{33}\, b_3(O_3)\, \beta_3(3)}$$

$$\xi_2(2,1) = \frac{\alpha_2(2)\, a_{21}\, b_1(O_3)\, \beta_3(1)}{\alpha_2(1)\, a_{11}\, b_1(O_3)\, \beta_3(1) + \ \alpha_2(2)\, a_{22}\, b_2(O_3)\, \beta_3(2) + \ \alpha_2(3)\, a_{33}\, b_3(O_3)\, \beta_3(3)}$$

$$\xi_2(2,2) = \frac{\alpha_2(2)\, a_{22}\, b_2(O_3)\, \beta_3(2)}{\alpha_2(1)\, a_{11}\, b_1(O_3)\, \beta_3(1) + \ \alpha_2(2)\, a_{22}\, b_2(O_3)\, \beta_3(2) + \ \alpha_2(3)\, a_{33}\, b_3(O_3)\, \beta_3(3)}$$

$$\xi_2(2,3) = \frac{\alpha_2(2)\, a_{23}\, b_3(O_3)\, \beta_3(3)}{\alpha_2(1)\, a_{11}\, b_1(O_3)\, \beta_3(1) + \alpha_2(2)\, a_{22}\, b_2(O_3)\, \beta_3(2) + \alpha_2(3)\, a_{33}\, b_3(O_3)\, \beta_3(3)}$$

$$\xi_2(3,1) = \frac{\alpha_2(3)\, a_{31}\, b_1(O_3)\, \beta_3(1)}{\alpha_2(1)\, a_{11}\, b_1(O_3)\, \beta_3(1) + \alpha_2(2)\, a_{22}\, b_2(O_3)\, \beta_3(2) + \alpha_2(3)\, a_{33}\, b_3(O_3)\, \beta_3(3)}$$

$$\xi_2(3,2) = \frac{\alpha_2(3)\, a_{32}\, b_2(O_3)\, \beta_3(2)}{\alpha_2(1)\, a_{11}\, b_1(O_3)\, \beta_3(1) + \alpha_2(2)\, a_{22}\, b_2(O_3)\, \beta_3(2) + \alpha_2(3)\, a_{33}\, b_3(O_3)\, \beta_3(3)}$$

$$\xi_2(3,3) = \frac{\alpha_2(3)\, a_{33}\, b_3(O_3)\, \beta_3(3)}{\alpha_2(1)\, a_{11}\, b_1(O_3)\, \beta_3(1) + \alpha_2(2)\, a_{22}\, b_2(O_3)\, \beta_3(2) + \alpha_2(3)\, a_{33}\, b_3(O_3)\, \beta_3(3)}$$

$$\xi_3(1,1) = \frac{\alpha_3(1)\, a_{11}\, b_1(O_4)\, \beta_4(1)}{\alpha_3(1)\, a_{11}\, b_1(O_4)\, \beta_4(1) + \alpha_3(2)\, a_{22}\, b_2(O_4)\, \beta_4(2) + \alpha_3(3)\, a_{33}\, b_3(O_4)\, \beta_4(3)}$$

$$\xi_3(1,2) = \frac{\alpha_3(1)\, a_{12}\, b_2(O_4)\, \beta_4(2)}{\alpha_3(1)\, a_{11}\, b_1(O_4)\, \beta_4(1) + \alpha_3(2)\, a_{22}\, b_2(O_4)\, \beta_4(2) + \alpha_3(3)\, a_{33}\, b_3(O_4)\, \beta_4(3)}$$

$$\xi_3(1,3) = \frac{\alpha_3(1)\, a_{13}\, b_3(O_4)\, \beta_4(3)}{\alpha_3(1)\, a_{11}\, b_1(O_4)\, \beta_4(1) + \alpha_3(2)\, a_{22}\, b_2(O_4)\, \beta_4(2) + \alpha_3(3)\, a_{33}\, b_3(O_4)\, \beta_4(3)}$$

$$\xi_3(2,1) = \frac{\alpha_3(2)\, a_{21}\, b_1(O_4)\, \beta_4(1)}{\alpha_3(1)\, a_{11}\, b_1(O_4)\, \beta_4(1) + \alpha_3(2)\, a_{22}\, b_2(O_4)\, \beta_4(2) + \alpha_3(3)\, a_{33}\, b_3(O_4)\, \beta_4(3)}$$

$$\xi_3(2,2) = \frac{\alpha_3(2)\, a_{22}\, b_2(O_4)\, \beta_4(2)}{\alpha_3(1)\, a_{11}\, b_1(O_4)\, \beta_4(1) + \alpha_3(2)\, a_{22}\, b_2(O_4)\, \beta_4(2) + \alpha_3(3)\, a_{33}\, b_3(O_4)\, \beta_4(3)}$$

$$\xi_3(2,3) = \frac{\alpha_3(2)\, a_{23}\, b_3(O_4)\, \beta_4(3)}{\alpha_3(1)\, a_{11}\, b_1(O_4)\, \beta_4(1) + \alpha_3(2)\, a_{22}\, b_2(O_4)\, \beta_4(2) + \alpha_3(3)\, a_{33}\, b_3(O_4)\, \beta_4(3)}$$

$$\xi_3(3,1) = \frac{\alpha_3(3)\, a_{31}\, b_1(O_4)\, \beta_4(1)}{\alpha_3(1)\, a_{11}\, b_1(O_4)\, \beta_4(1) + \alpha_3(2)\, a_{22}\, b_2(O_4)\, \beta_4(2) + \alpha_3(3)\, a_{33}\, b_3(O_4)\, \beta_4(3)}$$

$$\xi_3(3,2) = \frac{\alpha_3(3)\, a_{32}\, b_2(O_4)\, \beta_4(2)}{\alpha_3(1)\, a_{11}\, b_1(O_4)\, \beta_4(1) + \alpha_3(2)\, a_{22}\, b_2(O_4)\, \beta_4(2) + \alpha_3(3)\, a_{33}\, b_3(O_4)\, \beta_4(3)}$$

$$\xi_3(3,3) = \frac{\alpha_3(3)\, a_{33}\, b_3(O_4)\, \beta_4(3)}{\alpha_3(1)\, a_{11}\, b_1(O_4)\, \beta_4(1) + \alpha_3(2)\, a_{22}\, b_2(O_4)\, \beta_4(2) + \alpha_3(3)\, a_{33}\, b_3(O_4)\, \beta_4(3)}$$

Model Parameter Estimation using the Expected Frequencies

Determining new state transition probability

$$\hat{a}_{ij} = \frac{\text{expected number of transitions from i to j}}{\text{expected number of transitions from i}}$$

$$\hat{a}_{\mathrm{ij}} = = \frac{\sum_{\mathrm{t}=1}^{\mathrm{T}-1} \xi_t(i,j)}{\sum_{\mathrm{t}=1}^{\mathrm{T}-1} \gamma_t(i)}$$

$$\hat{a}_{11} = \frac{\xi_1(1,1) + \xi_2(1,1) + \xi_3(1,1)}{\gamma_1(1) + \gamma_2(1) + \gamma_3(1)}$$

$$\hat{a}_{12} = \frac{\xi_1(1,2) + \xi_2(1,2) + \xi_3(1,2)}{\gamma_1(1) + \gamma_2(1) + \gamma_3(1)}$$

$$\hat{a}_{13} = \frac{\xi_1(1,3) + \xi_2(1,3) + \xi_3(1,3)}{\gamma_1(1) + \gamma_2(1) + \gamma_3(1)}$$

$$\hat{a}_{21} = \frac{\xi_1(2,1) + \xi_2(2,1) + \xi_3(2,1)}{\gamma_1(2) + \gamma_2(2) + \gamma_3(2)}$$

$$\hat{a}_{22} = \frac{\xi_1(2,2) + \xi_2(2,2) + \xi_3(2,2)}{\gamma_1(2) + \gamma_2(2) + \gamma_3(2)}$$

$$\hat{a}_{23} = \frac{\xi_1(2,3) + \xi_2(2,3) + \xi_3(2,3)}{\gamma_1(2) + \gamma_2(2) + \gamma_3(2)}$$

$$\hat{a}_{31} = \frac{\xi_1(3,1) + \xi_2(3,1) + \xi_3(3,1)}{\gamma_1(3) + \gamma_2(3) + \gamma_3(3)}$$

$$\hat{a}_{32} = \frac{\xi_1(3,2) + \xi_2(3,2) + \xi_3(3,2)}{\gamma_1(3) + \gamma_2(3) + \gamma_3(3)}$$

$$\hat{a}_{33} = \frac{\xi_1(3,3) + \xi_2(3,3) + \xi_3(3,3)}{\gamma_1(3) + \gamma_2(3) + \gamma_3(3)}$$

Computing $\hat{b}_j(e_k)$, defined by

$$\hat{b}_j(e_k) = \frac{\text{expected number of times } \mathrm{e_k} \text{ is emmited from state j}}{\text{expected number of visits to state j}}$$

$$\hat{b}_j(e_k) = \frac{\sum_{\mathrm{t}=1|O_t=e_k}^{\mathrm{T}} \gamma_t(j)}{\sum_{\mathrm{t}=1}^{\mathrm{T}} \gamma_t(j)}$$

$$\hat{b}_1(e_k) = \frac{\gamma_1(1) + \gamma_4(1)}{\gamma_1(1) + \gamma_2(1) + \gamma_3(1) + \gamma_4(1)}$$

$$\hat{b}_2(e_k) = \frac{\gamma_1(2) + \gamma_4(2)}{\gamma_1(2) + \gamma_2(2) + \gamma_3(2) + \gamma_4(2)}$$

$$\hat{b}_3(e_k) = \frac{\gamma_1(3) + \gamma_4(3)}{\gamma_1(3) + \gamma_2(3) + \gamma_3(3) + \gamma_4(3)}$$

Computing the estimated initial state probability π_i (the expected number of times in state S_i at time t=1)

$$\hat{\pi}_i = \alpha_1(i)\beta_1(i)$$

$$\hat{\pi}_1 = \alpha_1(1)\beta_1(1)$$

$$\hat{\pi}_2 = \alpha_1(2)\beta_1(2)$$

$$\hat{\pi}_3 = \alpha_1(3)\beta_1(3)$$